

1-1-2001

## Change of support correction in mineral resource estimation

Marek J. Janas  
*Edith Cowan University*

Follow this and additional works at: <https://ro.ecu.edu.au/theses>



Part of the [Applied Statistics Commons](#), and the [Earth Sciences Commons](#)

---

### Recommended Citation

Janas, M. J. (2001). *Change of support correction in mineral resource estimation*. <https://ro.ecu.edu.au/theses/1051>

This Thesis is posted at Research Online.  
<https://ro.ecu.edu.au/theses/1051>

# Edith Cowan University

## Copyright Warning

You may print or download ONE copy of this document for the purpose of your own research or study.

The University does not authorize you to copy, communicate or otherwise make available electronically to any other person any copyright material contained on this site.

You are reminded of the following:

- Copyright owners are entitled to take legal action against persons who infringe their copyright.
- A reproduction of material that is protected by copyright may be a copyright infringement. Where the reproduction of such material is done without attribution of authorship, with false attribution of authorship or the authorship is treated in a derogatory manner, this may be a breach of the author's moral rights contained in Part IX of the Copyright Act 1968 (Cth).
- Courts have the power to impose a wide range of civil and criminal sanctions for infringement of copyright, infringement of moral rights and other offences under the Copyright Act 1968 (Cth). Higher penalties may apply, and higher damages may be awarded, for offences and infringements involving the conversion of material into digital or electronic form.



**Change of Support Correction in Mineral Resource Estimation**

by

**Marek J. Janas**

A Thesis Submitted in Partial Fulfilment of the  
Requirements for the Award of  
Master of Science (Mathematics and Planning).

Faculty of Communications, Health and Science  
School of Engineering and Mathematics  
Edith Cowan University

November 2001

## USE OF THESIS

The Use of Thesis statement is not included in this version of the thesis.

## **Abstract**

The success of any mining operation greatly, if not entirely, depends on the accuracy of prediction of recoverable mining reserves. However, prior to mining, knowledge about the distribution of the Selective Mining Unit (SMU) is limited. The SMU represents the volume on which extraction of ore takes place and on which recoverable mining reserves are based. Realistic recoverable reserve estimates can be obtained from the grade-tonnage curve that corresponds to the unknown distribution of the SMU rather than to the distribution of exploration sample data. In general, if the reserve calculation, at the given cut-off grade, is based upon exploration drill samples, with much smaller support than the SMU, then there is a high probability of incorrect estimation of the tonnage and the grade of ore, and this can have serious implications for the economic side of the mining project.

Various techniques for correction for the change of support of data, in other words change of the volume on which the data are defined, enable more accurate estimates of the distribution of the variable of interest (that is grade of a precious metal). The fact that the volume (support) represented by the variable is taken into account makes the estimates more reliable and, as we will show in the study, closer to reality. The

distribution of the SMU is derived from the known distribution of samples by applying a correction model.

Among these techniques are two recent methods these are a conditional simulation method detailed by I. Glacken and a kriging method due to A. Arik. This study aims to examine these two methods and compare them with the standard techniques. The methods will be applied to real data acquired from the Boddington Gold Mine in the south-west of Western Australia. In addition to accuracy, the practicality and simplicity of implementation of each method will also be discussed.

## DECLARATION

I certify that this thesis does not incorporate without acknowledgment any material previously submitted for a degree or diploma in any institution of higher education; and that to the best of my knowledge and belief it does not contain any material previously written by another person except where due reference is made in the text.

Signature\_\_

Date 23-11-2001

## ACKNOWLEDGMENTS

This document would not have become a reality if not the help from several people and institutions, which I would like to acknowledge gratefully.

My supervisor Associate Professor Lyn Bloom for providing valuable advice and extraordinary help.

I.M. Glacken for making available his thesis and the programs used for conditional simulation in this study.

A. Arik for making available a pre-print of his paper and the program for the Nearest Neighbour Kriging estimations performed in the study.

Boddington Gold Mine Pty. Ltd. for providing data sets, software and computer equipment.

My wife, Malgorzata, and my family for giving me a lot of support, help and being extremely patient.

Computerised processing of the data necessary for this study was done using the following packages:

Medsystem/MineSight® – general statistics, data manipulation, semivariograms, contouring, surface and solids modelling and visualisation, kriging, plotting. (BGM copies)

GSLIB – conditional simulation (private copy)

3Plot – plotting (public domain)



## Table of Contents

Abstract .....	3
DECLARATION .....	5
ACKNOWLEDGMENTS.....	6
1. Introduction.....	8
1.1 Background and significance .....	8
1.2 Aims and objectives .....	13
1.3 Methodology and notation.....	16
2. Random function model.....	21
2.1 Overview .....	21
2.2 Assumption and moments of stationarity.....	24
2.3 Semivariogram .....	29
2.4 Kriging .....	33
2.5 Simulation .....	37
2.5.1 The multiGaussian approach .....	39
2.5.2 Sequential Gaussian simulation.....	42
2.5.3 The LU decomposition algorithm.....	45
3. Change of support and volume - variance relationship .....	49
4. Correction for the support effect .....	56
4.1 Overview .....	56
4.2 Affine correction .....	59
4.3 Indirect lognormal correction and discrete Gaussian transformation.....	61
4.4 Change of support by conditional simulation.....	63
4.5 Nearest neighbour kriging .....	65
5. Data set and treatment .....	69
5.1 Introduction.....	69
5.1.1 Exploration and grade control practices at BGM .....	69
5.2 Exploration data set.....	71
5.2.1 Descriptive statistics of <i>excomp</i> .....	75
5.2.2 Definition of sample data set.....	76
5.3 Grade control data set.....	80
5.3.1 Descriptive statistics of the grade control data set.....	82
6. Variography of <i>finexcomp</i> .....	87
6.1 Analysis of spatial continuity of <i>finexcomp</i> .....	87
6.2 <i>Finexcomp</i> variography modelling.....	96
6.3 Cross validation of the ordinary kriging estimates .....	103
7. Change of support and grade estimation using <i>finexcomp</i> .....	110
7.1 Introduction.....	110
7.2 Ordinary kriging and the nearest neighbour kriging estimation .....	112
7.2.1 Background .....	112
7.2.2 <i>Finexcomp</i> grade estimation results .....	115
7.2.3 Analysis of the kriging estimation results .....	133
7.3 Change of support by conditional simulation.....	141
7.3.1 Background .....	141
7.3.2 Sequential Gaussian conditional simulation.....	142
7.3.3 Sequential Gaussian conditional simulation results analysis.....	147
8. Conclusions .....	152
APPENDICES .....	158
Appendix 1.....	159
Appendix 2.....	160
Appendix 3.....	161
REFERENCES.....	162

# 1. INTRODUCTION

## 1.1 Background and significance

The main focus of this study is to show the importance to recoverable ore reserve estimation of the effect of the volume, also referred to as the support, on which an attribute (for example grade of a precious metal) is defined. For a mining operation to be successful correct estimation of recoverable mining reserves is essential and so the correction for the change in support from sample data to Selective Mining Unit (SMU) is an issue that should not be neglected.

The identification of a potentially mineable ore body always raises the question of the minimum amount of sampling necessary to determine a reliable estimate of its physical limits and economic viability. At the development stage of any mining prospect, one of the main sources of costs is the exploration drilling and sampling. Hence, taking a very simple approach, minimising the sampling will also minimise the costs. On the other hand, even overlooking the economic side and assuming that financial resources are available to conduct a rigorous sampling program, the volume of samples taken from the project area is usually

very small in comparison to the volume of potentially mineable reserves; therefore the potential for error is high.

A sample set of some geological attribute obtained from an exploration drilling program provides valuable information regarding the location and values of that attribute. Based on the definition, originally derived from the geology of the region of interest, further interpretation of an ore body can be undertaken using this set. In geostatistical terminology, the modelling of the mineralised region is carried out. A model of an ore body is based on the spatial distribution of the samples taken and hence the quality of the model is directly dependent on the relevant sampling. In general, the more samples the better the estimate should be, providing that the samples are evenly distributed (no clustering or preferential drilling). However, more samples will mean at least higher financial expenditure. That forces the decision to be made on the minimum level of confidence in the final results that can be accepted and on the minimum amount of data necessary to provide such a level of confidence (Recny, 1982). Usually there is no easy answer to this question. To help in solving this complex problem a number of geostatistical methods have been developed.

For an ore body the property of prime concern is the content of a mineral per unit of weight of the ore. This is called the grade and is usually expressed in grams per tonne (g/t). The grade can be measured numerically and changes from one location to the other. Taking a geostatistical approach, the grade can be seen as a variable. There are also other variables, which may be of interest during the process of geological modelling. Geological modelling attempts to determine the spatial variability of the attributes of interest. Further examination of the spatial properties enables us to define a grade shell. The grade shell is a volume, whose limits and location are determined by a given cut-off value. The amount of ore inside grade shells, defined by an ore cut-off based on actual economic parameters, is called a *reserve*. The term *reserves*, or better *recoverable reserves*, can be used at the stage where this economic cut-off is determined and applied to a physically “possible to mine” deposit. Any material extracted with the grade content above the cut-off will generate profit. Material below the cut-off is usually wasted. Without loss of generality it will be assumed here that the study area is a mineable deposit and that the cut-offs that we are using are economic cut-offs.

However, mining occurs on a volume different from the sample volume. Hence the statistical distribution of the mineable unit can be expected to be different from the distribution of the sample data. Applying the same cut-off grade to different distributions (eg. the sample distribution and the mineable unit distribution) may result in different amounts of tonnage at the different grades. This is where the problem arises. The recoverable reserves, in most cases, cannot be accurately predicted from sample data only, without applying any correction for the volume (support) change.

There are several methods available to estimate ore reserves, ranging from simple contouring methods to sophisticated geostatistical kriging and simulation techniques. Each of these methods has its advantages and disadvantages. Yet sometimes not enough consideration is given to making an appropriate choice to best suit the specifics of the data used.

Generally, the estimation is done by building a block model of the mineralised zone of interest. Using available sample data, the grade of each block in the block model is estimated by the chosen technique. Blocks are of regular shape, usually rectangular, their dimensions mainly dependent on the drill spacing and the bench height. By performing the

process of estimation of the grade and tonnages of blocks using sample data, we move from a sample volume (smaller support) to a much larger support and bigger volume, which is the volume of a block. The result of the change from point distribution to block distribution is known as the *change of support effect* and allowance may be made for this change by means of a variance correction factor (Isaaks and Srivastava, 1989; Rossi and Parker 1993). In practice, as previously said, mining takes place at a volume different from sample and block volumes. This mining volume is usually called the Selective Mining Unit (SMU) and is the smallest volume that can be selectively mined. It is primarily defined by the equipment which is to be used during the ore extraction. This is, in fact, a very general approach to the problem of the SMU. A good practice in defining the SMU requires that a thorough consideration should be given to the exploration drill spacing, the intended grade control technique as well as the machinery. This is an interrelated system and, to some extent, the size of the mining bench and therefore equipment is indirectly dependent on the exploration drilling. For the purpose of this study we will assume that the size of a block from the models used is equal to the SMU. This does not affect the results of our calculation because once the SMU size is determined an additional model can be built with the block size equal to the SMU in order to estimate the relevant distribution.

The choice of the correction for change of support is not a simple one. Prior to the actual mining, the distribution of blocks in the block model is not fully known. Extraction of ore takes place on the volume of the SMU and therefore a realistic recoverable reserve estimate can be derived from the grade-tonnage curve that corresponds to the SMU distribution. However, at the modelling stage only the estimated point distribution is known, in other words, the global distribution of the exploration samples (composites). The complexity of this topic may be the reason why the correction and the change of support are sometimes neglected. Such an approach during the development of any geostatistical model can introduce a bias on estimated recoverable reserves. It can also result in a serious over- or underestimation of the percentage of blocks above a given cut-off grade.

## **1.2 Aims and objectives**

Due to its significance with respect to mineral resource estimation, the change of support and the need for correction for it are well recognised in the geostatistical literature. A number of techniques have been developed that enable such a correction to be performed in order to obtain unbiased estimates. The “standard” techniques which are

currently used include: *affine correction*, *indirect lognormal correction* and *discrete Gaussian transformation*. Each has its advantages as well as limitations. The research in the field of the support correction has been continuing with the aim of developing a practical and a robust method. We shall consider here two relatively recent methods suggested for correcting for the change of support. One of these methods is called Nearest Neighbour Kriging (NNK) (Arik, 1998), designed especially for use when estimating recoverable reserves with skewed grade distribution. It has a built-in mechanism which allows for honouring the volume on which data is defined.

In the second method (Glacken, 1996) the use of conditional simulation is proposed as the way of accounting for the differences in support. This method also allows for the incorporation of economic measures during a process of block delineation as ore and waste.

As stated in Section 1.1 this study aims, first of all, to show the influence that the data volume may have on recoverable reserve estimation. By the data volume, or support of data, we mean the volume represented by a datum, which in our case will be a sample from the exploration or grade control data set and a block from the block model. We examine here the



effect of change in the support of the data on the grade and tonnage of the estimated reserves. The two recent correction methods, referred to earlier, along with the standard affine correction will be used. These will be done in the context of a comparison using real data from the Boddington Gold Mine in the south-west of Western Australia. Moreover, during this process, the practicality and simplicity of implementation of the chosen methods will also be investigated. Based on the results from these exercises and available data from the mine, the degree of influence that the change of support effect may have on recoverable reserves will be addressed. In other words, this study will investigate the effect on the estimated grades and tonnages introduced by applying the chosen correction techniques. The results generated by the two new correction methods will be analysed individually due to the inherent differences between the estimation process, which includes kriging algorithms, and simulation. These techniques are designed with different objectives as will be shown in the course of this study.

As an additional check, the grade control data set adjusted by the affine correction method (in order to represent the same volume as the kriging estimates) will be compared to the results obtained from the kriging (ordinary kriging OK and NNK).

### 1.3 Methodology and notation

In this section the methodology is briefly summarised. It is divided into several stages for clarity. Each of these stages contains subsequent tasks. Next the notation that is going to be used through the study is presented.

#### Methodology

Stage 1.

Review the mathematical background and theory of:

- a) Random function model;
- b) The volume – variance relationship and the change of support; and
- c) The standard change of support correction techniques.

Stage 2.

Investigate the theory and the mathematical framework of the chosen correction methods:

- a) Correction using conditional simulation;
- b) Nearest Neighbour Kriging developed by Arik (1998); and
- c) Sequential Gaussian simulation.

Stage 3.

The chosen methods (Stage 2), the standard method (that is the affine correction) and the ordinary kriging (OK) method will be applied to real

exploration data from the Boddington Gold Mine (BGM) in South-west Western Australia. This data set consists of two subsets. One is the sample set obtained from exploration drilling and the other is the complete grade control set, very often referred to as “reality”. The practicality and the level of complexity of use of the methods from Stage 2 will be examined. In addition, for the sake of a theoretical comparison, the affine correction method will be applied to the grade control data and compared with the kriging estimates (for both OK and NNK).

#### Stage 4.

The results obtained in Stage 3 will be compared with the grade control data from the BGM. Attention will be given primarily to the comparison between the grade-tonnage curves generated from the grade estimations carried out in Stage 3 and the grade-tonnage curves from the grade control data set. The results obtained will be analysed in order to determine how the methods performed in this particular case. An attempt will be made to evaluate the level of impact of the support changes on mineral resource estimation. In addition, OK estimation will be performed without applying any correction for the support changes. Along with the results from the methods from Stage 2, especially from

NNK, this shall form a base for a comparison of how serious an effect the support problem may have on the reserve estimation.

### List of Symbols

$\forall$	for all
$a$	range of semivariogram
$C()$	covariance
$c_0$	nugget variance (nugget effect)
$c$	partial sill of semivariogram
$CV$	coefficient of variation (abbreviation)
$E\{ \}$	expected value
$F$	cumulative distribution function
$f$	nearest neighbour kriging smoothing correction factor
$f_v$	variance correction factor
$\gamma(\mathbf{h})$	semivariogram function
$G(y)$	standard normal cumulative distribution function
$g_i(h)$	basic semivariogram model, $h= \mathbf{h} $
$\mathbf{h}$	separation vector
$k$	number of emphasised nearest samples for nearest neighbour kriging
$m$	stationary mean

$\lambda(\mathbf{u}_\alpha)$	kriging weights associated with datum at location $\mathbf{u}_\alpha$
$\lambda_{nnk}$	nearest neighbour kriging weights
$\lambda_{ok}$	ordinary kriging weights
$\mu$	Lagrange parameter
$q$	quantile function
$r$	ordinary kriging residuals
$\sigma^2$	variance of the random variable $Z$
$\sigma_b^2$	block variance from a block model
$\hat{\sigma}_p^2$	composite variance
$\sigma_{OK}^2$	ordinary kriging variance
$s^2, s^2(v, V)$	experimental dispersion variance of values with support $v$ within region $V$
$v(\mathbf{u}_\alpha)$	support volume at $\mathbf{u}_\alpha$
$V$	support of a block (for instance SMU)
$\text{Var}\{ \}$	variance
$A$	region (also denotes the support or measure of the volume of the study region)
$S_n$	set of $n$ measurements of an attribute – sample set
$\mathbf{u}$	location vector $(u^x, u^y, u^z)$
$\alpha, \beta$	location indices e.g. $\mathbf{u}_\alpha$

$Y = \varphi(Z)$	transform function $\varphi(\cdot)$ relating two random variables $Y$ and $Z$
$Z = \varphi^{-1}(Y)$	inverse transform function $\varphi(\cdot)$ relating random variables $Z$ and $Y$
$Z(\mathbf{u}_\alpha)$	random variable at a sample location
$Z(\mathbf{u})$	random function
$Z_{OK}^*(\mathbf{u})$	ordinary kriging estimator
$Z_{SK}^*(\mathbf{u})$	simple kriging estimator
$Z_{NNK}^*(\mathbf{u})$	nearest neighbour kriging estimator
$z(\mathbf{u}_\alpha)$	$z$ value at location $\mathbf{u}_\alpha$
$z(\mathbf{u})$	true value at unsampled location $\mathbf{u}$
$z^{(l)}(\mathbf{u})$	$l$ th realisation of random variable $Z(\mathbf{u})$
$z_c^{(l)}(\mathbf{u})$	$l$ th realisation conditional to some neighbouring data

## 2. RANDOM FUNCTION MODEL

### 2.1 Overview

Our aim here is to describe mathematically the “behaviour” of natural phenomena such as the grade of a gold deposit. Of main interest is the distribution of the grade values in three dimensional space, i.e. within the deposit. It is known from experience that properties like grade are often structurally controlled. For example there are rich zones (high grade) and poorer zones (low grade). Therefore a kind of spatial continuity may be assumed. This means that the values are related in a certain way. If we know this relation we can model the entire distribution providing that some grade values, obtained from sampling at the discrete points, are available. Yet, looking at this attribute, that is the grade, at a smaller scale, say a low-grade zone itself, we may find a behaviour that seems to appear totally random. Samples taken next to each other may have extremely different values. To be able to capture this random component within the spatial continuity we need a model. A model which is capable accounting for both the structural and the random aspects is a *probabilistic model*. It provides the information of how the variable

changes with distance and location. Furthermore, the model will contain information for any location and not only the sampled locations.

We give here an overview of the theory of the *random function* model. This description, in the main, follows Goovaerts (1997), but Journel and Huijbregts (1978) is also used as a major reference text.

Description of a sample data set  $S_n$  (this can be any sample data set including drill samples), in statistical terms, is very rarely, if ever, the goal per se. Usually we want to characterise the whole population from which the samples have been drawn. If  $S_n = \{z(\mathbf{u}_\alpha), \alpha = 1, \dots, n\}$  is the set of samples taken from the study area  $A$ , the population will comprise all possible measurements over the area  $A$  and can be denoted as  $\{z(\mathbf{u}), \forall \mathbf{u} \in A\}$ , where  $\mathbf{u}$  is the location vector within area  $A$  with up to three  $(u^x, u^y, u^z)$  components and  $\alpha$  represents a certain location. As shown,  $S_n$  does not contain all the information that may be required since it is only a subset of the whole population. Therefore we need to set up an appropriate probability model to enable us to estimate reality, together with some measure of the estimation error involved.



A *random variable* (RV) is a real-valued function defined on the set of outcomes of an experiment. Random variables can be divided into two categories, discrete and continuous according to the type of values it takes.

In this thesis we consider only continuous random variables. The RV itself will be denoted by an upper case letter and its value by the corresponding lower case letter.

A continuous RV  $Z(\mathbf{u})$  is described by its cumulative distribution function (cdf) in the following way:

$$F(\mathbf{u}; z) = \text{Prob}\{Z(\mathbf{u}) \leq z\} \quad \forall z \quad (2 - 1)$$

Also the following relations must be satisfied:

$$F(\mathbf{u}; z) \in [0,1] \quad \forall z \quad (2 - 2)$$

$$F(\mathbf{u}; z) \leq F(\mathbf{u}; z') \quad \forall z' > z \quad (2 - 3)$$

In this context the sample data set is considered to be a set of outcomes from an unknown *random process*. A sample value  $z(\mathbf{u}_\alpha)$  at location  $\mathbf{u}_\alpha$ , for example gold grade from an exploration drilling, is considered as a realisation of a random variable  $Z(\mathbf{u}_\alpha)$ .

A *random function* (abbreviated to RF) is defined as a set  $\{Z(\mathbf{u}), \forall \mathbf{u} \in A\}$  of RV's  $Z(\mathbf{u})$  which are not, in general, independent but are related by a correlation expressing the spatial structure of the random variables. Following this definition, for multiple sample locations  $\mathbf{u}_k, k = 1, \dots, N$  within region  $A$ , there will be a vector of  $N$  random variables, such as  $\{Z(\mathbf{u}_1), \dots, Z(\mathbf{u}_N)\}$ , that corresponds to these locations. Because it is a vector of  $N$  random variables it is described by an  $N$ -point (or  $N$ -variate) cdf:

$$F(\mathbf{u}_1, \dots, \mathbf{u}_N; z_1, \dots, z_N) = \text{Prob}\{Z(\mathbf{u}_1) \leq z_1, \dots, Z(\mathbf{u}_N) \leq z_N\} \quad (2 - 4)$$

For any combination of locations  $\mathbf{u}_k$  and positive integer  $N$ , the set of such cdf's (2-4) is referred to in geostatistics as the *spatial law* of the RF  $Z(\mathbf{u})$ .

## 2.2 Assumption and moments of stationarity

The use of the RF model as a geostatistical tool is applicable when its probability law can be inferred (or at least a part of the probability law) so that the RF is defined in its entirety. This is only possible when multiple realisations  $\{z^{(l)}(\mathbf{u}), z^{(l)}(\mathbf{u}'); l = 1, \dots, L\}$  of the RF are available for

each of the locations. This is almost never the case in practice<sup>1</sup>. Furthermore, most often there is only a single measurement  $z(\mathbf{u})$  with a finite number of sample points  $\mathbf{u}_i$ . In order to solve this problem certain assumptions are required. These assumptions are called the *hypothesis of stationarity*. The main idea behind them is that the considered set of sample data must demonstrate a spatial *homogeneity* within the study area  $A$ . In practice, all the pairs of measurements  $\{z(\mathbf{u}_\alpha), z(\mathbf{u}_\alpha + \mathbf{h}); \alpha = 1, \dots, n\}$ , recorded a vector  $\mathbf{h}$  apart within  $A$  are treated as repetitions. Effectively they are now the multiple realisations available to infer the probability law of the RF. This also implies that the pairs of RVs  $\{Z(\mathbf{u}_\alpha), Z(\mathbf{u}_\alpha + \mathbf{h}); \alpha = 1, \dots, n\}$  originate from the same two-point distribution. In more general terms, the RF  $Z(\mathbf{u})$  is defined to be stationary if any two vectors of  $N$  random variables  $\{Z(\mathbf{u}_1), \dots, Z(\mathbf{u}_N)\}$  and  $\{Z(\mathbf{u}_1 + \mathbf{h}), \dots, Z(\mathbf{u}_N + \mathbf{h})\}$  have the same multivariate cdf for any translation vector  $\mathbf{h}$ . In other words the multivariate cdf is said to be invariant under translation:

$$F(\mathbf{u}_1, \dots, \mathbf{u}_N; z_1, \dots, z_N) = F(\mathbf{u}_1 + \mathbf{h}, \dots, \mathbf{u}_N + \mathbf{h}; z_1, \dots, z_N) \quad \forall \mathbf{u}_1, \dots, \mathbf{u}_N \text{ and } \mathbf{h} \quad (2 - 5)$$

In practical applications geostatistical analyses do not go beyond the two-point cdf's and the first and second order moments, if they exist.

---

<sup>1</sup> Even if the measurements for the same location are repeated in time then the RF is defined in space and time and should be denoted  $Z(\mathbf{u}, t)$

$$F(\mathbf{u}, \mathbf{u}'; z, z') = \text{Prob}\{Z(\mathbf{u}) \leq z, Z(\mathbf{u}') \leq z'\} = E\{I(\mathbf{u}; z) \cdot I(\mathbf{u}'; z')\} \quad (2 - 6)$$

where

$$I(\mathbf{u}; z) = \begin{cases} 1 & \text{if } Z(\mathbf{u}) \leq z \\ 0 & \text{otherwise} \end{cases} \quad \forall z \quad (2 - 7)$$

The first moment is the mean (expected value)  $E\{Z(\mathbf{u})\}$  of the distribution denoted by:

$$E\{Z(\mathbf{u})\} = m(\mathbf{u}) \quad (2 - 8)$$

The second order moments considered here include:

- the covariance

$$C(\mathbf{u}, \mathbf{u}') = E\{Z(\mathbf{u}) \cdot Z(\mathbf{u}')\} - E\{Z(\mathbf{u})\} \cdot E\{Z(\mathbf{u}')\} \quad (2 - 9)$$

- the correlogram

$$\rho(\mathbf{u}, \mathbf{u}') = \frac{C(\mathbf{u}, \mathbf{u}')}{\sqrt{C(\mathbf{u}, \mathbf{u}) \cdot C(\mathbf{u}', \mathbf{u}')}} \quad (2 - 10)$$

- the variogram

$$2\gamma(\mathbf{u}, \mathbf{u}') = \text{Var}\{Z(\mathbf{u}) - Z(\mathbf{u}')\} \quad (2 - 11)$$

Each of the moments (2-8) to (2-11) listed above is location dependent.

However under the assumption of stationarity the location is no longer needed and can be replaced by the separation vector  $\mathbf{h}$ . Therefore we have:

- two point cdf

$$F(\mathbf{h}; z, z') = \text{Prob}\{Z(\mathbf{u}) \leq z, Z(\mathbf{u} + \mathbf{h}) \leq z'\}$$

- expected value

$$E\{Z(\mathbf{u})\} = m$$

- covariance

$$C(\mathbf{h}) = E\{Z(\mathbf{u}) \cdot Z(\mathbf{u} + \mathbf{h})\} - E\{Z(\mathbf{u})\} \cdot E\{Z(\mathbf{u} + \mathbf{h})\}$$

- correlogram

$$\rho(\mathbf{h}) = \frac{C(\mathbf{h})}{C(0)}$$

- variogram

$$2\gamma(\mathbf{h}) = \text{Var}\{Z(\mathbf{u}) - Z(\mathbf{u} + \mathbf{h})\} = E\{[Z(\mathbf{u}) - Z(\mathbf{u} + \mathbf{h})]^2\}$$

If the variogram function  $2\gamma(\mathbf{h})$  and the covariance function  $C(\mathbf{h})$  depend only on the distance  $|\mathbf{h}|$  then we say that they are *isotropic*. Whereas if  $2\gamma(\mathbf{h})$  and  $C(\mathbf{h})$  depend on both the distance and the direction of the separation vector  $\mathbf{h}$  then they are said to be *anisotropic*. There are two types of anisotropy: (i) *geometric anisotropy* – the range of directional semivariograms varies and the sill remains the same for every direction and (ii) *zonal anisotropy* – the sill changes with direction. Modelling anisotropy in two-dimensions is described in Goovaerts (1997, pp. 90-95) and in three-dimensions in Isaaks and Srivastava (1989, pp. 377-991).

In a situation where the expected value  $E\{Z(\mathbf{u})\}$  exists and is invariant within  $A$ , and the two-point covariance function  $C(\mathbf{h})$  exists and depends only on the separation vector  $\mathbf{h}$ , the RF model is said to be stationary of order two or second-order stationary. Under these circumstances the following relations hold:

$$\gamma(\mathbf{h}) = C(0) - C(\mathbf{h}) \quad (2 - 12)$$

$$\rho(\mathbf{h}) = 1 - \frac{\gamma(\mathbf{h})}{C(0)} \quad (2 - 13)$$

It is worth noting here that stationarity is not a property of the attribute under consideration. It is an assumption made by the user. In fact it cannot be verified or refuted from the data. Stationarity is a property of the RF model that is necessary for inference.

If the increments  $Z(\mathbf{u}) - Z(\mathbf{u}+\mathbf{h})$  are second-order stationary then the RF is said to be intrinsic stationary or to satisfy the intrinsic hypothesis. Second-order stationarity implies the intrinsic hypothesis but the converse is not true.

### 2.3 Semivariogram

In this chapter the mathematical background of one of the statistics, commonly used in geostatistical studies, is presented. This summary statistic is referred to as the *semivariogram*.

It was established in the previous section that the RF model is used in order to determine the statistical parameters of the population represented by the sample data set  $S_n$ . Using the sample measurements from  $S_n$  parameters of the RF are inferred. The parameter of interest is the semivariogram or more precisely the sample semivariogram denoted  $\hat{\gamma}(\mathbf{h})$ . The sample semivariogram is expressed by the following equation:

$$\hat{\gamma}(\mathbf{h}) = \frac{1}{2N(\mathbf{h})} \sum_{\alpha=1}^{N(\mathbf{h})} [z(\mathbf{u}_\alpha) - z(\mathbf{u}_\alpha + \mathbf{h})]^2 \quad (2 - 14)$$

where  $N(\mathbf{h})$  is the number of the sample pairs located vector  $\mathbf{h}$  apart. The semivariogram is sensitive to outliers and there are more robust measures available to help to produce a clearer description of the spatial continuity. One group of these is introduced under a general name of *relative semivariograms* (Isaaks and Srivastava, 1989). General relative semivariograms adjust each of the semivariograms  $\hat{\gamma}(\mathbf{h})$  by a function of

the mean  $f(\hat{m}(\mathbf{u}))$  of all the data values used to calculate  $\hat{\gamma}(\mathbf{h})$ . This relationship is expressed as follows:

$$\gamma_{GR}(\mathbf{h}) = \frac{\hat{\gamma}(\mathbf{h})}{f(\hat{m}(\mathbf{h}))} \quad (2 - 15)$$

where 
$$\hat{m}(\mathbf{h}) = \frac{1}{2N(\mathbf{h})} \sum_{\alpha=1}^{N(\mathbf{h})} [z(\mathbf{u}_{\alpha}) + z(\mathbf{u}_{\alpha} + \mathbf{h})] = \frac{m_{-\mathbf{h}} + m_{+\mathbf{h}}}{2} \quad (2 - 16)$$

The function  $f$  used in (2-15) is usually derived from a scatter diagram where on one axis there are local means and on the other axis local variances. If these values are linearly correlated with non-zero slope such a data set is said to exhibit *proportional effect*.

Another type of the relative semivariogram is called pairwise relative semivariogram  $\hat{\gamma}_{PR}(\mathbf{h})$  and is computed as follows:

$$\hat{\gamma}_{PR}(\mathbf{h}) = \frac{1}{2N(\mathbf{h})} \sum_{\alpha=1}^{N(\mathbf{h})} \frac{[z(\mathbf{u}_{\alpha}) - z(\mathbf{u}_{\alpha} + \mathbf{h})]^2}{\left[ \frac{z(\mathbf{u}_{\alpha}) + z(\mathbf{u}_{\alpha} + \mathbf{h})}{2} \right]^2} \quad (2 - 17)$$

This relative semivariogram (2-17) re-scales each of the sample pairs by their average value. Unlike the semivariogram given in (2-14) the relative semivariograms have denominators that serve as a scaling factor to minimise the influence of large values.



Computation of a sample semivariogram gives a set of values corresponding to the finite number of lags  $h$  and direction used during computation. To enable computation of the semivariogram for any lag and direction a continuous function is required. This function is fitted to the experimental values of the semivariogram, and the process is called a modelling of the semivariogram. Permissible semivariogram models need to be conditionally negative definite (Goovaerts, 1997, p. 88) and are usually taken as a linear combination of standard models  $g(h)$ . The standard models written in isotropic form, most often used include:

- Nugget effect model

$$g(h) = \begin{cases} 0 & \text{if } h = 0 \\ 1 & \text{otherwise} \end{cases} \quad (2 - 18)$$

- Spherical model with range  $a$

$$g(h) = \text{Sph}\left(\frac{h}{a}\right) = \begin{cases} \left(\frac{3}{2}\right) \cdot \frac{h}{a} - \left(\frac{1}{2}\right) \cdot \left(\frac{h}{a}\right)^3 & \text{if } h \leq a \\ 1 & \text{otherwise} \end{cases} \quad (2 - 19)$$

- Exponential model with practical range  $a$

$$g(h) = 1 - \exp\left(\frac{-3h}{a}\right) \quad (2 - 20)$$

- Gaussian model with practical range  $a$

$$g(h) = 1 - \exp\left(\frac{-3h^2}{a^2}\right) \quad (2 - 21)$$

- Power model

$$g(h) = h^\omega \quad \text{with } 0 < \omega < 2 \quad (2 - 22)$$

These are illustrated in Figure 2. 1. Another feature that is illustrated in

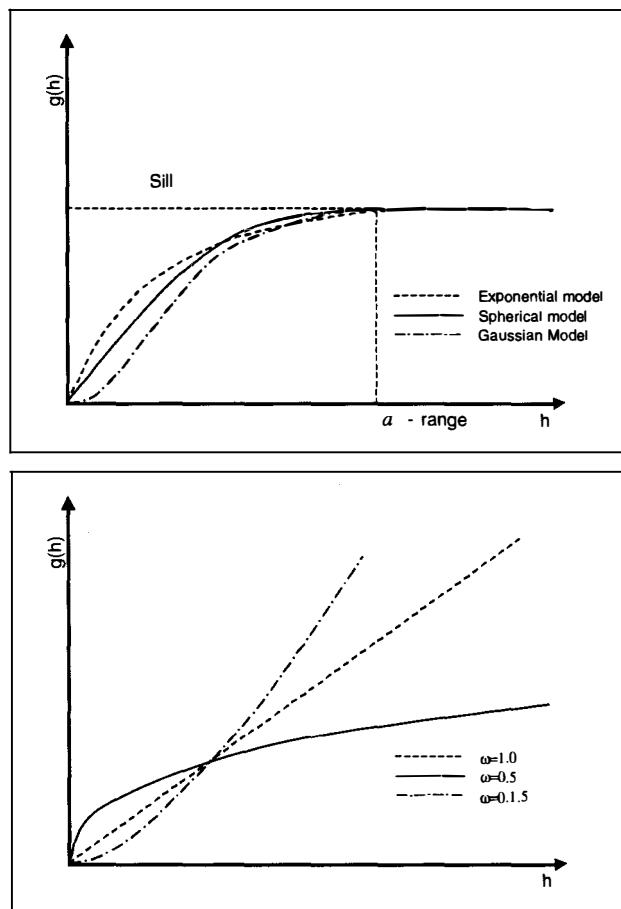


Figure 2. 1 Bounded semivariogram models (top graph) and power models (bottom graph) for different values of  $\omega$ .

the first four (bounded) models is the *sill*. For the nugget effect model the sill is reached as soon as  $h>0$ . The spherical model reaches its sill at

the range  $a$ , whereas the exponential and Gaussian models reach their sill at the practical range, defined as the distance at which the model value is 95% of the sill. In the cases presented here (2-18) to (2-21) the sills are equal to 1 since the models are standardised. The fifth model, that is the power model (2-22), does not have a sill.

Very often experimental semivariograms calculated in different directions exhibit different values for the range  $a$  and sill. We say that the spatial continuity of the attribute changes with the direction of the vector  $\mathbf{h}$  and not only with the distance  $h = |\mathbf{h}|$ . As earlier mentioned this type of behaviour is called anisotropy.

## 2.4 Kriging

Kriging is a term used for a group of algorithms that use a least-squares regression technique. Kriging is a best linear unbiased estimator (BLUE) method. The linear regression estimator, being a basis of kriging, can be expressed as follows:

$$Z^*(\mathbf{u}) - m(\mathbf{u}) = \sum_{\alpha=1}^{n(\mathbf{u})} \lambda_{\alpha}(\mathbf{u}) [Z(\mathbf{u}_{\alpha}) - m(\mathbf{u}_{\alpha})] \quad (2 - 23)$$

In (2-23)  $\mathbf{u}$  and  $\mathbf{u}_\alpha$  denote an unsampled location and a sampled point respectively. A sample value  $z(\mathbf{u}_\alpha)$  is a realisation of a RV  $Z(\mathbf{u}_\alpha)$  and  $\lambda_\alpha(\mathbf{u})$  is the weight assigned to a sample value  $z(\mathbf{u}_\alpha)$ . In this equation  $m(\mathbf{u})$  and  $m(\mathbf{u}_\alpha)$  are the expected values of two RV's  $Z(\mathbf{u})$  and  $Z(\mathbf{u}_\alpha)$  respectively.

*Simple kriging* (SK) assumes that  $m(\mathbf{u})$  is known constant within the study region A. Therefore the SK estimate can be expressed by the equation:

$$Z_{SK}^*(\mathbf{u}) = \sum_{\alpha=1}^{n(\mathbf{u})} \lambda_\alpha^{SK}(\mathbf{u}) [Z(\mathbf{u}_\alpha) - m] + m \quad (2 - 24)$$

During the estimation only the  $n(\mathbf{u})$  neighbouring data are retained and the  $n(\mathbf{u})$  kriging weights are derived so that the error variance  $\sigma_E^2(\mathbf{u})$  is minimised under the unbiasedness condition (2-26).

$$\sigma_E^2(\mathbf{u}) = \text{Var}\{Z_{SK}^*(\mathbf{u}) - Z(\mathbf{u})\} \quad (2 - 25)$$

$$E\{Z_{SK}^*(\mathbf{u}) - Z(\mathbf{u})\} = 0 \quad (2 - 26)$$

Where  $\mathbf{u}$  is the location of the RV being estimated and  $Z_{SK}^*(\mathbf{u})$  is the SK estimate. The SK minimum error variance is given by:

$$\sigma_{SK}^2(\mathbf{u}) = C(0) - \sum_{\alpha=1}^{n(\mathbf{u})} \lambda_\alpha^{SK}(\mathbf{u}) C(\mathbf{u}_\alpha - \mathbf{u}) \quad (2 - 27)$$

The SK weights can be written as:

$$\sum_{\beta=1}^{n(\mathbf{u})} \lambda_{\beta}^{SK}(\mathbf{u}) C(\mathbf{u}_{\alpha} - \mathbf{u}_{\beta}) = C(\mathbf{u}_{\alpha} - \mathbf{u}) \quad \alpha = 1, \dots, n(\mathbf{u}) \quad (2 - 28)$$

The assumption made on the mean for the SK may sometimes be difficult to satisfy. *Ordinary kriging* (OK) allows for variation of the local mean. The stationarity of the mean is limited only to a local neighbourhood. Therefore the estimator (2-23) can be written as:

$$Z^*(\mathbf{u}) = \sum_{\alpha=1}^{n(\mathbf{u})} \lambda_{\alpha}(\mathbf{u}) Z(\mathbf{u}_{\alpha}) + \left[ 1 - \sum_{\alpha=1}^{n(\mathbf{u})} \lambda_{\alpha}(\mathbf{u}) \right] m(\mathbf{u}) \quad (2 - 29)$$

Because the OK estimate is *unbiased* the weights  $\lambda_{\alpha}(\mathbf{u})$  have to add up to one. In effect the second term from the right hand side of (2-29) vanishes. The OK estimate can be then written as:

$$Z_{OK}^*(\mathbf{u}) = \sum_{\alpha=1}^{n(\mathbf{u})} \lambda_{\alpha}^{OK}(\mathbf{u}) Z(\mathbf{u}_{\alpha}) \quad \text{and} \quad \sum_{\alpha=1}^{n(\mathbf{u})} \lambda_{\alpha}^{OK}(\mathbf{u}) = 1 \quad (2 - 30)$$

The OK estimate  $Z_{OK}^*(\mathbf{u})$  is a linear combination of  $n(\mathbf{u})$  RV's  $Z(\mathbf{u}_{\alpha})$ .  $\lambda_{\alpha}^{OK}(\mathbf{u})$  are the OK weights whose estimation variance  $\sigma_{OK}^2(\mathbf{u})$  is minimum. The average error of the OK estimates is equal to zero under the unbiasedness condition:

$$E\{Z_{OK}^*(\mathbf{u}) - Z(\mathbf{u})\} = \sum_{\alpha=1}^{n(\mathbf{u})} \lambda_{\alpha}^{OK}(\mathbf{u}) m(\mathbf{u}) - m(\mathbf{u}) = m(\mathbf{u}) - m(\mathbf{u}) = 0 \quad (2 - 31)$$

The OK error variance can be written as

$$\sigma_{OK}^2(\mathbf{u}) = E\{[Z_{OK}^*(\mathbf{u}) - Z(\mathbf{u})]^2\} \quad (2 - 32)$$

As already mentioned the OK variance has to be minimised. To do this under the unbiasedness condition, i.e.  $\sum_{\alpha=1}^{n(\mathbf{u})} \lambda_{\alpha}^{OK}(\mathbf{u}) = 1$ , the Lagrange multiplier method is used (for detailed presentation see Goovaerts, 1997). The final result of this derivation is the OK system (2-33) with  $n+1$  linear equations in  $n+1$  unknowns, that is  $n$  data weights and the Lagrange parameter  $\mu_{OK}(\mathbf{u})$

$$\left\{ \begin{array}{l} \sum_{\beta=1}^{n(\mathbf{u})} \lambda_{\beta}^{OK}(\mathbf{u}) C(\mathbf{u}_{\alpha} - \mathbf{u}_{\beta}) + \mu_{OK}(\mathbf{u}) = C(\mathbf{u}_{\alpha} - \mathbf{u}) \quad \alpha = 1, \dots, n(\mathbf{u}) \\ \sum_{\beta=1}^{n(\mathbf{u})} \lambda_{\beta}^{OK}(\mathbf{u}) = 1 \end{array} \right. \quad (2 - 33)$$

The minimum OK variance then takes the following form:

$$\sigma_{OK}^2(\mathbf{u}) = C(0) - \sum_{\alpha=1}^{n(\mathbf{u})} \lambda_{\alpha}^{OK}(\mathbf{u}) C(\mathbf{u}_{\alpha} - \mathbf{u}) - \mu_{OK}(\mathbf{u}) \quad (2 - 34)$$

The OK system (2-33) is expressed in terms of covariances. On the other hand most of the geostatistical modelling of the variability of the study data is done in terms of the semivariogram. Taking into account the relation between the semivariogram and the covariance function (2-12) the OK system (2-33) can be re-written:

$$\left\{ \begin{array}{l} \sum_{\beta=1}^{n(\mathbf{u})} \lambda_{\beta}^{OK}(\mathbf{u}) [C(0) - \gamma(\mathbf{u}_{\alpha} - \mathbf{u}_{\beta})] + \mu_{OK}(\mathbf{u}) = C(0) - \gamma(\mathbf{u}_{\alpha} - \mathbf{u}) \quad \alpha = 1, \dots, n(\mathbf{u}) \\ \sum_{\beta=1}^{n(\mathbf{u})} \lambda_{\beta}^{OK}(\mathbf{u}) = 1 \end{array} \right. \quad (2 - 35)$$

The equation shown in (2-35) can be simplified considering the fact that

$\sum_{\beta=1}^{n(\mathbf{u})} \lambda_{\beta}^{OK}(\mathbf{u}) = 1$ . In its simpler form (2-35) is presented as:

$$\left\{ \begin{array}{l} \sum_{\beta=1}^{n(\mathbf{u})} \lambda_{\beta}^{OK}(\mathbf{u}) \gamma(\mathbf{u}_{\alpha} - \mathbf{u}) - \mu_{OK} = \gamma(\mathbf{u}_{\alpha} - \mathbf{u}) \quad \alpha = 1, \dots, n(\mathbf{u}) \\ \sum_{\beta=1}^{n(\mathbf{u})} \lambda_{\beta}^{OK}(\mathbf{u}) = 1 \end{array} \right. \quad (2 - 36)$$

There are a number of other variations of the kriging algorithm. They are not used in this study and so discussion of them is not given here. References can be found for example in Goovaerts (1997), Deutsch and Journel (1998), Journel and Huijbregts (1978) and Verly and Sullivan (1985).

## 2.5 Simulation

The following discussion is based on Goovaerts (1997) unless otherwise stated. Simulation is designed to reproduce the spatial variability of a data set. It aims to give the best reproduction of properties such as the histogram and the covariance of the model. However, as opposed to

estimation, it does not give the best estimate at unsampled locations. It does not concentrate on the local scale yet generates global representation of patterns of spatial continuity (Deutsch and Journel; 1998). As a result of simulation a map of realisations of  $z$ -values within the study region  $A$ , i.e.  $\{z^{(l)}(\mathbf{u}), \mathbf{u} \in A\}$ , is produced, where  $l$  denotes the  $l$ -th realisation at location  $\mathbf{u}$ . In conditional simulation data values are honoured at their locations; that is

$$z^{(l)}(\mathbf{u}) = z(\mathbf{u}_\alpha) \quad \forall \mathbf{u} = \mathbf{u}_\alpha, \quad \alpha = 1, \dots, n \quad (2 - 37)$$

Usually a large number of alternative realisations over the study area  $A$  is generated. This set of realisations models the *spatial uncertainty*. The joint probability of exceeding the value of a certain threshold at a given location  $\mathbf{u}_j$  can be numerically calculated. Each of the realisations represents a possible “picture” of the spatial distribution of the attribute under study. In effect for every point (or node) being simulated we have a distribution of possible values. Yet most practical applications call for only one value for a given location  $\mathbf{u}_j$ . Therefore often the results of simulation constitute input data for further post processing such as via a loss function as in the case presented by Glacken (1996).



A number of different simulation algorithms have been developed. In this work we shall examine in more detail *sequential Gaussian simulation* and *LU decomposition*. References to other algorithms can be found, for instance, in Goovaerts (1997) and in Deutsch and Journel (1998).

### 2.5.1 The multiGaussian approach

Both sequential Gaussian simulation and LU decomposition are performed under the assumption of the multivariate Gaussian random function model. Recall, to infer the cdf we need to know the spatial law of the RF (Section 2.2). More precisely, in the case of conditional simulation the cdf is conditioned to the  $(n)$  local data and is called *conditional cumulative distribution function* (ccdf) and is expressed by :

$$F(\mathbf{u}; z | (n)) = \text{Prob}\{Z(\mathbf{u}) \leq z | (n)\} \quad (2 - 38)$$

The fact that the Gaussian RF model is fully defined by the covariance function makes it extremely useful with respect to the inference of its ccdf. The properties characterising a multiGaussian RF model  $\{Y(\mathbf{u}), \mathbf{u} \in A\}$  with covariance function  $C_Y(\mathbf{h})$  are listed below (Goovaerts, 1997):

- All subsets of that RF are multivariate normal i.e.  $\{Y(\mathbf{u}), \mathbf{u} \in D \subset A\}$ ;

- The one-point cdf of any linear combination of RV components is normal, i.e.  $X = \sum_{\alpha=1}^n \lambda_{\alpha} Y(\mathbf{u}_{\alpha})$  is normal for any  $\lambda_{\alpha}$  and at any location  $\mathbf{u}_{\alpha} \in R$ ;
- The distribution of any pair of RV's  $Y(\mathbf{u})$  and  $Y(\mathbf{u} + \mathbf{h})$  is normal and fully defined by the covariance function  $C_Y(\mathbf{h})$ ;
- If two RV's are uncorrelated they are also independent, i.e. if  $\text{Cov}\{Y(\mathbf{u}), Y(\mathbf{u}')\} = 0$ , then  $Y(\mathbf{u})$  and  $Y(\mathbf{u}')$  are independent;
- All conditional distributions of any subset of the RV  $Y(\mathbf{u})$  are multivariate normal, given realisations of any other subset of  $Y(\mathbf{u})$ .

If we consider a single RV  $Y(\mathbf{u})$ , under the multiGaussian model, its conditional distribution is fully defined by its mean and variance, given  $n(\mathbf{u})$  data  $y(\mathbf{u}_{\alpha})$ . Further, the mean and variance of the cdf at location  $\mathbf{u}$  are identical to the simple kriging estimate  $y_{SK}^*(\mathbf{u})$  and simple kriging variance  $\sigma_{SK}^2(\mathbf{u})$  from  $n(\mathbf{u})$  data  $y(\mathbf{u}_{\alpha})$ . The cdf can then be expressed as:

$$[G(\mathbf{u}; y | (n))]_{SK}^* = G\left(\frac{y - y_{SK}^*(\mathbf{u})}{\sigma_{SK}(\mathbf{u})}\right) \quad (2 - 39)$$

where  $G(\cdot)$  is the standard normal cdf (Abramovitz and Stegun, 1972, p.932) and

$$y_{SK}^*(\mathbf{u}) = m(\mathbf{u}) + \sum_{\alpha=1}^{n(\mathbf{u})} \lambda_{\alpha}^{SK}(\mathbf{u}) [y(\mathbf{u}_{\alpha}) - m(\mathbf{u}_{\alpha})] \quad (2 - 40)$$

$$\sigma_{SK}^2(\mathbf{u}) = C_R(0) - \sum_{\alpha=1}^{n(\mathbf{u})} \lambda_{\alpha}^{SK}(\mathbf{u}) C_R(\mathbf{u}_{\alpha} - \mathbf{u}) \quad (2 - 41)$$

The weights  $\lambda_{\alpha}^{SK}(\mathbf{u})$  are given by (2-28). The RV's  $Y(\mathbf{u}_{\alpha})$  and  $Y(\mathbf{u})$  do not have to be identical therefore the RF  $\{Y(\mathbf{u}), \mathbf{u} \in A\}$  does not have to be stationary. As it turns out, it is enough to solve the SK system, at a given location  $\mathbf{u}$ , to infer the ccdf, under multiGaussian RF model. To be able to take advantage of the model it has to be assumed that the study data satisfy the multiGaussian assumption. Yet, in reality, it would be very difficult, if not impossible, to find a variable, such as the grade, in any of the earth sciences with perfect multiGaussian distribution. Therefore the distribution of the variable has to be transformed into normal space prior to the simulation being performed. This transformation involves the steps presented below.

Firstly, the original  $z$  data are transformed to  $y$  values which have a standard normal histogram. This procedure is referred to as a *normal score transform* and the  $y$  values  $y(\mathbf{u}_{\alpha}) = \phi(z(\mathbf{u}_{\alpha}))$  are called normal scores. Secondly, the multiGaussian model is applied to the normal scores. This enables us to derive the Gaussian conditional cdf at any unsampled location  $\mathbf{u}$ , such as:

$$G(\mathbf{u}; y | (n)) = \text{Pr ob}\{Y(\mathbf{u}) \leq y | (n)\}$$

With respect to the last equation there is another requirement which has to be satisfied that is the two-point cdf of  $Y(\mathbf{u})$  should also be normal see (Goovaerts, 1997, pp. 271-275) and (Deutsch and Journel, 1998, pp.142-144).

In the third step the conditional cdf of the original variable is retrieved

$$\begin{aligned} F(\mathbf{u}; z | (n)) &= \text{Pr ob}\{Z(\mathbf{u}) \leq z | (n)\} \\ &= \text{Pr ob}\{Y(\mathbf{u}) \leq \phi(z) | (n)\} \\ &= G(\mathbf{u}; \phi(z) | (n)) \end{aligned}$$

$\phi(\cdot)$  is the normal transform function and is monotonic increasing.

If all the assumptions are satisfied and the multiGaussian RF model holds for the normal score variable  $y$ , then the simulation with the sequential paradigm can proceed.

### 2.5.2 Sequential Gaussian simulation

The sequential simulation paradigm is based on Bayes' axiom (Goovaerts, 1997 pp.376-377) by which any two-point ccdf can be expressed as a product of two one-point ccdf's:

$$F(\mathbf{u}'_1, \mathbf{u}'_2; z_1, z_2 | (n)) = F(\mathbf{u}'_2; z_2 | (n+1)) \cdot F(\mathbf{u}'_1; z_1 | (n)) \quad (2 - 42)$$

It is possible to decompose the  $N$ -point conditional cdf  $F(\mathbf{u}'_1, \dots, \mathbf{u}'_N; z_1, \dots, z_N | (n))$  so that it can be expressed as a product of  $N$  one-point conditional cdf's based on Bayes' theorem. The sequential simulation proceeds in the following steps:

- At the first location  $\mathbf{u}'_1$  the cdf is modelled conditional to the  $n$  existing data  $z(\mathbf{u}_\alpha)$ , i.e.  $F(\mathbf{u}'_1; z | (n)) = \text{Prob}\{Z(\mathbf{u}'_1) \leq z | (n)\}$ ;
- From the modelled cdf a realisation is drawn  $z^{(1)}(\mathbf{u}'_1)$ . This realisation becomes a conditioning datum for all further drawings;
- The two steps are repeated until all  $N$  nodes are simulated.

As a result of this process a set of values  $\{z^{(j)}(\mathbf{u}'_j), j = 1, \dots, N\}$ , referred to as realisation of the RF  $\{Z(\mathbf{u}), \mathbf{u} \in R\}$  is obtained.

If the multiGaussian RF model is used with the sequential paradigm then this type of simulation is called *sequential Gaussian simulation*. The algorithm of sequential Gaussian simulation of a continuous attribute  $z$  will be considered. The area over which the simulation is done has to be gridded and the calculation is performed at the grid nodes. The grid does not need to be regular. The variable is conditioned to the data values  $\{z(\mathbf{u}_\alpha), \alpha = 1, \dots, n\}$ . We assume that  $z$ -data were transformed to the normal

score  $y$ -data and that the multiGaussian RF model is retained. Following Goovaerts (1997) this process can be presented in the subsequent phases:

- For each realisation define a random path to visit all grid nodes only once;
- For each node  $\mathbf{u}'$  estimate the mean and the variance of the Gaussian ccdf,  $G(\mathbf{u}'; y | (n))$  by carrying out simple kriging. The semivariogram model of the normal score data  $\gamma_Y(h)$  should be used. Here  $(n)$  denotes the conditioning information, i.e. the number  $n(\mathbf{u}')$  of normal score data  $y(\mathbf{u}_\alpha)$  and values  $y^{(l)}(\mathbf{u}'_j)$  previously simulated from the neighbourhood that should be used during simple kriging;
- Draw a simulated value  $y^{(l)}(\mathbf{u}'_j)$  from this ccdf and add it to the simulated data set;
- Continue to the next grid node according to the random path and repeat the last two phases;
- Iterate until all nodes are simulated;
- Back-transform the simulated normal scores  $\{y^{(l)}(\mathbf{u}'_j), j = 1, \dots, N\}$  where  $N$  is the number of nodes, into simulated values for the original variable

$$z^{(l)}(\mathbf{u}'_j) = \phi^{-1}(y^{(l)}(\mathbf{u}'_j)) \quad j=1, \dots, N$$

$\phi^{-1}(\cdot) = F^{-1}(G(\cdot))$ , where  $F^{-1}(\cdot)$  is the inverse cdf of the variable  $Z$  and  $G(\cdot)$  the standard Gaussian cdf. The number of realisations can be arbitrary. This means that other realisations are obtained by repeating the steps outlined above beginning with the step where the random path is defined.

### 2.5.3 The LU decomposition algorithm

This is another example of a simulation technique that relies on the multiGaussian RF model. The simulation is realised by decomposition of the covariance matrix. This method is usually used when simulating a small number  $N$  of points with sparse conditioning data (Goovaerts, 1997). Since the decomposition algorithm is performed in the normal space therefore the original  $z$ -data is first transformed into normal score  $y$ -data. The simulation is conditioned to the sample data set  $\{z(\mathbf{u}_\alpha), \alpha = 1, \dots, n\}$  and we have  $N$  grid nodes with location  $\mathbf{u}'_j$ . The subsequent steps of the LU decomposition algorithm are as follows:

- The covariance matrix  $\mathbf{C}$  is constructed between all  $(n + N)$  sample points and simulated grid nodes:

$$\mathbf{C} = \begin{bmatrix} \mathbf{C}_{11} & \mathbf{C}_{12} \\ \mathbf{C}_{21} & \mathbf{C}_{22} \end{bmatrix} = \begin{bmatrix} [C_Y(\mathbf{u}_\alpha - \mathbf{u}_\beta)] & [C_Y(\mathbf{u}_\alpha - \mathbf{u}'_j)] \\ [C_Y(\mathbf{u}'_i - \mathbf{u}_\beta)] & [C_Y(\mathbf{u}'_i - \mathbf{u}'_j)] \end{bmatrix}$$

where  $C_Y(\mathbf{h})$  is the covariance function of the standard normal RF  $Y(\mathbf{u})$  and  $\mathbf{C}_{11}$ ,  $\mathbf{C}_{22}$ , and  $\mathbf{C}_{12} = \mathbf{C}_{21}^T$  are the  $n \times n$  sample-to-sample covariance matrix, the  $N \times N$  node-to-node covariance matrix and the data-to-node covariance matrix, respectively.

- The matrix  $\mathbf{C}$  is then decomposed and written as a product of a lower and an upper triangle matrix, such as:

$$\mathbf{C} = \mathbf{L} \cdot \mathbf{U} = \begin{bmatrix} \mathbf{L}_{11} & \mathbf{0} \\ \mathbf{L}_{21} & \mathbf{L}_{22} \end{bmatrix} \cdot \begin{bmatrix} \mathbf{U}_{11} & \mathbf{U}_{12} \\ \mathbf{0} & \mathbf{U}_{22} \end{bmatrix}$$

- A realisation  $\{y^{(l)}(\mathbf{u}'_j), j = 1, \dots, N\}$ , conditioned to the neighbouring sample data, is derived as the following linear combination:

$$\mathbf{y}^{(l)} = [y^{(l)}(\mathbf{u}'_j)] = \mathbf{L}_{21} \cdot \mathbf{L}_{11}^{-1} \cdot \mathbf{y}_\alpha + \mathbf{L}_{22} \cdot \boldsymbol{\omega}^{(l)} \quad (2 - 43)$$

In (2-43)  $\mathbf{y}_\alpha$  is the vector of the  $n$  conditioning data and  $\boldsymbol{\omega}^{(l)}$  is the vector of  $N$  standard normal deviates.

- The last step involves the back-transform of the simulated normal scores to the simulated original values  $\{z^{(l)}(\mathbf{u}'_j) = \phi^{-1}(y^{(l)}(\mathbf{u}'_j)), j = 1, \dots, N\}$ .

Subsequent realisations are generated by multiplying of  $\boldsymbol{\omega}^{(l')}, l' \neq l$  by the matrix  $\mathbf{L}_{22}$  from (2-43). This allows the generation of a large number of realisations in a short computation time.



As one would expect, the results of simulation, both sequential Gaussian and LU decomposition, may contain values that are higher than the largest original sample value and others that are lower than the smallest sample value. Therefore to back-transform from the simulated normal scores to the original attribute data it is necessary to model the sample distribution beyond the smallest  $z$ -data value  $z_1$  (*lower tail*) and above the largest  $z_k$  (*upper tail*). Three different models are suggested (Deutsch and Journel, 1998), (Goovaerts, 1997) for extrapolation. The models include:

- *Power cdf model* for the lower tail

$$[F(z)]_{Pow.} = \left[ \frac{z - z_{\min}}{z_1 - z_{\min}} \right]^{\omega} \cdot F^*(z_1) \quad \forall z \in (z_{\min}, z_1] \quad (2 - 44)$$

where  $\omega > 1$ ,  $z_1$  is the smallest  $z$ -data value,  $z_{\min}$  is the chosen minimum  $z$ -value. If  $\omega = 1$  than we have a particular case of (2-44) which is the *linear model*. Distributions with  $\omega > 1$  are negatively skewed and with  $\omega < 1$  are positively skewed.

- *Power cdf model* for the upper tail

$$[F(z)]_{Pow} = F^*(z_k) + \left[ \frac{z - z_k}{z_{\max} - z_k} \right]^{\omega} \cdot [1 - F^*(z_k)] \quad \forall z \in (z_k, z_{\max}] \quad (2 - 45)$$

where  $\omega < 1$ ,  $z_K$  is the largest  $z$ -data value and  $z_{\max}$  is the maximum data value chosen by the user.

- *Hyperbolic cdf model* for the upper tail

$$[F(z)]_{Hyp.} = 1 - \frac{\lambda}{z^\omega} \quad \forall z > z_K \quad (2 - 46)$$

$$\text{and } \lambda = z_K^\omega \cdot [1 - F^*(z_K)], \quad \omega \geq 1$$

The magnitude of  $\omega$  affects the tail being extrapolated, that is the larger the value of  $\omega$  the shorter the tail. A suggested value of  $\omega = 1.5$  gives good results in most cases.

### 3. CHANGE OF SUPPORT AND VOLUME - VARIANCE RELATIONSHIP

In the discussion so far the data values  $z(\mathbf{u}_\alpha)$  were treated as point samples. In reality, however, the variable of interest (for instance grade of a gold deposit) represents a particular volume or sometimes a surface. This can be the volume of a drill sample  $v(\mathbf{u}_\alpha)$  or the volume  $V$  of a block in a mining block model. This value is called the *support* of the variable of interest. There is a relation, discussed later in this chapter, between the support of data and the distribution of their values. Intuitively, data with smaller support, e.g. the grade of drill samples, will have a larger variance than data with a larger support, e.g. the grade of blocks (often containing hundreds of tonnes of rock each) from a block model.

Let us consider the same property of a gold deposit, that is the grade, but with different supports, i.e. different size samples arising from distinct drilling types. In effect, we have two different variables because the volumes/supports they exhibit are not equal. That also implies individual statistical characteristics. The question is whether these two variables are related in any way, and whether two variables with different supports

can be related. Also of interest is the problem of modelling the distribution of one of the variables knowing, or having estimated, the distribution of the other one. In our case where we wish to determine the distribution of the SMU (block) knowing the distribution of the exploration data, because in practice, when mining commences, one will rely on the SMU to calculate the recoverable reserves.

From the statistical point of view, a variable with smaller support, sample values in our case, is more *dispersed* than a variable with larger support, in our example SMU. However, the global mean, at the zero cut-off, of the point distribution is not affected by change of support. Samples are most often considered as point samples since the volume  $v(u_\alpha)$  they represent is very small compared to the larger SMU volumes whose average we are trying to estimate.

The *support effect* has a practical impact on mining. Estimating recoverable reserves, at the given cut-off grade, based on the point support grade–tonnage curve may be biased if actual mining uses an SMU with much larger volume. In general, at a given cut-off, as the size of the SMU increases, the average grade of ore decreases. For cut-off grades below the average grade of a deposit, increasing the volume of

the SMU often results in an increase in the estimated tonnage of ore. For cut-off grades above the average grade, larger SMU usually results in a decrease in the estimated tonnage of ore (Isaaks and Srivastava, 1989). In particular, if a selection of blocks as waste or ore, based on a given cut-off grade, is made on the basis of exploration drill samples then there is the possibility of overestimating the percentage of blocks above the cut-off grade. This equates to overestimating the tonnages above the cut-off grade. Now, depending on the magnitude of the error this can have very serious, sometimes even disastrous, financial implications for a mining project.

Increase in support reduces the spread of the data as illustrated in Figure 3. 1. By increasing the support the values of the variable are averaged over increasing volume. To illustrate this we can imagine a situation where the whole model contains only one block, which covers the whole study area *A*. In such a hypothetical situation the frequency distribution of the variable would become a spike with the value equal to the value of the mean of the considered deposit. Summarising, we can say that the larger the support the smaller the variance.

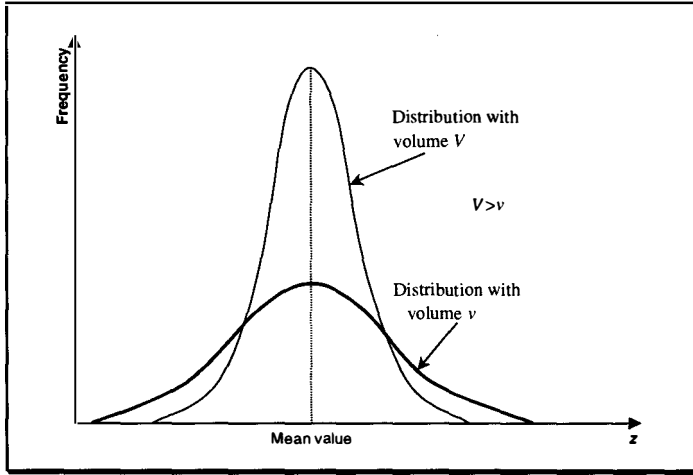


Figure 3. 1 Example of the frequency distributions of data with volume  $V$  and  $v$ , where  $V > v$

Denote by  $V(\mathbf{u})$  an SMU of volume  $V$  centered on location  $\mathbf{u}$ . Suppose that  $V(\mathbf{u})$  is divided into  $N$  production units  $v(\mathbf{u}_\alpha)$ , centred on location  $\mathbf{u}_\alpha$  and having volume  $v$ . Then the mean value (grade) of  $Z$  over the volume  $v(\mathbf{u}_\alpha)$  is given by

$$z_v(\mathbf{u}_\alpha) = \frac{1}{v} \int_{v(\mathbf{u}_\alpha)} z(\mathbf{u}) d\mathbf{u}$$

and mean value (grade) on  $V(\mathbf{u})$  is given by

$$z_v(\mathbf{u}) = \frac{1}{V} \int_{V(\mathbf{u})} z(\mathbf{u}) d\mathbf{u} = \frac{1}{N} \sum_{\alpha=1}^N z_v(\mathbf{u}_\alpha)$$

The *dispersion* of the  $N$  grades  $z_v(\mathbf{u}_\alpha)$  about their mean value  $z_v(\mathbf{u})$  can be described by the mean square deviation (Journel and Huijbregts, 1978):

$$s^2(\mathbf{u}) = \frac{1}{N} \sum_{\alpha=1}^N [z_v(\mathbf{u}) - z_v(\mathbf{u}_\alpha)]^2 \quad (3 - 1)$$

If we consider each of the components of (3-1) as realisations of RV's then this equation can be re-written as:

$$S^2(\mathbf{u}) = \frac{1}{N} \sum_{\alpha} [Z_v(\mathbf{u}) - Z_v(\mathbf{u}_{\alpha})]^2 \quad (3 - 2)$$

The *dispersion variance* of the RV  $S^2(\mathbf{u})$  is the expectation of this variable, assuming the hypothesis of stationarity (Section 2.2). The dispersion variance of smaller volume (support)  $v$  within larger volume (support)  $V$  is defined by

$$D^2(v/V) = E\{S^2(\mathbf{u})\} = E\left\{\frac{1}{N} \sum_{\alpha} [Z_v(\mathbf{u}) - Z_v(\mathbf{u}_{\alpha})]^2\right\} \quad (3 - 3)$$

In more general terms the variance of dispersion  $D^2(v/V)$  can be also expressed as the mean value over  $V(\mathbf{u})$  of the estimation variance  $\sigma_E$  of grade  $Z_v(\mathbf{u})$  (e.g. grade of SMU) by grade  $Z(\mathbf{u}_{\alpha})$  (grade of samples) with volume  $v(\mathbf{u}_{\alpha})$  within  $V(\mathbf{u})$  (for more details see Journel and Huijbregts, 1978):

$$\begin{aligned} D^2(v/V) &= \frac{1}{V} \int_{v(\mathbf{u})} E\{[Z_v(\mathbf{u}) - Z_v(\mathbf{u}_{\alpha})]^2\} d\mathbf{u}_{\alpha} \\ &= \frac{1}{V} \int_{v(\mathbf{u})} \sigma_E^2(V(\mathbf{u}), v(\mathbf{u}_{\alpha})) d\mathbf{u}_{\alpha} \quad v \ll V \end{aligned} \quad (3 - 4)$$

In (3-4)  $V$  is significantly larger than  $v$ , as in case of drill sample data and, for instance, SMU blocks. In practical applications the dispersion

variance can be calculated from (3-1). In this case  $z_v(\mathbf{u}) = \bar{z} = \frac{1}{n} \sum_{\alpha} z_v(\mathbf{u}_{\alpha})$ ,

where  $n$  is the number of grade samples and  $n \leq N$ . The equation (3-1)

has now the form

$$s_n^2 = \frac{1}{n} \sum_{\alpha=1}^n [\bar{z} - z_v(\mathbf{u}_{\alpha})]^2 \quad (3 - 5)$$

The equation (3-4) can also be written in terms of semivariograms:

$$D^2(v/V) = \bar{\gamma}(V, V) - \bar{\gamma}(v, v) \quad (3 - 6)$$

and this form is often used for computation of the dispersion variance.

Another relationship involving the dispersion variance is the volume variance relationship, which was derived experimentally by D.G. Krige is frequently referred to as “Krige’s relation”:

$$D^2(v/A) = D^2(v/V) + D^2(V/A) \quad (3 - 7)$$

where  $v \leq V \leq A$ , with  $A$  here denoting the measure of the volume of the deposit.

Equation (3-7) illustrates quite well the way the different supports affect the variability. Using it we can calculate by how much the total variance  $D^2(v/A)$  needs to be reduced to more accurately reflect the variance between blocks  $D^2(V/A)$ . The *variance adjustment factor*  $f_v$  is defined as



the ratio of the block variance to the point variance (Isaaks and Srivastava, 1989):

$$f_v = \frac{D^2(V/A)}{D^2(v/A)} = \frac{D^2(v/A) - D^2(v/V)}{D^2(v/A)} = 1 - \frac{D^2(v/V)}{D^2(v/A)} \quad (3 - 8)$$

From the discussion presented above it can be seen that a change in the support may have significant effect on the results of mineral resource estimation. Hence, there is a definite need for an effective way of dealing with this issue. In the current geostatistical literature several methods of correcting for the change of support are proposed. Some of these are examined in detail in the following chapter.

## 4. CORRECTION FOR THE SUPPORT EFFECT

### 4.1 Overview

Firstly a brief insight into research on the correction for the change of support is given. Subsequently, different correction methods are presented.

Since the theory of regionalised variables was developed by G. Matheron (1971) the volume – variance relationship and the change of support problem have been well recognised within the field of geostatistics. One of the first studies that demonstrated the significance of accounting for the change of support during mineral resource estimation was that of M. David (1977). The theoretical foundations for the most commonly used methods of change of support correction were devised and presented by Journel and Huijbregts (1978). These formed the basis for several ways to correct the point variance into the block variance, eg. *affine correction*, *indirect lognormal correction* (Isaaks and Srivastava, 1989), *discrete Gaussian correction* (Journel and Huijbregts, 1978). Each of these assumes a certain type of underlying distribution. The models are typically applied to the “global” distribution (derived from all available data), yet in practice mineral resources need to be estimated on a local

scale. Rossi and Parker, (1993) presented a case study to test the most commonly used correction techniques, affine correction, indirect lognormal and Gaussian method. In the conclusion the authors suggest their own approach for handling the change of support. This involves kriging and conditional simulation in order to derive the support correction factor on a global and local scale.

There are a number of publications investigating the theory as well as the limitations of the topic (David, 1972; Huijbregts, 1976; Journel, 1985). In these cases special attention is given to the grade-tonnage relationships. Properly used, the volume-variance relationship may be employed for production planning. It also helps to compute fluctuation in grade over different periods of time (Parker, 1980). Resolving the optimal mining as well as the milling method depends strongly on estimated ore body characteristics – grade, tonnage, and variability. Hence, the accuracy of the estimates is critical (Parker, 1980; Recny, 1978).

There is also a method known as *lognormal short cut*, developed by David (1972, 1977). However, it was developed mainly for a porphyry copper-type deposit and may produce biased results in some other cases,

eg. gold deposits, following Rossi and Parker (1993). Those authors also refer to Sullivan and Verly (1983) whose results demonstrate biased estimates, in case of a gold deposit, produced by the lognormal short cut.

A number of papers regarding change of support was collected and published by Dimitrakopoulos (1994). Various techniques are discussed, along with case studies, also including use of conditional simulation. Literature that relates to the different methods of conditional simulation and the volume – variance relationship is well developed. References can be found in many sources, eg. (Goovaerts, 1997; Deutsch & Journel, 1998; Dagdelen et al, 1997)

Summarising, the volume – variance relationship and the problem of accurate prediction of mineral resources, hence accounting for the change of support, has received a great deal of attention in the geostatistical literature. There have been many methods developed to help in solving this problem. In general, they can be classified into two groups:

- Direct methods: recoverable reserves are estimated directly from the data available (eg. Disjunctive Kriging (Matheron, 1975b), Probability Kriging, MultiGaussian Kriging)

- Indirect methods: recoverable reserves are estimated by applying one of the correction methods to build a block grade model.

Each of these approaches has its own advantages and disadvantages. The following sections present methods deemed to be the most commonly used in practice.

## 4.2 Affine correction

Possibly the most frequently used procedure for correcting for the support effect is the *affine correction*. The affine correction transforms values (in this case quantiles  $q_z$ ) of one distribution into values (or quantiles  $q_y$ ) of another distribution (Isaaks and Srivastava, 1989; Journel and Huijbregts, 1978) and it is described by the following equation:

$$q_y = \sqrt{f_v} * (q_z - m) + m \quad (4 - 2)$$

where  $m$  is the common stationary mean of both distributions and the factor  $f_v$  is the variance correction factor defined by (3-8). Equation (4-2) is illustrated in Figure 4.1.

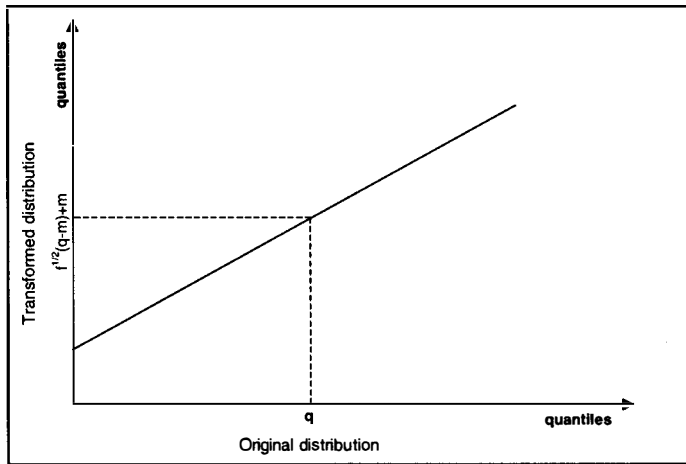


Figure 4.1 Affine correction transformation

According to the geostatistical literature (e.g. Isaaks and Srivastava, 1989; Rossi and Parker, 1993) the value of the correction factor  $f_v$  should fall between 0.7 – 0.8 for the affine correction method to be effective. With a reduction in variance above 30% (moving from smaller support  $v$  to larger support  $V$ ) a symmetrisation of the distribution may occur. Therefore the adjustment factor should not be smaller than 0.7. Too low a value of the factor may also produce a minimum value of the transformed distribution which is not realistic. The value of  $f_v$  can be also estimated as the ratio of the arithmetic variance  $\sigma_z^2$  of the original variable, say  $Z$ , and the variance  $\sigma_y^2$  of the variable  $Y$  whose distribution is being estimated. The support of  $Z$  is  $v$  and the support of  $Y$  is  $V$ , with  $v < V$ . Therefore we have:

$$f_v = \frac{\sigma_y^2}{\sigma_z^2} \quad (4 - 3)$$

This correction method is based on the assumption that the shape and the mean of the distribution do not change. Only the variance changes. Effectively, the variance of the original variable  $Z$  can be shrunk around the mean that is common and known, to obtain the distribution of other variable  $Y$ , usually of the SMU. The method is not difficult to apply and that is its main advantage. In practice the affine correction technique gives results very similar to those obtained from the *indirect lognormal correction* (Journel and Huijbregts, 1978) discussed in the next section.

### 4.3 Indirect lognormal correction and discrete Gaussian transformation

These two methods, i.e. *indirect lognormal correction* and the *discrete Gaussian transformation* are not used in our study and so will not be discussed in great detail in this thesis.

The Indirect Lognormal Correction is given by the following exponential equation:

$$q_Y = a q_Z^b \quad (4 - 4)$$

where:

$$a = \frac{m}{\sqrt{f_v * CV^2 + 1}} \left[ \frac{\sqrt{CV^2 + 1}}{m} \right]^2$$

and

$$b = \sqrt{\frac{\ln(f_v * CV^2 + 1)}{\ln(CV^2 + 1)}}$$

(Isaaks and Srivastava, 1989 pp. 472-476)

As before,  $m$  is the mean and  $f_v$  is the variance correction factor. The coefficient of variation is denoted by  $CV$  and is defined as the ratio of the standard deviation to the mean. References on this method can be also found in Journel and Huijbregts (1978).

The *discrete Gaussian transformation* is a more sophisticated method than the two discussed so far. It was developed by G. Matheron (1975a) and it involves a transformation of the original variable  $Z$  into the Gaussian distribution by means of Hermite polynomials. The mean and the variance of the transformed distribution are then determined. Based on the results the variance correction factor is obtained. Then the Gaussian histogram is back-transformed. The mean is preserved while the variance has been reduced. This is a very brief description of the method. References can be found in Journel and Huijbregts (1978). The discrete Gaussian method is considered more robust by some authors (Rossi and Parker, 1993), than the other methods discussed. Nevertheless it has not been widely used in practice due to its high level of complexity.



#### **4.4 Change of support by conditional simulation.**

*Change of support by conditional simulation* is one of the two relatively new correction methods of support changes chosen for this study. This method was detailed by Glacken (1996) who gave an example of its use as a tool for recoverable reserve estimation at different supports. Two simulation algorithms are suggested as the best suited for the purpose of correction the changes in the support of data. The algorithms include:

- The LU simulation (Section 2.5.3); and
- Sequential Gaussian simulation for blocks (Section 2.5.2).

The LU decomposition algorithm is limited to local change of support and is suggested as better suited for grade control purposes. The covariance between simulated block values is not reproduced since they are treated as separate entities. For the global change of support sequential Gaussian simulation is proposed. This simulation takes into consideration the relation between the simulated block values i.e. the covariance between blocks. This global approach enables reproduction of the recoverable reserves for a given support, which is what we would like to achieve in the study. Therefore the sequential Gaussian simulation method will be used for the purpose of this research. We also intend to compare the results of applying different change of support correction

methods in terms of the grade tonnage curves. These curves can be derived from resource estimates.

A brief summary of the change of support by use of conditional simulation is given here. For full details see Glacken (1996). The correction for the support change is accomplished directly during the conditional simulation and there is no need for the separate correction factor used by other methods. The main idea is to simulate the values of the variable at the discretised volume of a block. Then, if the variable averages linearly, those values can be averaged to calculate the value of the block at the desired support. In practice, nearly any simulation algorithm may be adopted for this purpose, however LU decomposition and sequential Gaussian simulation are the two methods proposed. Averaging the point values over many realisations produces a probability distribution of the values (i.e. grades) for each block simulated. This models the uncertainty at unsampled locations. In most cases we are interested in a single value per block to be returned. Yet having the distribution of the grade for each block gives the flexibility of applying different criteria (including economic) to determine the “optimal” grade. Use of the theory of profit and loss functions is suggested. The general assumption behind the definition of the function is that selection of any

value except for the true value, which is unknown, will incur a loss. It is possible to determine the value which minimises the expected loss for any given simulated probability distribution.

This method may have very practical application possibilities for mining operations. It allows the incorporation of economic parameters for a grade control during block selection, as well. The traditional block selection procedure, which uses a deterministic cut-off grade, is replaced with a probabilistic approach. The probability of the block exceeding the cut-off grade is compared with a “threshold probability”. If the probability is higher than the threshold probability then the block is selected, otherwise it is rejected. This threshold takes into account the uncertainty about the grade and economic parameters. What is even more interesting, the method does not require a grade estimate because it works in the probability space. A case study is given by Glacken (1997).

#### **4.5 Nearest neighbour kriging**

*Nearest neighbour kriging*, (NNK) is the second new method used in this study for correction for the support effect of the data. This method was developed by Arik (1998) and is a modification of ordinary kriging (OK)

designed especially to deal with skewed distributions when estimating recoverable reserves. It also accommodates the variance correction factor. Hence it honours the change of support effect. The NNK estimator  $Z_{NNK}^*$  is similar to the OK estimator  $Z_{OK}^*$  (2-30) and can be written as follows:

$$Z_{NNK}^*(\mathbf{u}) = \sum_{\alpha=1}^{n(\mathbf{u})} \lambda_{\alpha}^{NNK}(\mathbf{u})Z(\mathbf{u}_{\alpha}) \quad \text{and} \quad \sum_{\alpha=1}^{n(\mathbf{u})} \lambda_{\alpha}^{NNK}(\mathbf{u}) = 1 \quad (4 - 5)$$

where  $\lambda_{\alpha}^{NNK}(\mathbf{u})$  are the NNK weights. The NNK estimation variance can be derived as in (2-32). The NNK estimator  $Z_{NNK}^*(\mathbf{u})$  is a linear combination of  $n(\mathbf{u})$  RV's  $Z(\mathbf{u}_{\alpha})$ . In general, more weight is given to the nearest neighbour sample value than to the other values. The weights are increased or decreased by a certain proportion, so that the sum of the weights is one in order to satisfy the general unbiasedness condition of the kriging technique. The proportion used to obtain NNK weights is called the *smoothing correction factor*. The suggested value for the factor is the square root of the ratio of the SMU block variance  $\sigma_b^2$  to the sample variance  $\hat{\sigma}_p^2$  (Arik, 1998).

$$f = \sqrt{\frac{\sigma_b^2}{\hat{\sigma}_p^2}} \quad (4 - 6)$$

This is the correction factor  $f$  which accounts for the changes in the variance moving from smaller support to larger support. Adjustment of the ordinary kriging (OK) weights  $\lambda_{\alpha}^{OK}(\mathbf{u})$  to determine the NNK weight  $\lambda_{\alpha}^{NNK}(\mathbf{u})$  can be carried out as follows:

$$\lambda_{\alpha}^{NNK}(\mathbf{u}) = \lambda_{\alpha}^{OK}(\mathbf{u}) + (1 - \lambda_{\alpha}^{OK}(\mathbf{u})) \cdot f \quad \text{for the nearest sample} \quad (4 - 7)$$

$$\lambda_{\alpha}^{NNK}(\mathbf{u}) = \lambda_{\alpha}^{OK}(\mathbf{u}) \cdot (1 - f) \quad \text{for all other samples} \quad (4 - 8)$$

Although the standard approach with NNK would be simply to consider the nearest sample, the algorithm does allow one to emphasise  $k$  nearest samples. (In practice, the actual value(s) taken for  $k$  would differ on the particular case under consideration). If  $\lambda_k(\mathbf{u})$  is the sum of OK weights of  $k$  nearest samples then,

$$\lambda_k(\mathbf{u}) = \sum_{i=1}^k \lambda_i^{OK}(\mathbf{u}) < 1$$

and each  $p_i$  is the ratio of the weights of one of  $k$  sample values to the sum  $\lambda_k(\mathbf{u})$  which can be written as follows

$$p_i = \frac{\lambda_i^{OK}(\mathbf{u})}{\lambda_k(\mathbf{u})} \quad i = 1, \dots, k$$

Then equations (4-7) and (4-8) can be written as

$$\lambda_{\alpha}^{NNK}(\mathbf{u}) = [\lambda_k(\mathbf{u}) + (1 - \lambda_k(\mathbf{u})) * f] * p_i \quad i = 1, \dots, k$$

$$\lambda_{\alpha}^{NNK}(\mathbf{u}) = \lambda_j(\mathbf{u}) * (1 - f) \quad j = k + 1, \dots, n$$

These two equations can be also presented in the simpler form (Arik, 1998)

$$\lambda_{\alpha}^{NNK}(\mathbf{u}) = \lambda_i(\mathbf{u}) + (p_i - w_i) * f \quad i = 1, \dots, k \quad (4 - 9)$$

$$\lambda_{\alpha}^{NNK}(\mathbf{u}) = \lambda_j(\mathbf{u}) * (1 - f) \quad j = k + 1, \dots, n \quad (4 - 10)$$

As shown, the NNK method is an effective way of reducing the smoothing (the closest samples are given most importance) usually introduced by the kriging algorithm and, at the same time, adjusting the estimate to take into account the changes in the support of the data. And indeed, emphasising the nearest sample (or samples if deemed appropriate) may prove beneficial with variables from the earth sciences which very often exhibit a skewed distribution. Further, this method, on top of employing all of the variographic parameters used by OK, determines in statistical terms, which of the nearest samples influence the estimate most. Different panel size estimates can be generated without a need for a separate change of support correction.

In the next chapter a description of the data set used in the study is given.

## **5. DATA SET AND TREATMENT**

### **5.1 Introduction**

The data for this study were acquired from the Boddington Gold Mine (BGM) database. The BGM is located in the Darling Scarp Jarrah Forest, approximately 130km south east of Perth in Western Australia. Ore is extracted from both weathered oxide and fresh bedrock zones utilising open cut mining methods. The data set used here comes from the oxide profile only. At the beginning a comprehensive description of the exploration and mining practices at BGM will be given, followed by the presentation of the data sets used throughout the study.

#### **5.1.1 Exploration and grade control practices at BGM**

An identified mineralised structure is usually defined further by an exploration drilling. Diamond, hammer or reverse circulation drilling is used. Solid cores of rock can be obtained only from the first type of drilling. The other two methods result in small chips of rock and rock dust. At BGM the drill holes are located on a pseudo regular grid (approximately 25 by 25 metres). Holes have widely varying azimuth and dip, and the density of drill holes is sometimes greater in high-grade

areas. They are sampled at one-metre intervals down the hole. The diameter of these holes can vary from 60 mm to 122.6 mm depending on the type of rod and drill rig used. The data from the exploration samples serve as an input for building a 3D model of the ore body and the grade and the tonnages are estimated using geostatistical techniques. This model is then optimised and the optimal pit envelope is defined (Boddington Gold Mine Internal Report, 1998). Before the mining phase begins another drilling campaign occurs, called a grade control infill drilling. This is done inside the optimised pit shell in order to confirm and further define the extent of the ore body. Effectively the drill spacing is denser. However, only the exploration data is used in geological modelling because the grade control data is not available at that stage. The grade control sampling occurs on each bench before it is actually mined.

Two raw data sets will be used in this study. The sets were primarily extracted from the data base covering the following region:

East 9193m – 9674m

North 10924m – 11549m

The coordinates used in this thesis are quoted from the mine grid. The mine grid north is 42° 20' 40'' to the west of true north. This, however, is not the final study area, which will be defined in section 5.2.2. The first



set contains the exploration drill data. After compositing it will be called *excomp*. This set will serve as our exploration sample set. The second set is the grade control data set. It consists of the grade control trench samples. At BGM the vast majority of grade control data come from channelling, which occurs on every bench prior to mining. This data set will be called *grchanraw*. Grade control data are very often used as data against which geostatistical estimates are reconciled. In this study the data from *grchanraw* will be used for a similar purpose. However, the estimation itself will be done using data from *excomp* only.

## 5.2 Exploration data set

Data for a total of 815 drill holes were extracted from the BGM database. The set consists of three different types of drilling:

- diamond drilling;
- reverse circulation drilling; and
- hammer drilling.

There are 265 holes of diamond drilling type, 322 holes drilled using the reverse circulation technique and 228 holes of hammer drilling type.

Samples, in most cases, are taken every metre down the hole.

Essentially, the holes were drilled on a pseudo regular square grid with grid spacing of approximately 25 metres. However, in some areas

drilling density appears to be higher than in the others. It should be noted that the set described here as the exploration set might also include some of the grade control drill holes (infill drilling) drilled before mining was commenced. Because of several campaigns of drilling within BGM it was found very difficult, in some cases even impossible, to distinguish some of the grade control holes from exploration holes. However, this should not affect, to any extent, the outcome of the study. A few drill holes were found with very high sample values in some cases even as high as 1000 grams per tonne of ore. Investigation of this anomaly (Khosrowshahi et al, 1992) showed that, in one of the pits there were three spatial domains with very high grade values of copper and gold identified in the lower part of the weathered profile. It should be noted that this pit constitutes the southern part of our study area.

Because of possible differences between drilling types, the exploration data set was split into three separate sets each containing only one type of drilling. The summary statistics calculated on each of them is presented in Table 5.1. Essentially, there is very little difference between the diamond and the hammer drilling types. The reverse circulation data is less variable than the other two.

Table 5.1 Summary statistics by drilling type. Raw exploration data set.

Type of drilling	Mean	Standard Deviation	Min.	Max.	Number	Coefficient of Variation
<b>Diamond</b>	1.702	18.508	0.010	1310.690	13503	10.874
<b>Reverse Circulation</b>	1.148	10.056	0.010	639.000	9299	8.760
<b>Hammer</b>	1.480	16.686	0.010	1310.690	8616	11.274

This could be attributed to many factors, for instance:

- the nature of reverse circulation drilling (it produces rock dust) can introduce some degree of smoothing; and
- there are only three holes, from the reverse circulation set, drilled in the high grade zone in the pit mentioned earlier.

For these reasons the data from the reverse circulation drilling is considered to be a complementary data set rather than a separate population. Hence, for the purpose of this study, it was decided to combine all three sample populations.

Our study will concentrate on one representative bench chosen from the entire data set. A bench or level is a horizontal (in the case of BGM inclined at 2%) slice of rock mined at one time or pass. This bench was selected to intersect with the described high grade zone. The reduced level (RL) of the bench is 228.0 m, it is not inclined and is three metres thick, hence the bottom RL is 225.0m. The fact that the bench is

horizontal is important from the point of view of the grade control trench data; this will be discussed further in the next sections.

To be able to compare the exploration data with the grade control data set in the same region of space, the samples must represent the same vertical thickness. In order to achieve this the samples needed to be composited. Compositing involves calculating and assigning values to specified segment lengths located at specified positions down the hole. These segments are generally different from the actual sections assayed. In this case the aim is to compare the sections that are contained within each bench at 3.0 metres vertical thickness. We have assumed here that the volume of a sample is the same for both data sets. At this point, it should be noted that the trench data from grade control are, in fact, already composited. The reason for this is that trenching occurs on every bench. Moreover, the channel depth is equal to 3.0 metres, which is the bench height. Hence, every channel sample represents the same thickness, which is equal to our chosen segment length for compositing. The composited exploration data set is called *excomp*.

### 5.2.1 Descriptive statistics of *excomp*

The statistics presented in this section are calculated for the chosen representative bench and over the primary region defined at the end of section 5.1.1. The summary statistics for *excomp* are presented in Table 5.2 below.

Table 5.2 Summary statistics calculated on *excomp* for the bench 228.0 RL.

<b>Data Set</b>	<b>Mean</b>	<b>Standard Deviation</b>	<b>Min.</b>	<b>Max.</b>	<b>Number</b>	<b>Coefficient of Variation</b>
<i>Excomp</i>	1.303	6.172	0.010	84.330	1 707	4.736

The frequency plot for the bench 228.0 RL and also the lognormal probability plot for *excomp* are shown in Figure 5.1. As can be seen, this is a relatively variable population, positively skewed with a tail of high values. It will be necessary later on to identify and separate the high grade composites from the rest of the population. Consideration of the lognormal probability plot indicates that the distribution may be regarded as approximately lognormal, although it should be noted that this assumption does not affect the results of the calculations performed in this study.

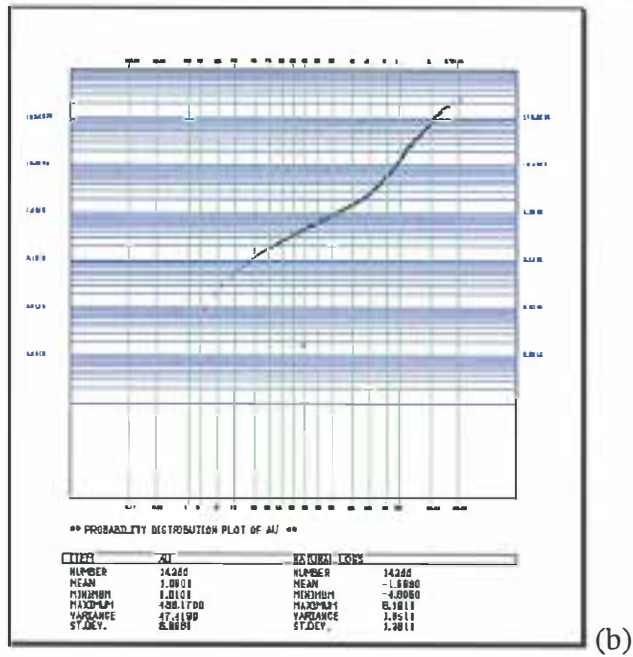
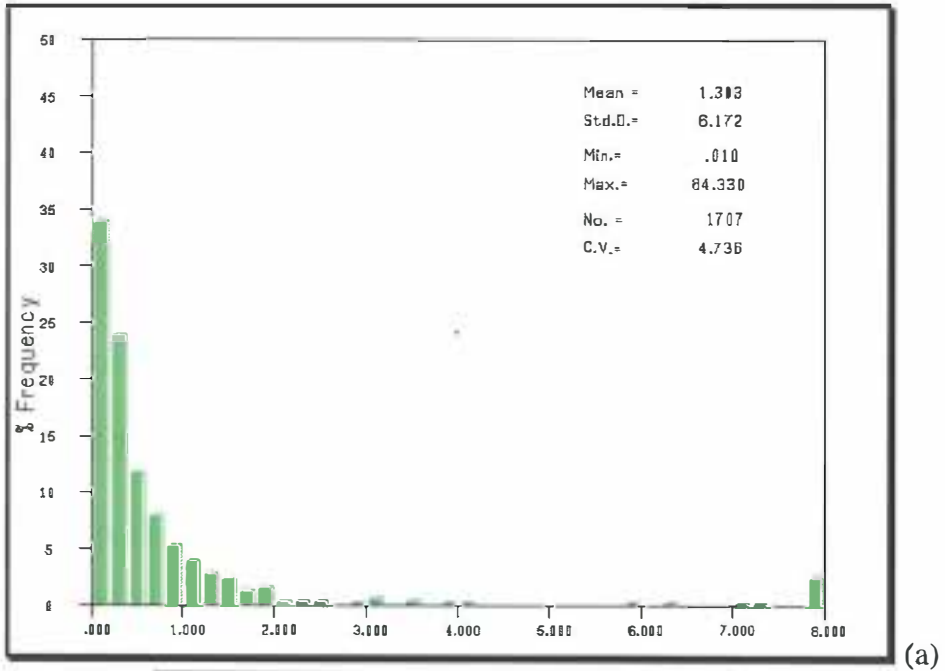


Figure 5.1 *Excomp* frequency plot (a) and lognormal probability plot (b), bench 228.0 RL.

### 5.2.2 Definition of sample data set

Within the region covered by *excomp*, apart from other geological formations, there are a few dolerite dykes present. The dolerites, based

on the BGM experience, are barren rocks and they do not host any gold mineralisation (Boddington Gold Mine Internal Report, 1998; 1996). Hence, taking any sample data from the intersection with dolerite dykes into the calculation of the statistics and experimental semivariograms would create a bias. There is also a high-grade zone, already mentioned in Section 5.2, located in the southern part of the project area. Since it is a separate population from both a geological and a statistical point of view, it has also been excluded from the calculations. In order to enable exclusion of the above-described populations every sample from *excomp* was assigned an integer code. If a sample came from an intersection with one of the dolerites or with the high-grade zone a special, three-digit code was attributed to it so that it could be excluded from the subsequent calculations.

The coding mentioned above was done using solids acquired from BGM. The solids were created based on the exploration drill data and they represent different dolerite dykes in the region. One solid represents the high-grade zone. After the coding was carried out, the coded drill data were listed in order to check the results. Any questionable drill holes, i.e. a sample with a gold grade within a dolerite dyke, were then edited, using MineSight® software, and the codes corrected. No alteration to the

sample values was made in any case. The coding was done within Medsystem® statistical suite.

As a result of these modifications to the *excomp* data set, effectively a new data set was generated. This new data set, referred to here as *finexcomp* is the exploration set that is used in this study. A plan view of the study area with *finexcomp* composite data is shown in Figure 5.2.

Summary statistics for *finexcomp* are given in Table 5.3.

Table 5.3 Summary statistics calculated for *finexcomp* for the bench 228.0 RL.

<b>Data Set</b>	<b>Mean</b>	<b>Standard Deviation</b>	<b>Min.</b>	<b>Max.</b>	<b>Number</b>	<b>Coefficient of Variation</b>
<i>Finexcomp</i>	1.464	4.906	0.010	52.860	143	3.351

The final study project limits, over which summary statistics were calculated, are:

E: 9410m – 9630m  
 N: 11100m – 11330m  
 Elevation: 225m – 228m RL



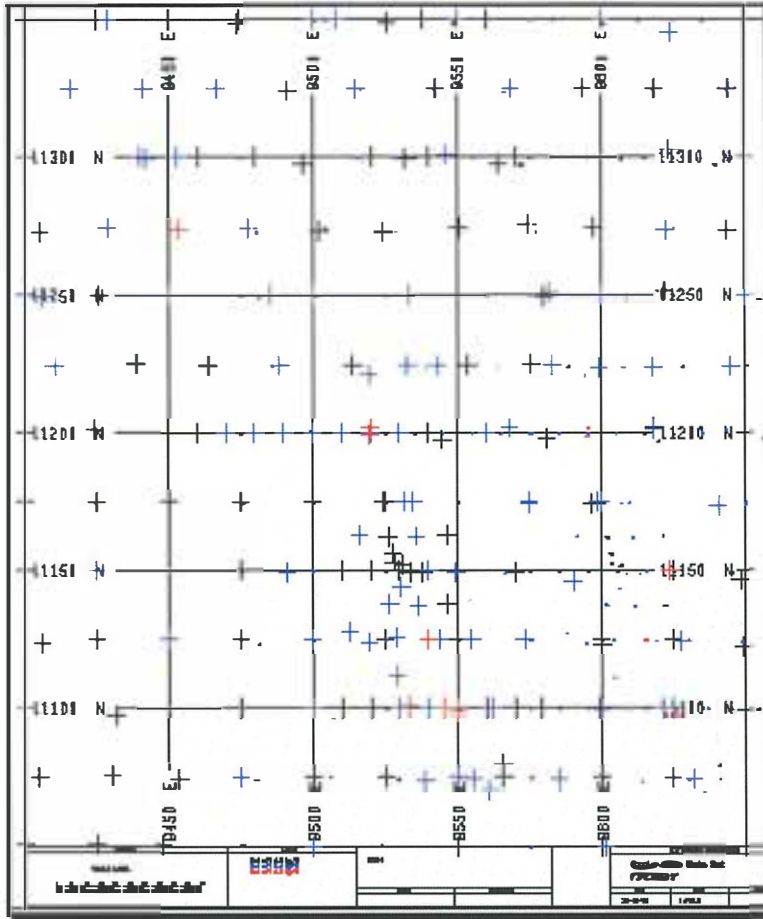


Figure 5.2 Final study area (E: 9410-9630m, N: 11100-11330m). Plan view *finexcomp* – 228.0 RL. Composites between 0.4 and 5.0 g/t shown in blue, greater than 5.0 g/t shown in red

The frequency plot and the lognormal probability plot for *finexcomp* are shown in Figure 5.3. As can be seen the majority of samples from *finexcomp* fall below 2.5 (g/t) cut-off grade and the data set is positively skewed. The lognormal probability plot indicates that the data exhibit an approximately lognormal distribution.

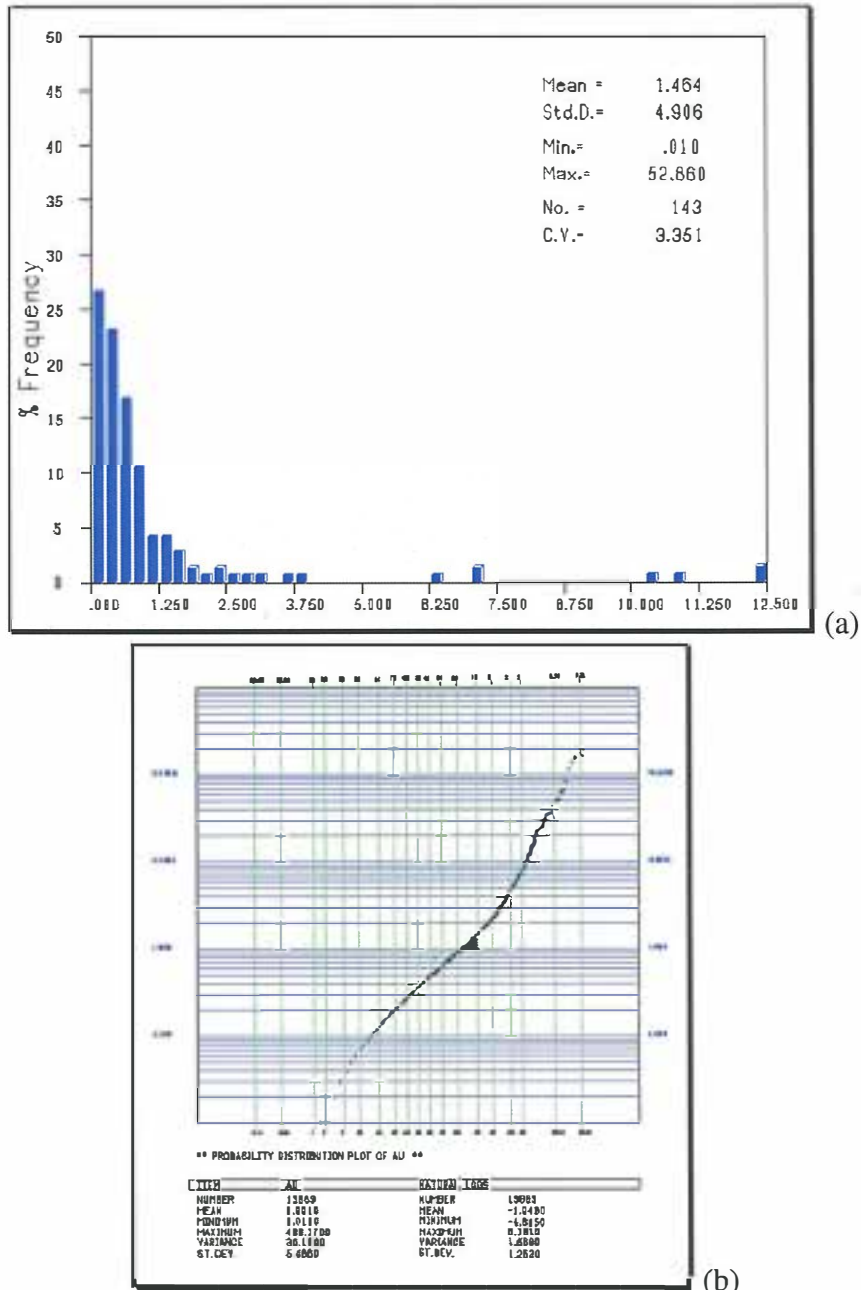


Figure 5.3 *Finexcomp* data set: (a) histogram and (b) lognormal probability plot

### 5.3 Grade control data set

After mining of the ore body has commenced, every mining bench is channelled. Channels are narrow trenches cut across the bench to its full depth of three metres. The trench spacing is equal to ten metres. A soil

pile builds up along the sides of a trench during the digging process. Samples are taken along the soil pile in two-metre increments. Therefore the support represented by one grade control sample can be defined by the following parameters X=2m, Y=10m and Z=3m. It should be noted that there is no need for blasting as long as the oxide material is soft enough to be mined in situ with an excavator. Grade control is done on inclined benches. The inclination is defined by the following parameters:

- hinge point coordinates: 10200 m South, 11500 m North
- inclination direction 180 (i.e. South)
- inclination 2 %

Grade control data for the chosen bench come from the trenching. The set containing these data is referred to as *grchanraw* and comprises approximately 23,913 samples, within the chosen horizontal bench within a range from 228.0 RL to 225.0 RL and the primary coordinates as defined at the end of Section 5.1.1.

The *grchanraw* set, similarly to *excomp*, contains mineralised and non-mineralised zones including the high grade structure. In order to be able to distinguish ore from waste, plan views of both populations were generated as shown in Figure 5.4. Because *grchanraw* covers a smaller area than *excomp*, both sets were constrained to the same region i.e. E:

9410m – 9630m, N: 11100m – 11330m and elevation: 225m – 228m RL (see Section 5.2.2), before the geostatistical analysis was carried out.

Figure 5.4 shows initial area larger than the final study area.

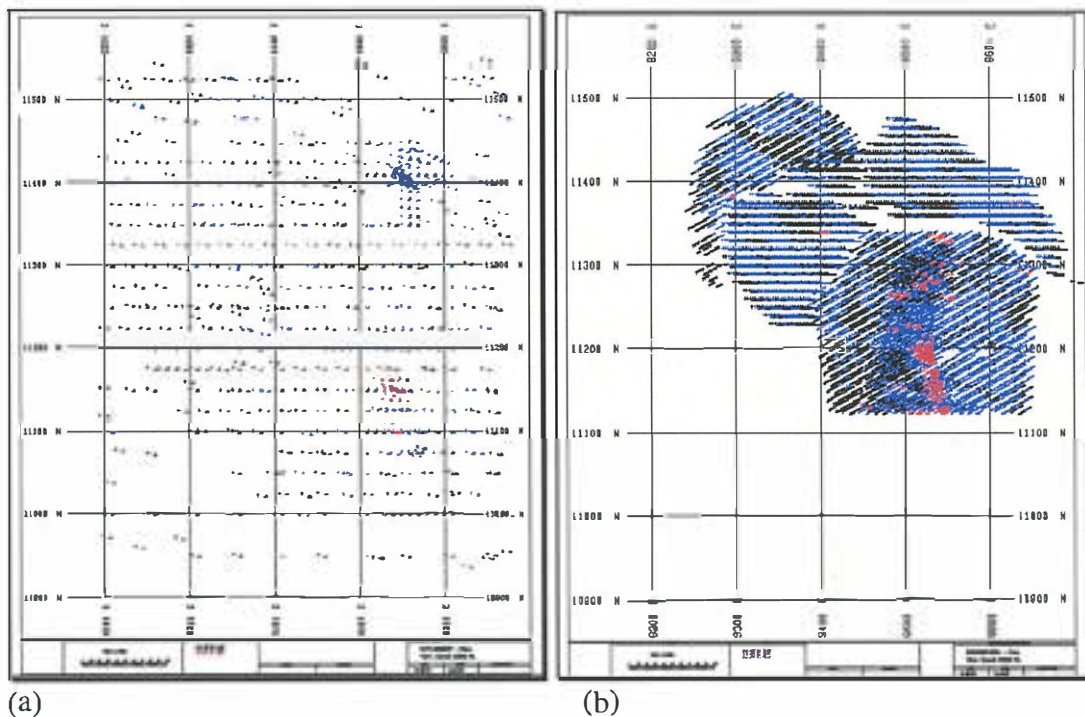


Figure 5.4 Plan view *excomp* (a) and *grchanraw* (b)– 228.0 RL. Composites between 0.4 and 0.5 g/t shown in blue, greater than 5.0 g/t shown in red.

### 5.3.1 Descriptive statistics of the grade control data set.

This section consists of two parts. The first refers to the statistical properties of *grchanraw* from the region defined in Section 5.1.1. The second part presents the summary statistics for *grchan*, the final grade control data set, which comes from the final study region as defined in Section 5.2.2.

## Part 1

Summary statistics for *grchanraw* are presented in Table 5.4

Table 5.4 Summary statistics calculated for *grchanraw* for the bench 228.0 RL (primary region see Section 5.1.1).

Data Set	Mean	Standard Deviation	Min.	Max.	Number	Coefficient of Variation
<i>Grchanraw</i>	0.929	2.149	0.010	42.340	23 913	2.314

The histogram for the bench 228.0 RL and the lognormal probability plot for *grchanraw* are shown in Figure 5.5 (a) and (b) respectively. This set contains a much larger number of samples/composites, and has a lower level of variability in comparison to *excomp*. Also *grchanraw* has a positively skewed distribution. The lognormal probability plot in Figure 5.5 shows that the distribution of this data set is approximately lognormal. The deviation from the straight line takes place especially at the upper end of the curve where high grade values occur.

## Part 2

As discussed in Section 5.2.2, the final study region was based on geological and statistical properties. Similarly to *finexcomp*, the samples within the *grchanraw* set that intersect with the high-grade zone and with the dolerite dykes were flagged so that they could be identified and excluded during the statistical calculations. As a result the final grade control data set was generated, and is referred to as *grchan*.

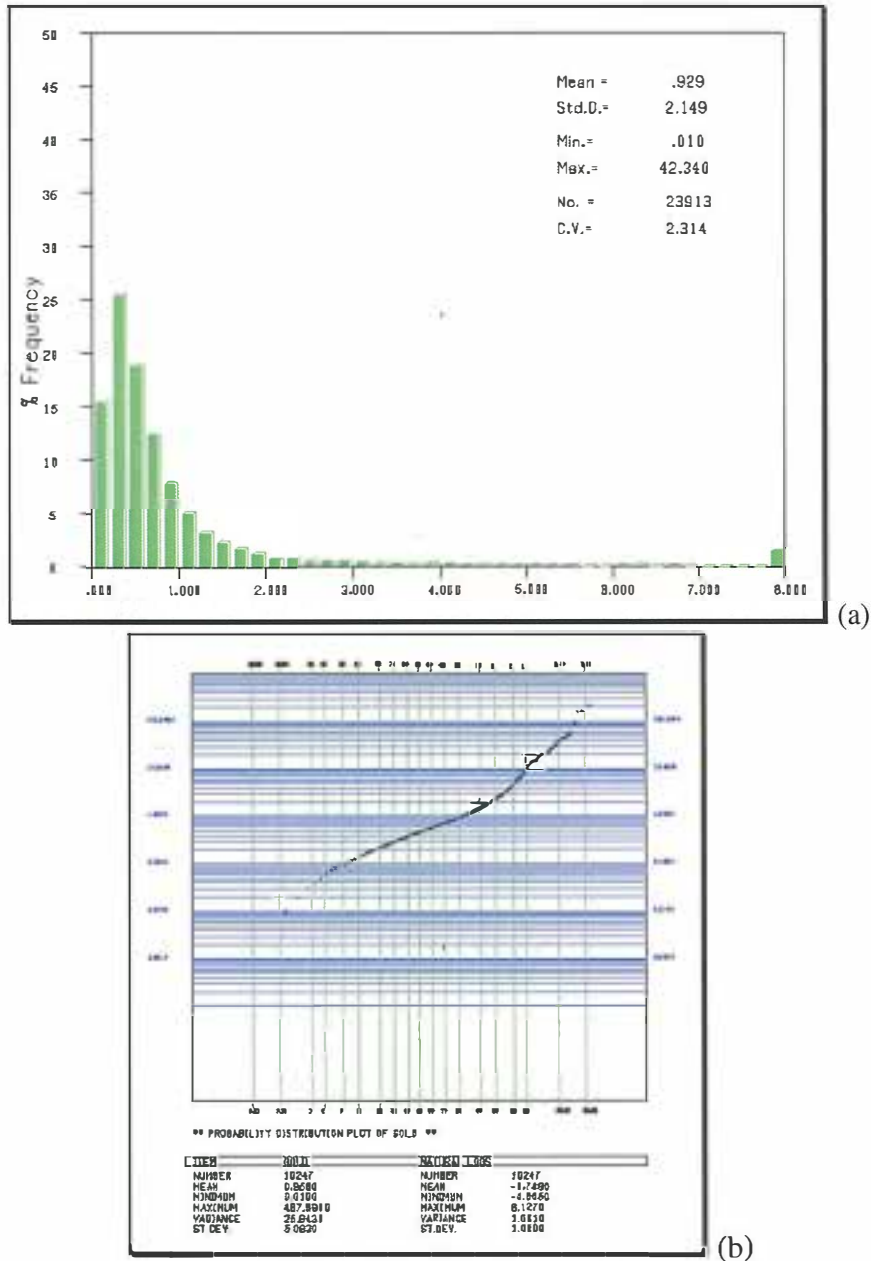


Figure 5.5 *Grchanrow* - frequency plot and (a) and lognormal probability plot. Initial region (see Section 5.1.1)

Summary statistics for *grchan* are presented in Table 5.5.

Table 5.5 *Grchan* summary statistics for the bench 228.0 RL

Data Set	Mean	Standard Deviation	Min.	Max.	Number	Coefficient of Variation
<i>Grchan</i>	1.095	2.419	0.010	42.340	3980	2.209

In Figure 5.6 the frequency plot and the lognormal probability plot, respectively, of *grchan* are shown.

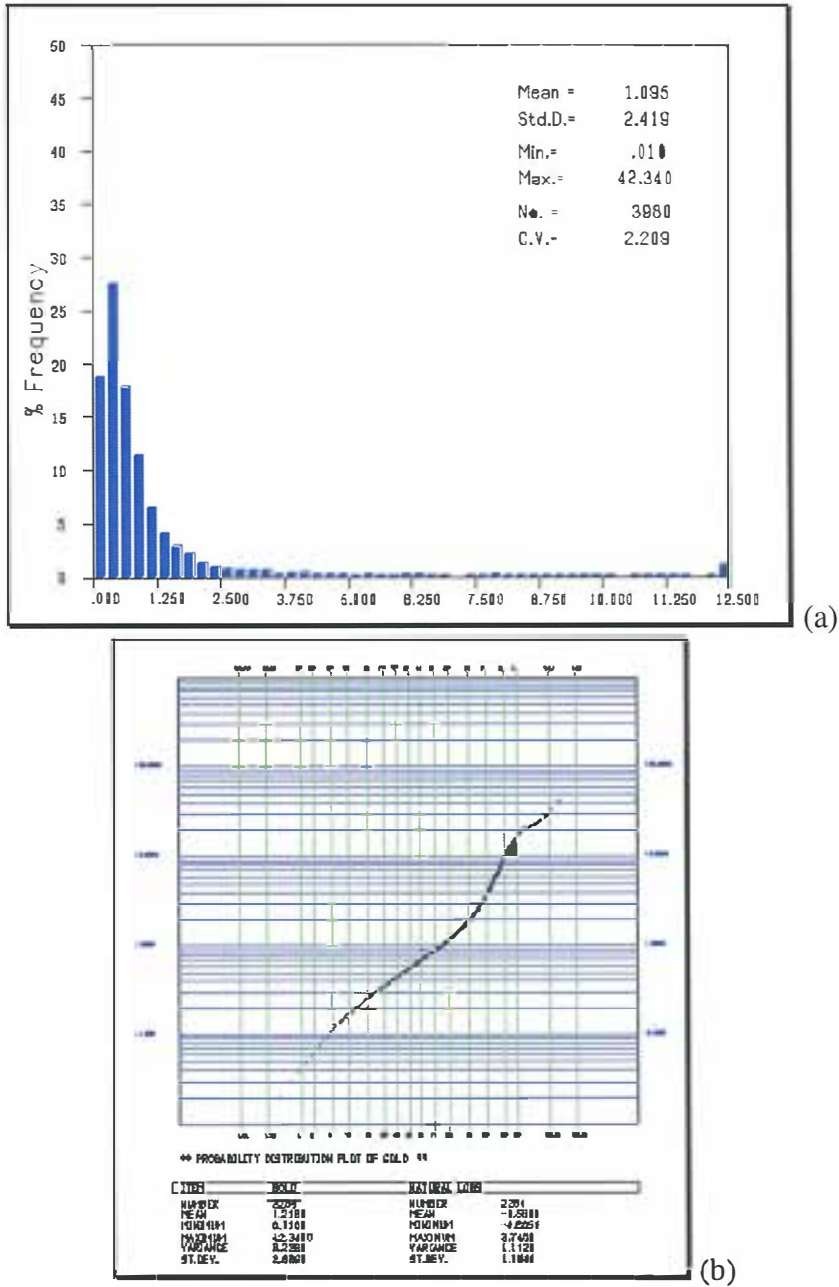


Figure 5.6 *Grchan* frequency plot (a) and lognormal probability plot (b)

Looking at the plots in Figure 5.6 and the plots presented earlier for *finexcomp* in Figure 5.3, some similarities can be seen. The grade control

data are certainly much smoother and contains many more data samples than the exploration data set (*finexcomp*). However the *grchan* statistics confirm the fact that our study region has a relatively high variability and includes considerably high sample values. It is positively skewed with an approximately lognormal distribution.



## 6. VARIOGRAPHY OF *FINEXCOMP*

### 6.1 Analysis of spatial continuity of *finexcomp*

The analysis of the spatial properties of *finexcomp* data set is done using the semivariogram function (Section 2.3). In order to achieve a better representation of the spatial continuity of the data set and a clearer picture of the directional semivariograms, data from benches adjacent to the bench of interest were used. The bench chosen for the study is described as follows: crest 228 RL and toe 225 RL and during the semivariogram calculations two additional benches above and two below the data set, each 3 m thick, were incorporated. Horizontal lag distance of 25 m was used, due to the drill spacing, with 12.5 m tolerance. Calculation was done for ten lags  $h$  (2-14).

In addition, several h-scatter plots of *finexcomp* were generated in the directions from N0°E to N180°E. These calculations helped in ascertaining the major direction of the continuity of the data set. It was found that the h-scatter plot for the N140°E yields the highest correlation coefficient amongst the all h-scatter plots generated. It should be noted that in the report, (Khosrowshahi et al, 1992), the major direction of the

continuity used for the semivariogram modelling, within approximately the same region, was also N140°E. However, the data set used in that report is different from that used in our study.

Raw data directional semivariograms were calculated for the range of the azimuths N0°E to N180°E. However, they did not give a clear representation of the spatial continuity of *finexcomp*. An example of these semivariograms is presented in Figure 6.1.

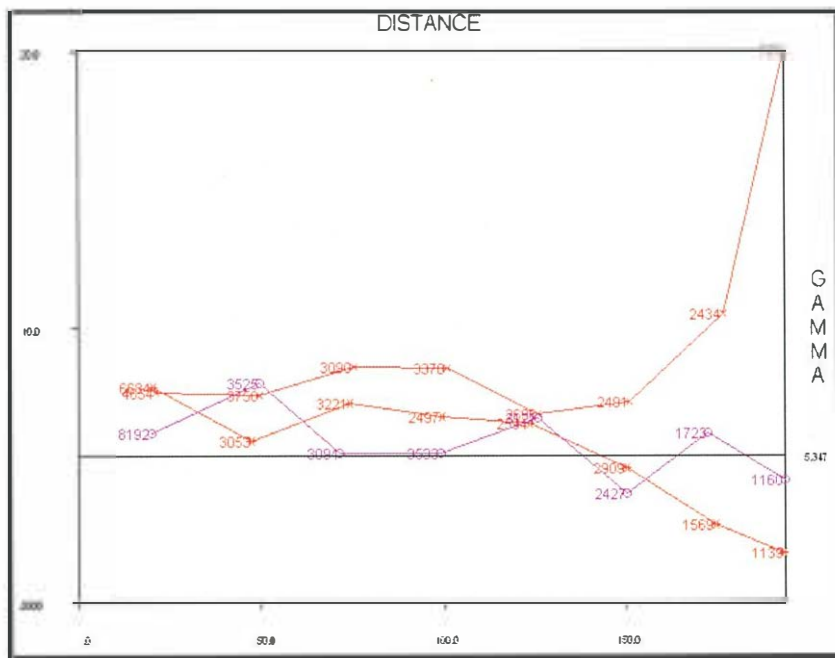


Figure 6.1 Experimental classical semivariograms. Directions: N10 E – red, N50°E – orange, N140°E – purple.

Since the data set contains some considerably high values, it was decided to use a more robust type of semivariogram which would help to reduce the influence of the outliers. The type of semivariogram chosen is the

pair-wise relative semivariogram (2-17) (Isaaks and Srivastava 1989, Goovaerts 1997, Arik 1997). Recall that this semivariogram is obtained from the classical one by adjusting the semivariogram calculation by a squared mean. The adjustment is done separately for each pair of sample values. The average of the two values is used as the local mean.

Another supporting factor for the computation of the pair-wise relative variogram is the fact that the relation between the local mean and the standard deviation in the case of *finexcomp* is approximately linear. This relation is presented graphically in Figure 6.2. This type of behaviour is known as *proportional effect* (Section 2.3). This type of semivariogram was also used by Khosrowshahi et al (1992).

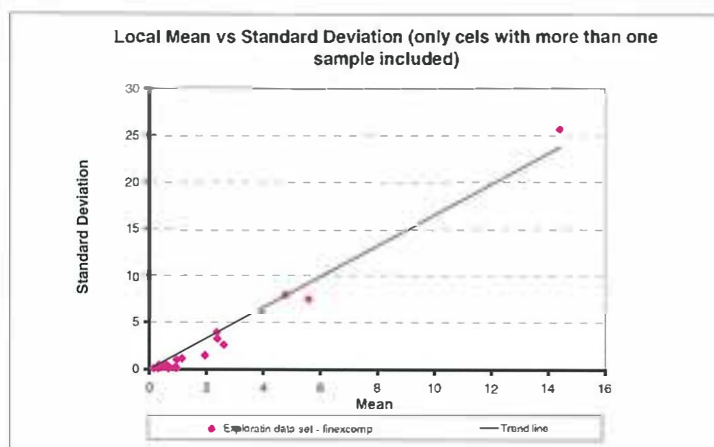


Figure 6.2 *Finexcomp* - local mean versus standard deviation

As discussed earlier in this section, the major direction of continuity of *finexcomp* was determined to be N140°E, based on the correlation

coefficient from the calculated h-scatter plots. In order to check this assumption further, a contour plot of the pair-wise semivariogram surface was generated. The parameters used for the contouring are:

- minimum contour value 0.01
- maximum contour value 2.0
- contour increment 0.025

It is noticeable that the values listed above are low. This is due to the re-scaling introduced by the pair-wise semivariogram algorithm (2-17). The contoured semivariograms were calculated from  $N0^{\circ}E$  to  $N180^{\circ}E$  azimuth on *finexcomp* with the parameters described earlier. The results of the contouring are given in Figure 6.3.

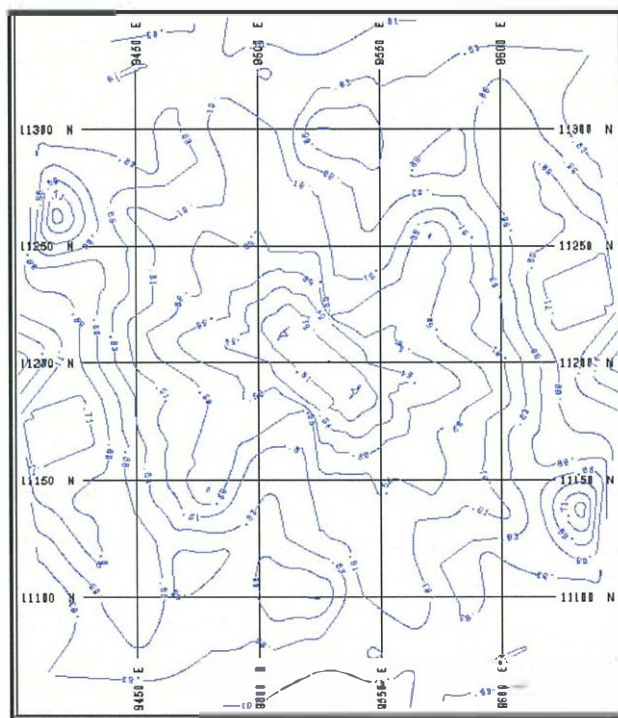


Figure 6.3 *Finexcomp* pair-wise experimental semivariogram surface contours.

From the plot it can be clearly seen that the major direction of the continuity was correctly determined.

As expected, the pair-wise relative semivariogram gave a much clearer picture of the spatial continuity of our exploration data set. The pair-wise relative semivariograms calculated in the major and the minor directions of continuity, along with the omnidirectional two-dimensional semivariogram are shown in the following Figure 6.4.

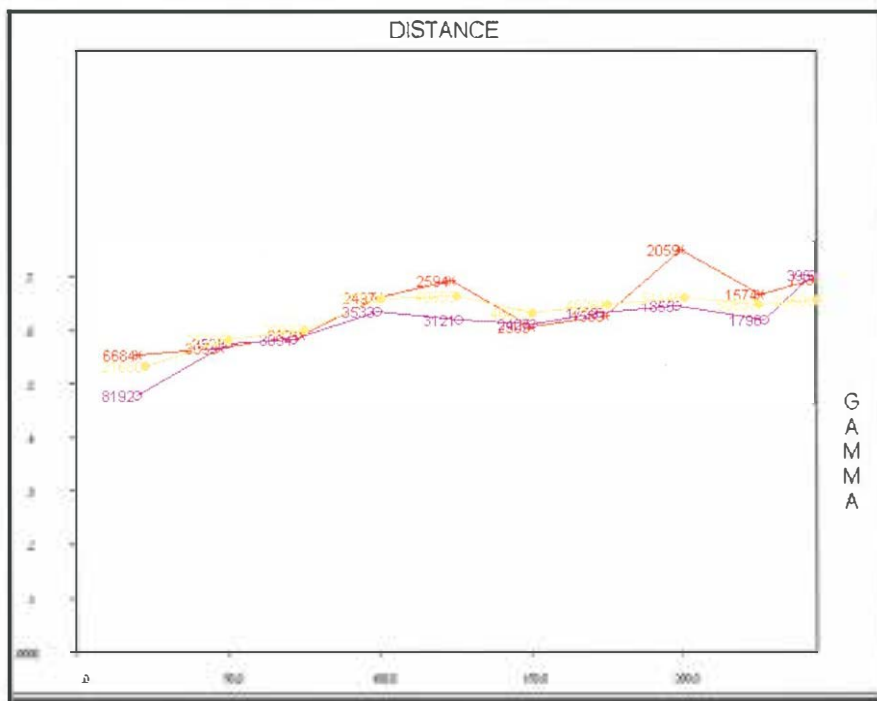


Figure 6.4 Experimental pair-wise semivariograms. Major direction, N140°E – purple; minor direction N50°E – red; omnidirectional 2-dimensional semivariogram – yellow.



two points with higher Y values than the value of corresponding points from the major and omnidirectional semivariograms. It is very likely that these two points are the effect of some isolated high grade pods in that direction. This also affects the omnidirectional two-dimensional semivariogram to some extent. Nevertheless, all three curves, in Figure 6.4 do stabilise with increasing distance. The lateral dimensions of our entire project, i.e. 220 m in X and 230 m in Y, imply that the major area of interest from the “variographic” point of view is that up to, approximately, a 110 m range. Having said that, it was assumed here that *finexcomp* demonstrates geometric anisotropy, i.e. the sill of the directional semivariograms stays the same and only the ranges are changing with the direction and also that the value of the nugget effect should be the same in every direction.

The nugget effect very much depends on the variability of a deposit (usually the more variable the deposit the higher the nugget) and also on the sampling error (and again the higher the error the larger the nugget effect). Yet, reading the value of the nugget directly from the experimental semivariogram curves presented in Figure 6.4 could prove difficult and not very accurate. The nugget is defined as the lack of continuity at a very short scale, smaller than the first lag of the





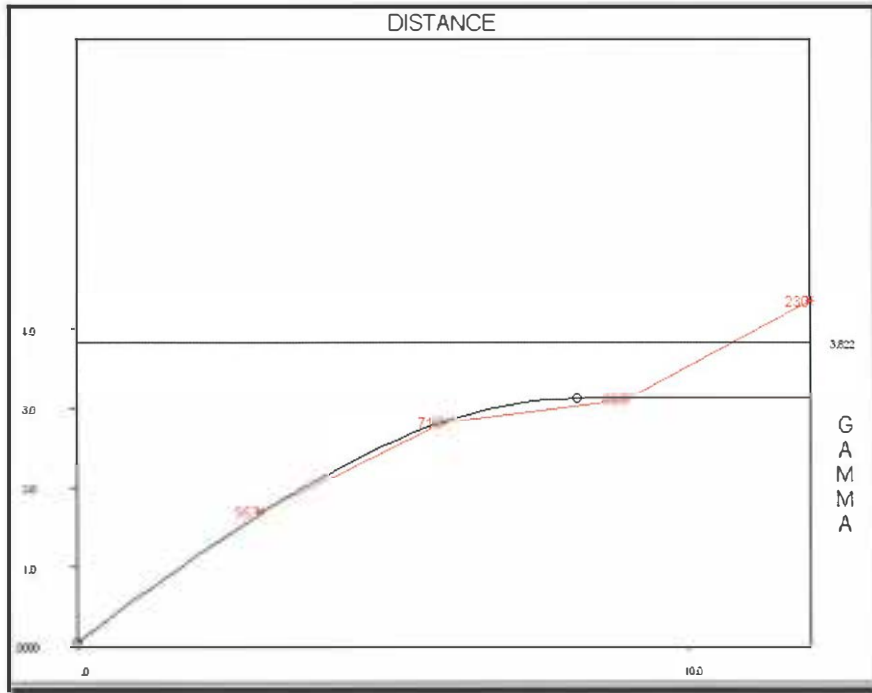


Figure 6.5 Raw data down-hole semivariogram (red) along with the modelled semivariogram.

The modelled value of the nugget effect is:

$$C_0=0.058 \quad (6 - 1)$$

This value was taken as the value of the nugget for the semivariogram models of *finexcomp*.

The available information, obtained from the calculation performed so far, enables us to model the variography of *finexcomp*. This process is described in Section 6.2.

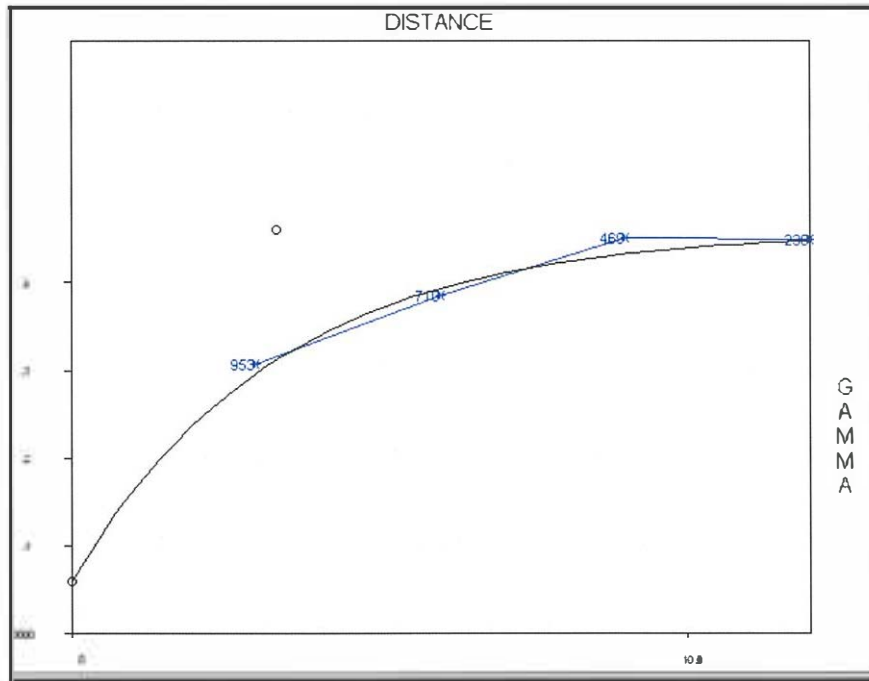


Figure 6.6 Pair-wise relative down-hole semivariogram (blue) along with the modelled semivariogram<sup>2</sup>.

## 6.2 *Finexcomp* variography modelling

Although the calculated set of directional sample semivariograms provides us with very useful information with respect to the spatial continuity of *finexcomp*, in most cases it cannot deliver all the semivariogram values required by the kriging system. Kriging algorithms (2-30 and 4-5) will be used later in the study to estimate grade for *finexcomp*. For the kriging system we need semivariogram values between the sampled locations and non-sampled locations where an estimate is going to be made. Therefore we have to build a

<sup>2</sup> The points (small circles or black dots appearing above the semivariograms) visible in Figure 6.6 and 6.5 are software specific. These points “define” the variogram being modelled and can be used to interactively fit the model to the experimental semivariogram by dragging them.

semivariogram model which will contain all the data required. The model also enables calculation of the semivariogram value for any separation vector  $\mathbf{h}$ .

Modelling a semivariogram involves fitting a curve to a given experimental semivariogram. Usually there are two models created first, for the major and minor direction of continuity of the data set. Subsequently, based on the built directional models, the model of anisotropy can be derived, if an anisotropy is present. There are several theoretical semivariogram models available, which can be used. The most common ones were listed in Section 2.3.

In the case of *finexcomp*, as was discussed in Section 6.1, we have geometric anisotropy. This means that the semivariograms in the major and minor directions need to be modelled. Then based on these models the anisotropy parameters can be derived.

The directional semivariogram for the major direction of continuity i.e. N140°E, was modelled first. The modelling was done using Medsystem® software (Arik 1997). This model, referred to as the major direction model, is a nested structure and consists of two basic

exponential models (2-20). The parameters describing the model are given in Table 6.1.

Table 6.1 Major direction of continuity N140°E semivariogram model

	Type	Anisotropy Type	Sill	Range
Structure 1	nugget		0.058	
Structure 2	exponential	geometric	0.492	16.48
Structure 3	exponential	geometric	0.010	101.70

A graphical presentation of the major direction model along with the experimental pair-wise relative semivariogram in this direction can be seen in Figure 6.7.

Similarly, a model for the minor direction of continuity of *finexcomp* was developed. The minor direction is perpendicular to the major direction of continuity. This model is also a nested structure which is a combination of two exponential basic models (2-20). The semivariogram model for the minor direction of spatial continuity is characterised by the parameters presented in Table 6.2.

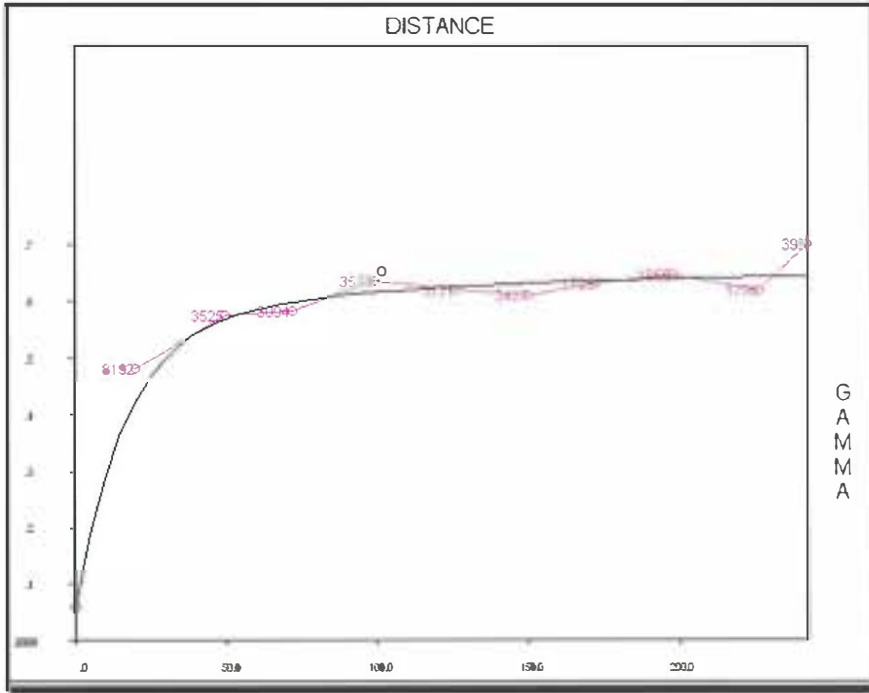


Figure 6.7 *Finexcomp*, major direction model and experimental pair-wise relative semivariogram for the major direction (N140°E) of continuity

Table 6.2 Minor direction of continuity, N50°E, semivariogram model

	Type	Anisotropy Type	Sill	Range
Structure 1	nugget		0.058	
Structure 2	exponential	geometric	0.492	4.65
Structure 3	exponential	geometric	0.010	51.21

Figure 6.8 shows the minor direction model and the experimental pair-wise relative semivariogram calculated in this direction.

The variography modelling based on the pair-wise relative semivariograms presented in this section enabled us to determine the major parameters of spatial continuity of *finexcomp*. Summarising, we have (see Table 6.3):

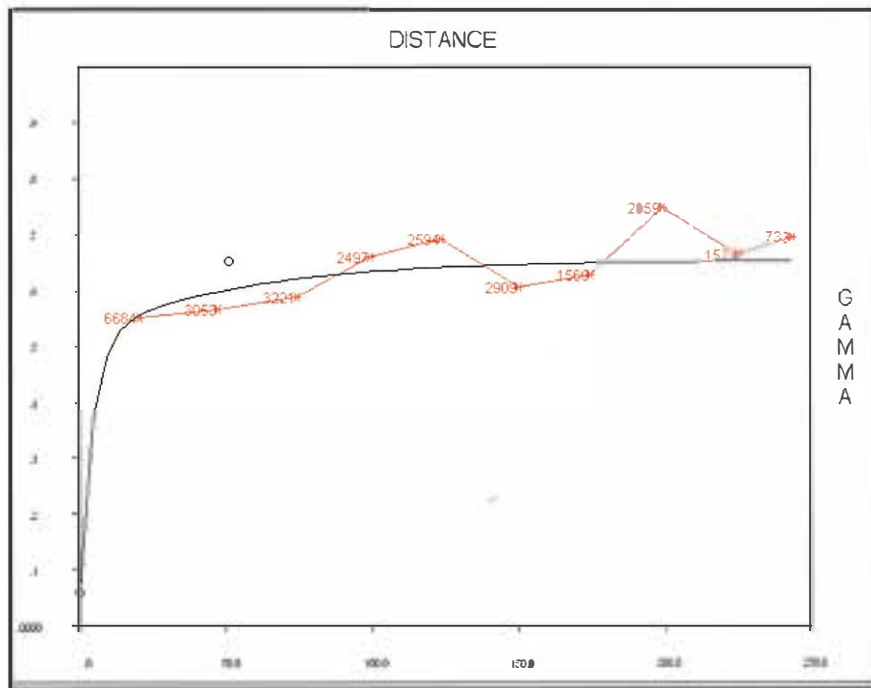


Figure 6.8 *Finexcomp*, minor direction model and experimental pair-wise semivariogram for the minor direction (N50°E) of continuity

Table 6.3 *Finexcomp* spatial continuity parameters based on pair-wise relative semivariograms

Nugget:  $C_0=0.058$  (6-1)

	Type of Variogram Model	Anisotropy Type	Sill	Range Max.	Range Min.
Structure 1	Exponential	geometric	0.49	16.48	4.65
Structure 2	Exponential	geometric	0.01	101.70	51.21

The chosen semivariogram model represents the spatial continuity of *finexcomp*. Using this the subsequent kriging will estimate the grade at every point of the ore body covered by the study project. The estimation will be done using composite data from *finexcomp*. However, not all parameters derived from the pair-wise relative semivariograms can be directly applied to kriging. Furthermore, use of the kriging variance from

the kriging algorithm calls for a variogram model based on the traditional (classical) semivariogram (Goovaerts, 1997). Therefore the parameters from the variogram models based on the relative semivariograms (anisotropy directions and ranges) will be used to model the classical semivariogram. Then the generated models, fitted to the classical experimental semivariograms, will be utilised during kriging. Of significance is the fact that these models do not deliver the actual sill values since the sill values already modelled (see Table 6.3) are affected by the re-scaling introduced by the chosen type of the relative semivariogram (2-17).

The model for the classical semivariograms are shown in Figure 6.9 and Figure 6.10 on the next page, while Table 6.4 summarises the properties of these models.

As for the pair-wise relative semivariograms, the models for the classical semivariograms are nested models consisting of two exponential single structures in each of the major and minor directions of continuity. The parameters presented in Table 6.4 characterise the semivariogram models that will be used to estimate the grade of the bench used for the study purpose.

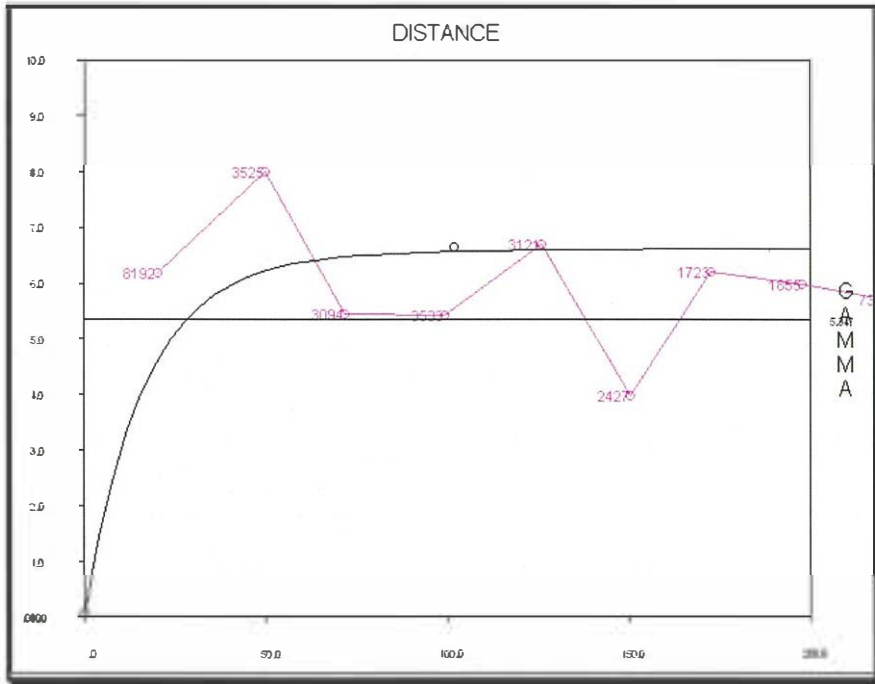


Figure 6.9 Major direction (N 140°E) semivariogram model with experimental classical semivariogram (major direction – purple).

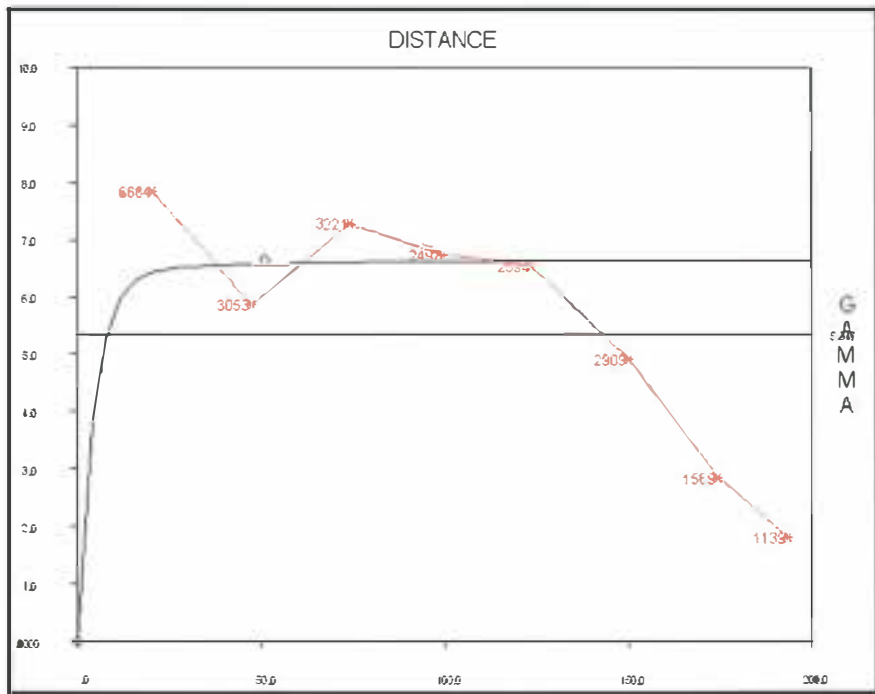


Figure 6.10 Minor direction (N 50°E) semivariogram model with experimental classical semivariogram (orange).



The estimation will be done by use of the kriging algorithms, that is ordinary kriging (2-30) and nearest neighbour kriging (4-5).

Table 6.4 *Finexcomp* spatial continuity parameters based on classical experimental semivariograms

Nugget:  $C_0=0.058$  (6-1)

	Type of Variogram Model	Anisotropy Type	Sill	Range Max.	Range Min.
Structure 1	Exponential	geometric	6.38	16.48	4.65
Structure 2	Exponential	geometric	0.22	101.70	51.21

### 6.3 Cross validation of the ordinary kriging estimates

Cross validation is one way of evaluating our chosen model. The value of a given sample is temporarily removed and then the estimation is performed, at the same location, using the remaining sample values. The process is repeated for each sample value. Results of the estimation can be compared with the true sample values (Isaaks and Srivastava, 1989; Goovaerts, 1997). Although cross validation can provide a good insight into the performance of the chosen method, it does not point specifically at any of particular parameters used. Hence, if the results are considered to be not satisfactory it is not evident whether it is due to the semivariogram model used, the search strategy parameter employed or, possibly, the technique itself. On the other hand, a good outcome from

the cross validation does not guarantee the best estimates at the unsampled locations. This may be the case when preferential sampling is present. Some authors (Goovaerts, 1997) even state that a decision on which model to use made on the basis of experience, available information and the purpose of the study may be more appropriate than the one based on the results of different statistical tests. Summarising, it can be said, that cross validation (also called point validation) is a good source of information but it should not be seen as the only or final judgement as to whether to accept or discard a certain estimation technique or its parameters. There are other factors such as experience, history of the deposit and geological input, to list only a few, that are also significant. These factors are very often deemed to be the most important in making a decision on the whole estimation system. In our case the grade estimates generated by OK method (2-30) will be validated using *finexcomp* data set. The search parameters used are described in Section 7.2.1. A Medsystem® procedure was used for to perform the cross validation.

The results from cross validation are presented below. Table 6.5 contains a comparison of the estimates calculated by OK and the *finexcomp* values.

Table 6.5 Summary statistics of the *finexcomp* and the kriging estimate

Item	Mean	Standard Deviation	Minimum	Maximum	Median	Skewness
Composite value	1.473	4.922	0.010	52.860	0.530	8.642
OK estimate	1.472	1.813	0.260	11.640	0.900	3.661
Kriging variance	5.768	1.137	2.709	6.923	6.241	-1.164

Table 6.6 summarises the statistical properties of the OK estimate residuals. Residuals (errors) are defined as the difference between the estimated values and the actual composite values.

Table 6.6 Summary statistics of residuals from OK estimate.

Item	Ordinary Kriging Estimate
Mean	0.0008
Standard Deviation	4.954
Minimum	-10.050
Maximum	48.060
Skewness	6.876
Weighted Squared Error	32.345

The weighted squared error *WSE* is defined by the following equation

$$WSE = \frac{\sum_{\alpha=1}^n \frac{1}{\sigma_{OK}^2(\mathbf{u}_{\alpha})} r^2}{\sum_{\alpha=1}^n \frac{1}{\sigma_{OK}^2(\mathbf{u}_{\alpha})}}$$

where  $r$  is the value of the residuals and  $\sigma_{OK}^2(\mathbf{u}_{\alpha})$  (2-32 and 2-34) is the kriging variance at location  $\alpha$ .

As expected, the distribution of the kriging estimates is much smoother than the distribution of the values used for the estimation. Also the minimum and the maximum value of *finexcomp* and the OK estimates show that the latter has a smaller range.

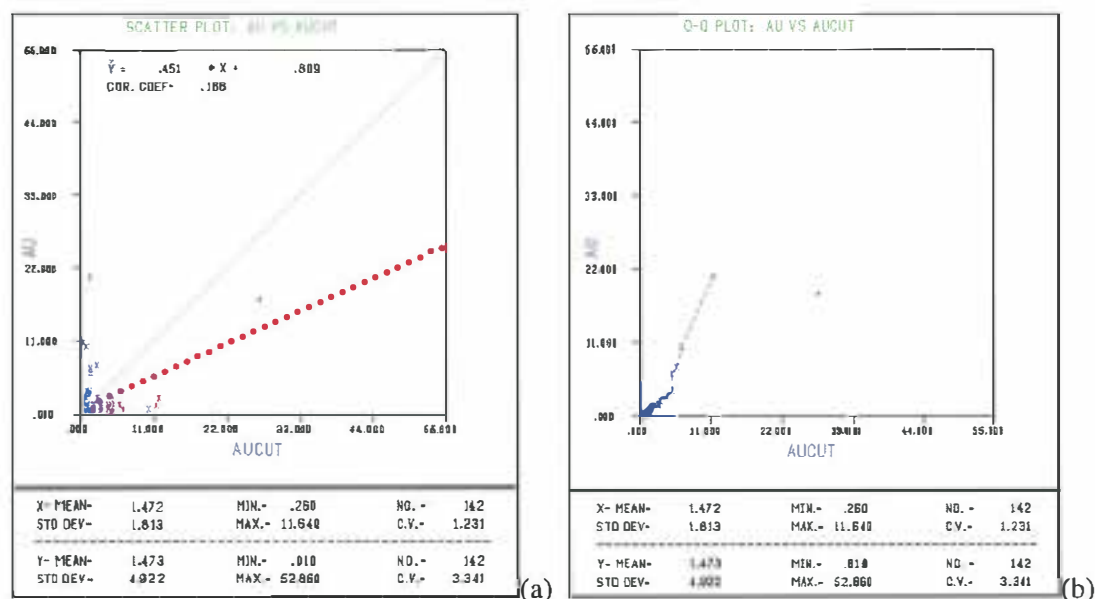


Figure 6.11 h-scatter plot with least square fit line (red) - (a) and q-q plot - (b) of the composite values (Y axis) and the OK grade estimates (X axis)

What is very important is that the average grade of the data set was estimated with a high degree of accuracy. The actual and the estimated means are virtually equal (see Table 6.5). The mean value of the distribution of the residuals (errors) and the variance of that distribution (see Table 6.6) show that the main objective of the kriging algorithm was achieved. The mean of the residuals is very close to zero. The variance

reflects the variability of the original composite values and is relatively high.

From the graphical presentation of the cross validation results in Figure 6.11 (a) and (b) it can be seen that some overestimation occurred within the range of grade values from zero to approximately five grams per tonne (g/t). Once the limit of five (g/t) is exceeded (high grade zones) underestimation seems to be present. The nature of *finexcomp* data set, that is high variability and positively skewed distribution (even though the high grade quartz vein was omitted during the statistical calculation) may exacerbate, to some extent, the differences between the smooth OK estimated and the actual composite values. The distribution of the residuals, shown in Figure 6.12, is reasonably symmetrical.

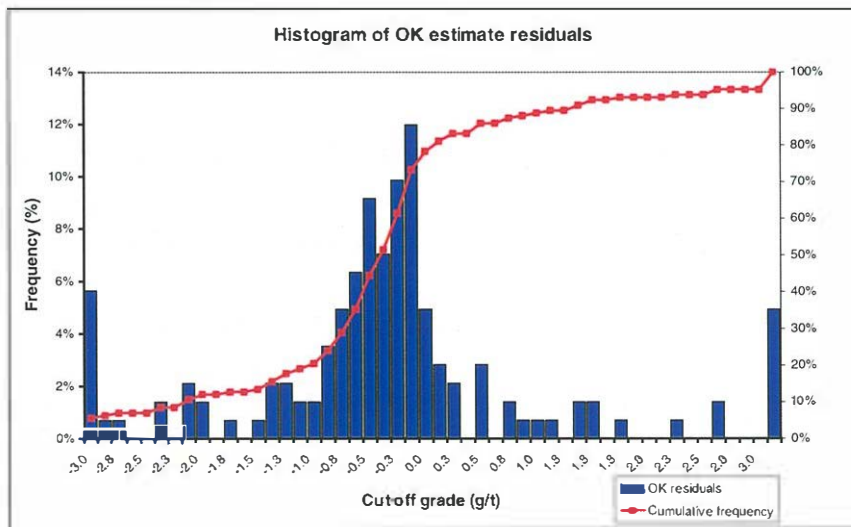


Figure 6.12 Histogram of the OK estimate residuals

Therefore it can be expected that, for the whole project considered, the grade estimate should be fairly accurate. Indeed, the mean grade of the original composite values used during the OK estimation and the mean value of the estimates are nearly identical. The mean of the composites is 1.473 (g/t) and the mean of the OK estimates is 1.472 (g/t).

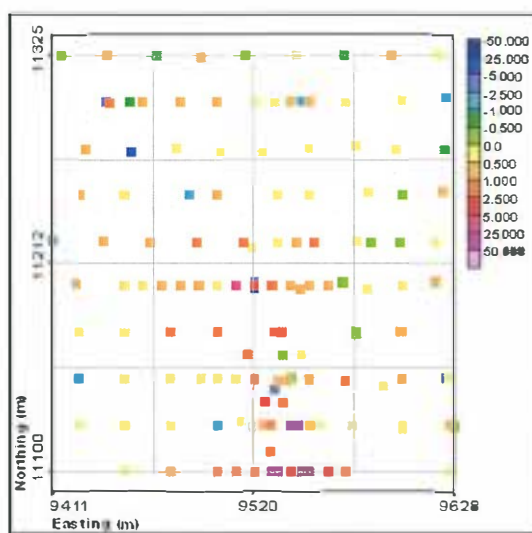


Figure 6.13 Position of residuals from the cross validation of the OK estimate. The legend bar specifies the magnitude of the residual

Figure 6.13 presents a bench plan with the residuals from the cross validation plotted. They are represented by small squares. The colour of a square reflects the magnitude of the error according to the legend bar. From this map it can be seen that even though the estimated grades seem to be higher than the actual grades of the composites the magnitude of the differences is not large. It is also evident that, in most cases, where the residuals appear to be higher there is usually a mixture of

overestimated and underestimated points. Hence the overall error should not be significant.

In view of the results of cross validation presented here, together with the information acquired from the BGM geology and mining departments, and the fact that the spatial continuity parameters derived in this study are similar to published results (Khosrowshahi et al, 1992), (BGM Inter. Report, 1996), it is deemed that the semivariogram model validated here is appropriate. This model (Table 6.4) along with the search parameters detailed later in Figure 7.1, Figure 7.2 and Figure 7.3, will be used in this study for further kriging grade estimations.

## **7. CHANGE OF SUPPORT AND GRADE ESTIMATION USING *FINEXCOMP***

### **7.1 Introduction**

The main purpose of a geostatistical study, with respect to mining applications, is to generate grade estimates of a geological attribute of interest such as grade of precious metal (such as gold, as in our case) or some other elements. Not only do we want the value of the grade but we would also like to know its spatial continuity and other statistical properties. Since the economic success of an operation greatly, if not entirely, depends on these factors it is crucial for our estimates to be as accurate as possible. There is no estimation which would give perfect results. Nevertheless a number of different methods have been developed to meet these requirements.

Many different factors can bias the estimation results. One of these factors, as already discussed, is the change of support. The level of impact of the change of support on the estimates may be increased if for instance the size of a panel which is estimated is not equal to the size of the SMU. The support effect can also be critical, if neglected, when



global estimation of recoverable resource at a given cut-off is based on the grade distribution of exploration data.

In the following sections grade estimations using *finexcomp* will be performed using three different methods:

- ordinary kriging (OK);
- nearest neighbour kriging (NNK); and
- sequential Gaussian conditional simulation.

Special attention will be given to the change of support effect on the estimation results. The latter two methods have a built-in mechanism that takes into account the support changes. The results from each of the methods will be compared with the grade control data *grchan* by means of grade-tonnage curves. This comparison is very important from a mine planning point of view. By calculating grade-tonnage curves (if calculated for the whole mineral deposit) the tonnage of the deposit can be determined for different minimum grades, often called cut-off grades. Furthermore, the average grade of the deposit can be readily derived at the given minimum cut-off grade. Then, if economic parameters are applied, the monetary value of the deposit can be calculated. The change of support correction on *finexcomp* will be carried out using the affine correction method (Section 4.2).

For theoretical purposes an affine correction will also be applied to the grade control data *grchan* to adjust its distribution according to the panel size used during the grade estimation. Then the grade-tonnage curves from the adjusted data will be compared with the appropriate grade estimates. In addition, using each of the listed methods, grade estimation will be carried out for the panel size equal to the support of our *grchan* data set, which is 2 m by 10 m laterally and 3 m vertically.

## **7.2 Ordinary kriging and the nearest neighbour kriging estimation**

### **7.2.1 Background**

The geostatistical estimation techniques used in this section include: ordinary kriging and the nearest neighbour kriging. Each of these techniques will be applied to estimate the grade of panels using sample data from *finexcomp*. The mathematical background of the first of the method, that is OK, is given in Section 2.4. The NNK algorithm is presented in Section 4.5. Recall, the nearest sample (or  $k$  nearest samples) is emphasised during the NNK estimation of the grade of a block. The proportion by which the NNK weight  $\lambda_{\alpha}^{NNK}(\mathbf{u})$  (4-9 and 4-10) of this sample (or  $k$  nearest samples) is increased, is directly proportional to the variability of the deposit being estimated. Intuitively a less smooth

estimated grade distribution could be expected from NNK than from OK, and NNK should be more robust, especially in a variable deposit such as our data set.

While performing an estimation we often talk about a sample neighbourhood. This term describes the search parameters required by the OK and NNK methods. These parameters determine the area around the unsampled location  $\mathbf{u}$  being estimated within which samples are accepted for use in the estimation. Often the search area has an ellipsoidal shape due to anisotropy of a data set, for example like in the case of *finexcomp* – geometric anisotropy. It is important to define the search parameters correctly and not to include samples which are too far away. Conversely, one has to retain enough data to make the estimate reliable. The determination of the parameters should be based on the geostatistical properties of the spatial continuity of the data set and geological input in the case of earth sciences (see also Arik, 1990). Other properties required by the kriging system are provided by the semivariogram model used during the estimation process.

Once all the necessary parameters are defined, the kriging estimation can be carried out. With respect to our *finexcomp* data set, appropriate

semivariogram models have been prepared as described in Section 6.2. The spatial continuity parameters of the models are listed in Table 6.4. Similarly the search parameters for the data have been determined. These parameters are listed in the form of the Medsystem ® software entries in the following figures: Figure 7.1, Figure 7.2 and Figure 7.3. Note that an explanation of the “Kriging Search Parameters” from Figure 7.1 is given in Appendix 1.

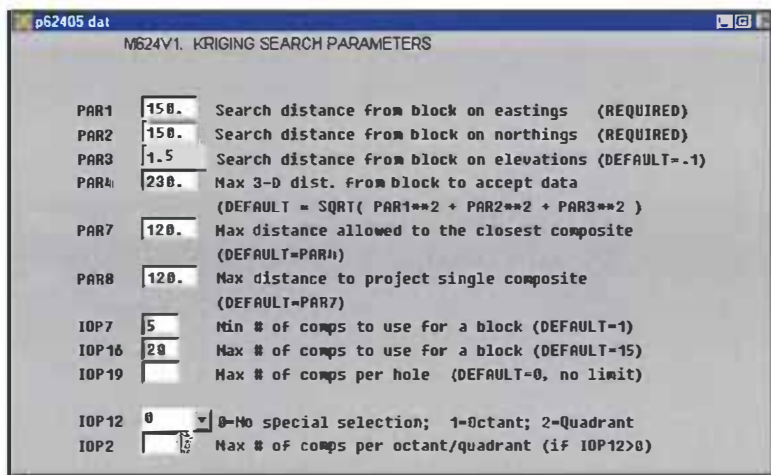


Figure 7.1 Primary search parameters for OK and NNK runs

The following section presents the results of the grade estimation obtained from the several kriging runs. These results are analysed in detail in Section 7.2.3.

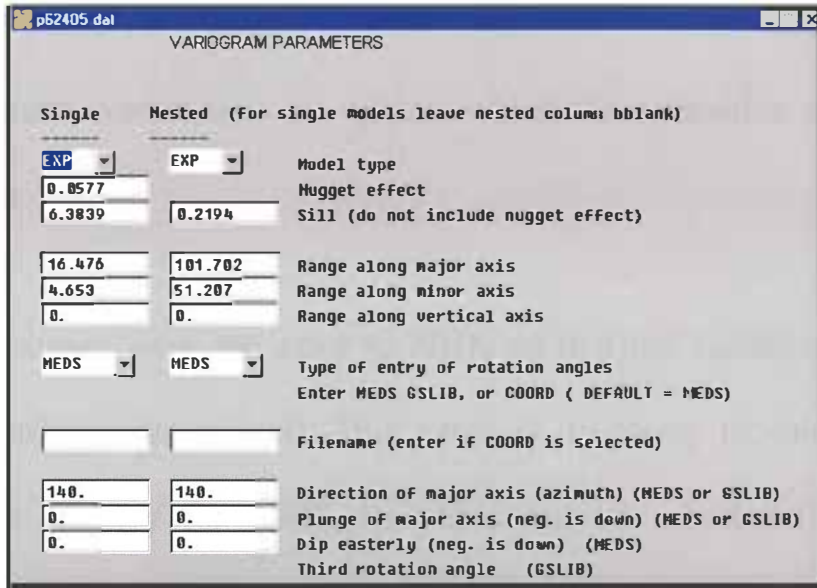


Figure 7.2 Semivariogram parameters for OK and NNK runs

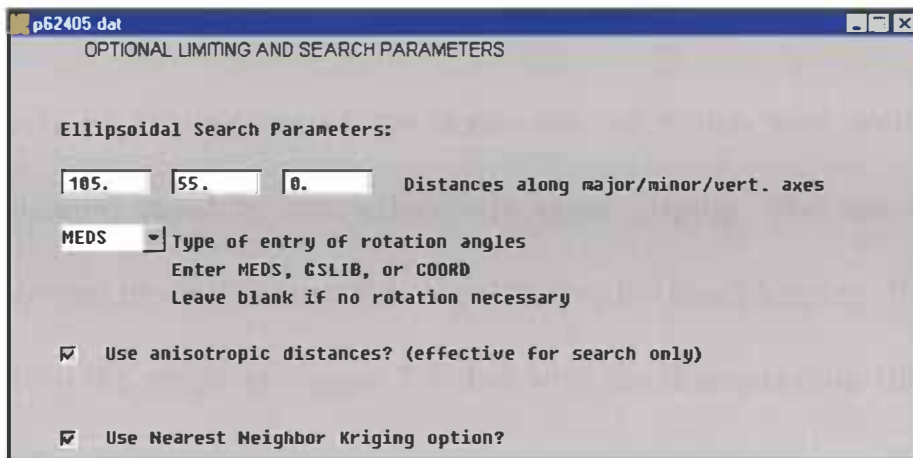


Figure 7.3 Ellipsoidal search parameters for OK and NNK runs

### 7.2.2 *Finexcomp* grade estimation results

The estimations were done using two panel sizes as follows:

- first X=12.5m by Y=12.5 m by Z=3m (referred to as **panel size 1**)  
and then
- X=2 m by Y=10m by Z=3m (referred to as **panel size 2**).

The latter panel size was used in order to achieve the same support as the *grchan* grade control data set against which the estimation results are compared.

OK estimations were run prior to NNK so that the variance of block values could be determined. This value is necessary to calculate the correction factor  $f$  for NNK. Its value can be calculated from the

equation (4-6) as 
$$f = \sqrt{\frac{\sigma_b^2}{\sigma_p^2}}$$

Two sets of kriging runs were done, one of which was with block discretisation equal to one, effectively point kriging. The second one incorporated block discretisation equal to five for block kriging. It can be seen from the graph in Figure 7.4 that with the discretisation (in the X and Y directions) above five there are no significant changes to the block variance.

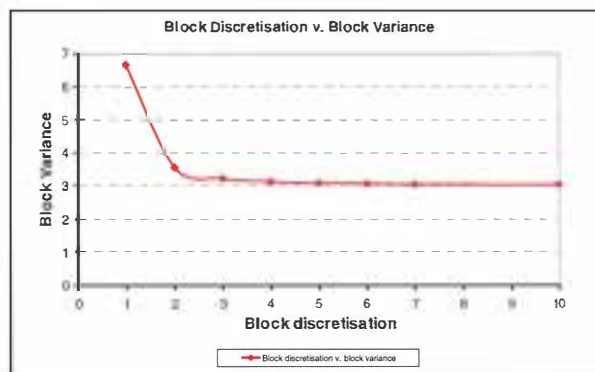


Figure 7.4 Block discretisation versus block variance

The block variance and standard deviation from the point kriging (panel size 1) are:

$$\sigma_{bp}^2 = 6.66 \quad \text{and} \quad \sigma_{bp} = 2.58 \quad (7 - 1)$$

whereas the block variance and standard deviation from the block kriging (panel size 1) are:

$$\sigma_{bb}^2 = 3.08 \quad \text{and} \quad \sigma_{bb} = 1.75 \quad (7 - 2)$$

It follows that the two factors  $f_{bp}$  for NNK point and  $f_{bb}$  block kriging respectively are:

$$f_{bp}=0.53 \quad \text{and} \quad f_{bb}=0.36 \quad (7 - 3)$$

The number  $k$  of nearest samples for NNK was varied from  $k=1$  to  $k=3$  for point and block kriging. Effectively three runs in each of these cases were carried out.

Figure 7.5 shows *grchan* channel data alone within the final study area. In Figure 7.6 the results of the point kriging from OK and NNK are presented in the form of bench plans overlaid with *grchan* channel data.

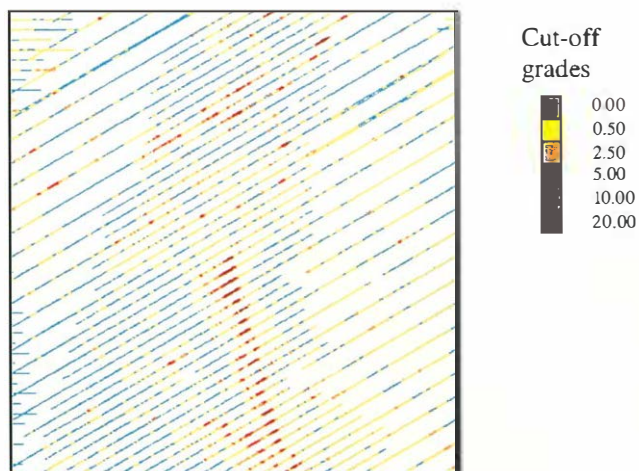


Figure 7.5 *Grchan* channel assay data – bench plan, final study area.

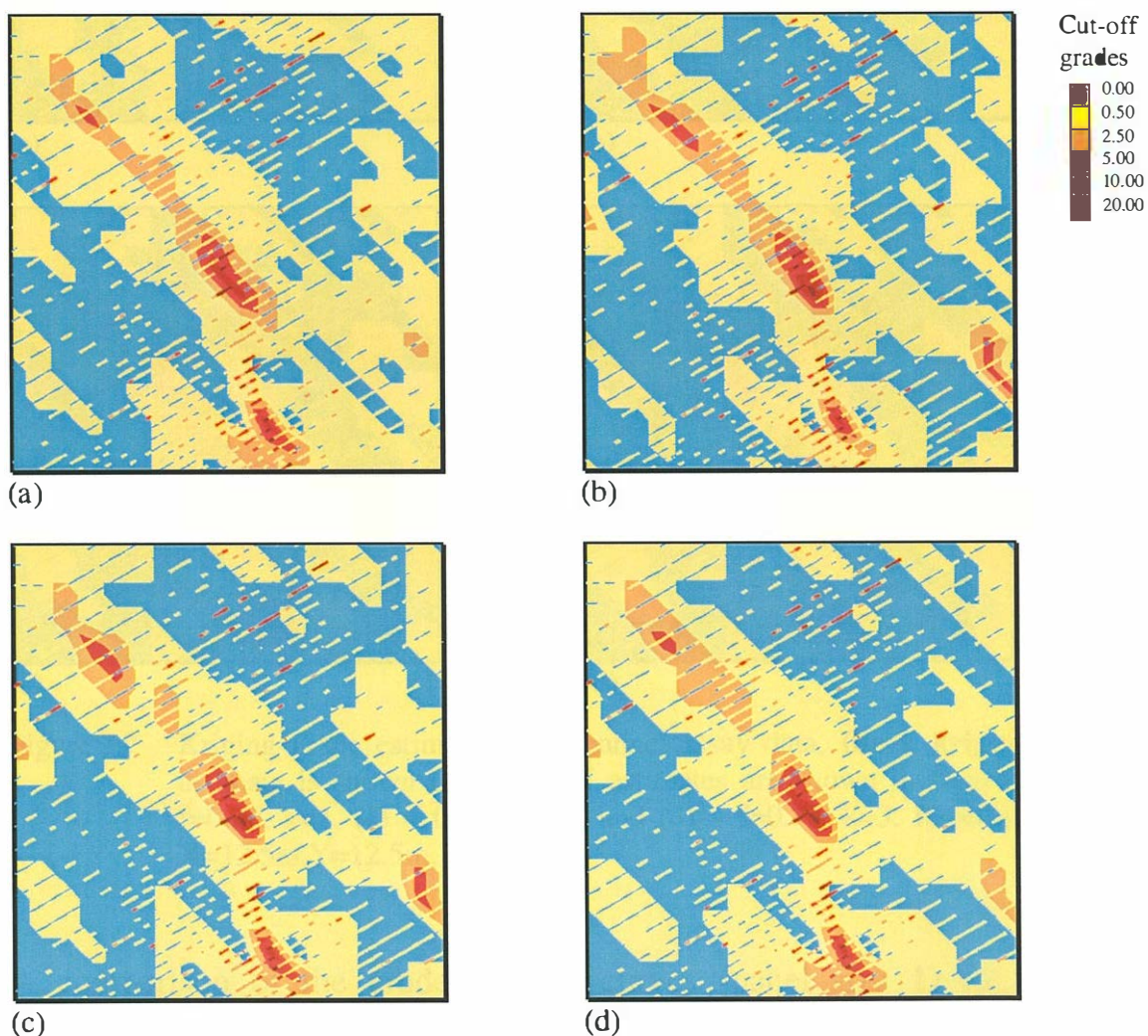


Figure 7.6 Kriging grade estimates and channel assay data. **Point kriging.** OK estimate is shown in (a), NNK estimates are shown in figures (b) –  $f=0.53$ ,  $k=1$ , (c) –  $f=0.53$ ,  $k=2$  and (d) –  $f=0.53$ ,  $k=3$ . Panel size  $1 - X=12.5m, Y=12.5m, Z=3m$ .



The four mosaic plots in Figure 7.7 present the results of the panel size 1 block kriging, again overlaid with *grchan* channel data.

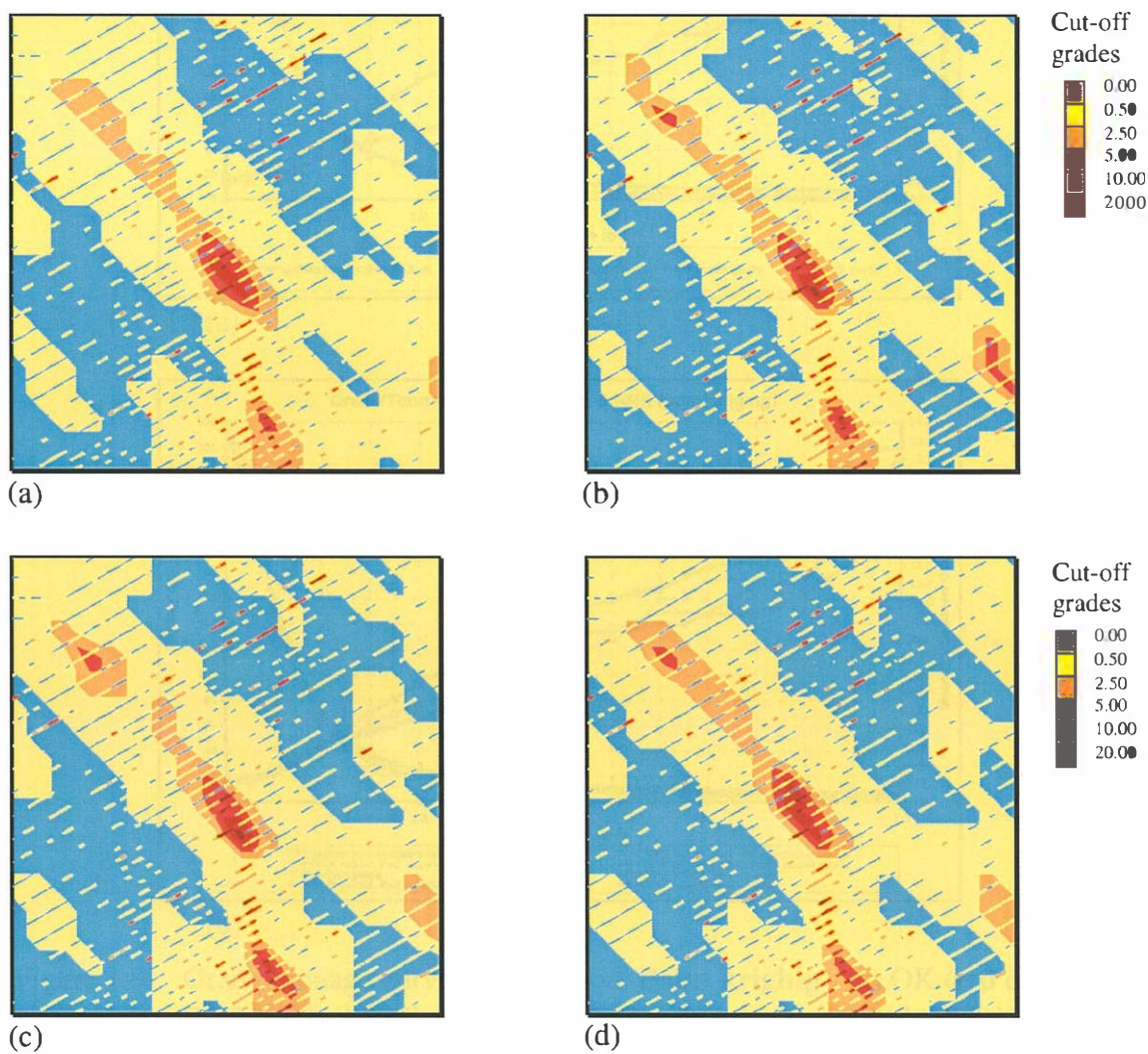
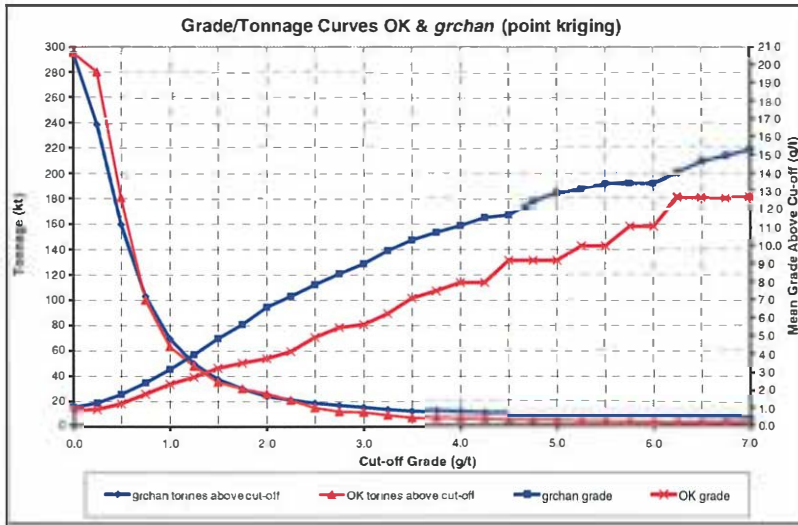
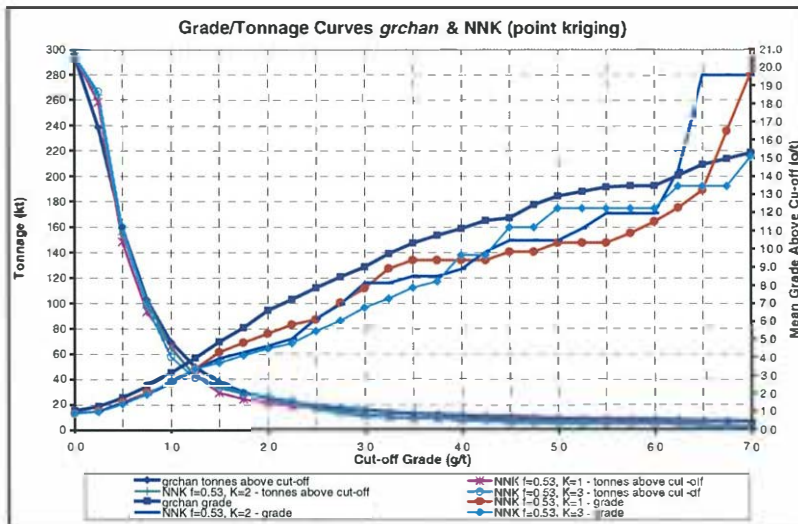


Figure 7.7 Kriging grade estimates and channel assay data. **Block kriging.** OK estimate is shown in (a), NNK estimates are shown in figures (b) –  $f=0.36, k=1$ , (c) –  $f=0.36, k=2$  and (d) –  $f=0.36, k=3$ . Panel size 1 –  $X=12.5m, Y=12.5m, Z=3m$ .

A comparison of the grade-tonnage curves (panel size 1) for point kriging is given in Figure 7.8. In every case the thick dark-blue curves represent the grade-tonnage curves of the *grchan* data set. Figure 7.8 (a)



(a)



(b)

Figure 7.8 Grade-tonnage curves comparison. **Point kriging** - (a) OK (red curves); (b) NNK  $f=0.53$  ( $k=1$  - brown,  $k=2$  - blue,  $k=3$  - light blue); (a) and (b) *grchan* (dark blue curves). Panel size 1 -  $X=12.5m, Y=12.5m, Z=3m$ .

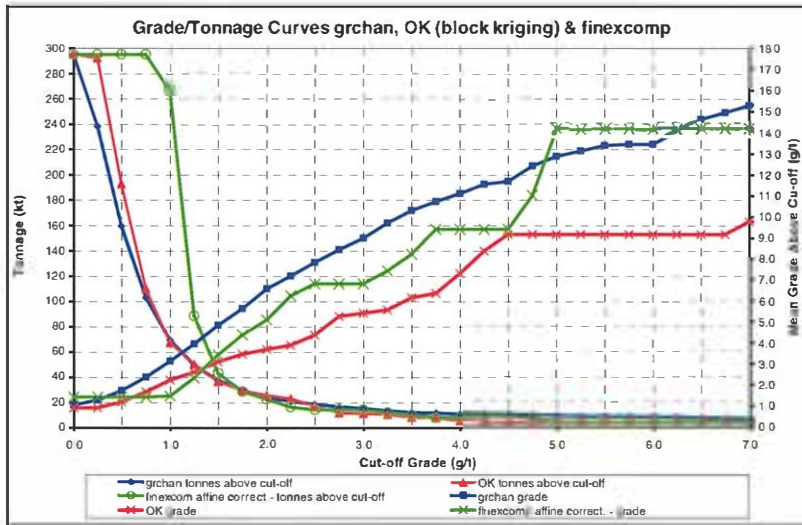
presents the grade-tonnage curves from OK estimates while Figure 7.8 (b) shows the grade-tonnage curves from NNK. There are three different estimates for three different numbers of samples  $k$  (equations 4-9, 4-10) emphasised during NNK estimation process, i.e.  $k=1$ ,  $k=2$  and  $k=3$ . Note that the *grchan* sample support is clearly defined, that is one sample

represents the volume contained within the dimensions X= 2m, Y=10m and Z= 3m. In order to avoid a bias, the declustering weights were used to calculate the *grchan* statistics prior to the comparisons presented from now on. Unless otherwise stated cell declustering was used with the cell size equal to the size represented by one sample from *grchan*. This data set is used throughout the study for comparison with the results from the different methods. There is only one exception, described later in this section, where affine corrected *grchan* was used (Figure 7.11 and Table 7.3).

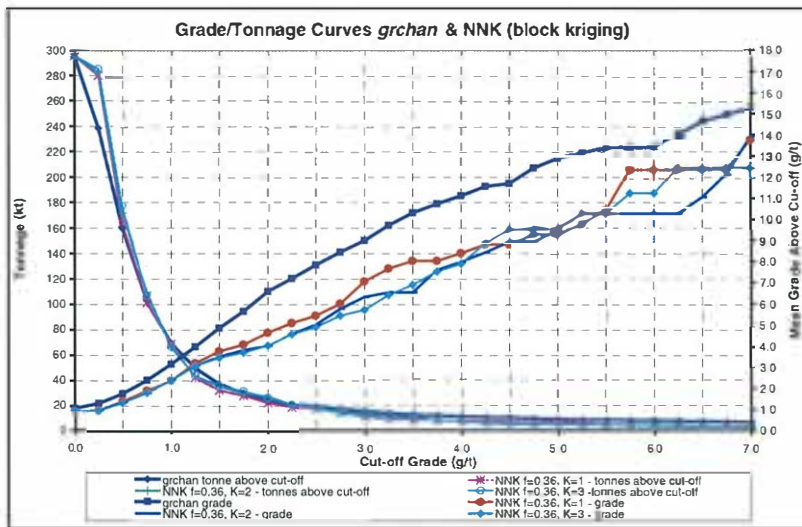
Figure 7.9 (a) and (b) present block kriging estimates from OK and NNK respectively. In addition the corrected *finexcomp* distribution using the affine correction method is presented in Figure 7.9 (a) in the form of grade-tonnage curves. The correction was done for the panel size 12.5m x 12.5m x 3 m. The affine correction factor  $\sqrt{f_v}$  was calculated as the ratio of the block variance  $\sigma_{bb}^2 = 3.08$  to the *finexcomp* point variance  $\hat{\sigma}_p^2$  (Table 5.3) and is equal to

$$\sqrt{f_v} = \sqrt{\frac{3.08}{24.07}} = 0.36$$

As already discussed in Section 4.2 the value of this factor should not be too small otherwise less reliable results may be expected from the affine



(a)



(b)

Figure 7.9 Grade-tonnage curves comparison. **Block kriging.** - (a) OK (red curves); (b) NNK  $f=0.36$  ( $k=1$ -brown,  $k=2$ -blue,  $k=3$ -light blue); (a) and (b) *grchan* (dark blue curves). Affine corrected *finexcomp* (a) green curves. Panel size 1 -  $X=12.5m, Y=12.5m, Z=3m$ .

correction method. Notwithstanding this, for the purpose of this research, we wanted to test and compare different correction methods therefore it was decided to use this method and apply the correction factor as

calculated above. This also gives us an opportunity to check in practice the assumption about the value of the factor  $\sqrt{f_v}$ .

Table 7.1 lists the summary statistics for *grchan* and the kriging grade estimates presented in Figure 7.8 and Figure 7.9 as well as the summary statistics of *finexcomp* after the affine correction was carried out.

Table 7.1 *Grchan* and grade estimates statistics summary. *Finexcomp* – affine corrected. Panel size 1 for kriging (12.5x12.5x3 m).

Data Set	Mean	Standard Deviation	Min.	Max.	Number	Coefficient of Variation
<i>Grchan</i>	1.089	2.514	0.010	42.340	2188	2.308
<i>Finexcomp</i> affine correct.	1.464	1.755	0.944	19.852	143	1.199
OK <sup>[1]</sup>	0.916	1.277	0.050	14.310	420	1.394
NNK <sup>[1]</sup> , f=0.53, k=1	0.926	2.093	0.050	34.740	420	2.260
NNK <sup>[1]</sup> , f=0.53, k=2	0.938	1.989	0.050	32.360	420	2.120
NNK <sup>[1]</sup> , f=0.53, k=3	0.927	1.696	0.050	23.450	420	1.830
OK <sup>[2]</sup>	0.947	1.165	0.200	11.560	420	1.230
NNK <sup>[2]</sup> , f=0.36, k=1	0.943	1.679	0.152	26.369	420	1.780
NNK <sup>[2]</sup> , f=0.36, k=2	0.946	1.514	0.174	22.836	420	1.600
NNK <sup>[2]</sup> , f=0.36, k=3	0.947	1.411	0.170	16.800	420	1.490

Note: [1] – point kriging (no block discretisation)  
 [2] – block kriging (block discretisation X=5, Y=5, Z=1)

The results presented in Figure 7.6 to 7.9 are the results obtained from the kriging estimates using panel size 1 support (X=12.5m by Y=12.5m by Z=3m) which is not equal to the support of *grchan*. If we consider the

grade control data set, one sample represents a support of  $X=2\text{m}$  by  $Y=10\text{m}$  by  $Z=3\text{m}$ . The direct comparison of the tonnage curves by the means of the percentage of the population above given cut-off is not possible, because the support of samples and the support of panels are different.

Consequently to enable such a comparison an average tonnage represented by a sample from *grchan* and by a panel from kriging was incorporated. In the case of *grchan*, the average tonnage per sample was calculated based on the volume of the study bench, the number of samples and the specific gravity (SG). The SG is expressed in tonnes per cubic metre ( $\text{t/m}^3$ ) and for the weathered (clay) profile at BGM is approximately equal to  $1.5 (\text{t/m}^3)$ . The volume of the panel is readily defined and so is the tonnage. Whenever the support of both samples and the panels from the estimation or simulation were equal, the grade-tonnage curves were calculated as the percentage of the population above given cut-off and the mean grade above cut-off, respectively. Assigning tonnage to the samples and the panels in such a case (tonnages would be equal because the support of both of these is the same) would re-scale the graph but would not affect the direct relationship between these curves.

To illustrate the results one would obtain from estimating the grade and tonnage of the study deposit based solely on *finexcomp*, the appropriate curves are presented in Figure 7.10. In the same figure there are also grade-tonnage curves obtained from affine corrected *finexcomp*. This time, however, the correction was done for the panel size 2, in order to achieve the same support as *grchan*. The new affine correction factor  $\sqrt{f_v}$  was based on the block variance  $\sigma_b^2 = 4.32$  from the panel size 2, and the *finexcomp* sample variance (Table 5.3). The correction factor is equal to

$$\sqrt{f_v} = \sqrt{\frac{4.32}{24.07}} = 0.42$$

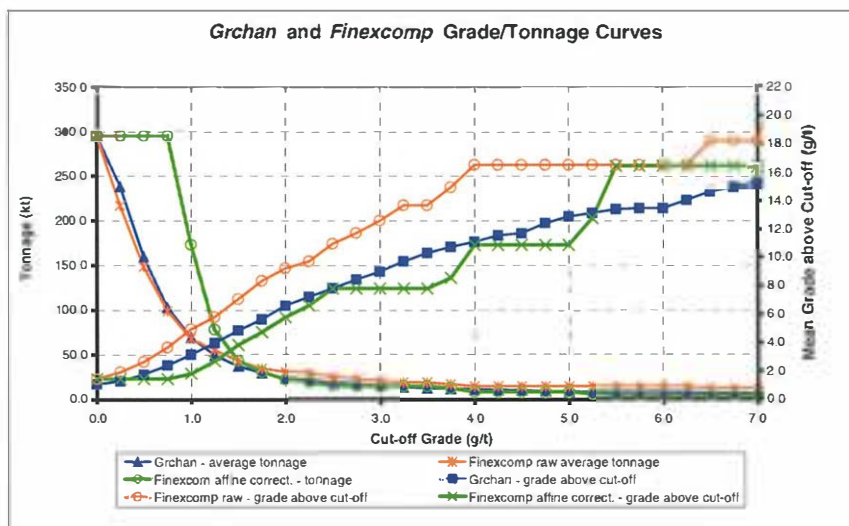


Figure 7.10 *Grchan* (blue), raw *finexcomp* (orange) and affine corrected *finexcomp* (green) grade-tonnage curves.

*Grchan* is presented by blue curves, raw *finexcomp* by orange curves and corrected *finexcomp* by green curves. For the raw *finexcomp* the tonnages are reasonably well estimated. However the grades of both the raw *finexcomp* and corrected *finexcomp* deviate from the *grchan* grade curve. Note that the summary statistics for *finexcomp* after this support correction are included later in Table 7.4.

Subsequently, to make the comparison more comprehensive the data from *grchan* had been subjected to some preparation in order to account for the change of support effect. Specifically, the set was first declustered using cell declustering with a cell size equal to  $X=12.5m$  and  $Y=12.5m$  (the same as the panel size from previous grade estimation). Then the composite values were corrected for the change of support using the affine correction method. This was done in order to test the performance of this method. It should be noted that the modifications described above were made for this exercise alone. The subsequent comparisons are not affected. The experimental variance correction factor  $\sqrt{f_v}$  used for the affine correction in this case is the ratio of the block variance  $\sigma_{bb}^2 = 3.08$  to the variance  $\sigma_p^2 = 3.21$  of the de-clustered *grchan*. Table 7.2 presents summary statistics of *grchan* after declustering was carried out.



Table 7.2 Summary statistics of de-clustered *grchan*. Cells size 12.5m x 12.5x3m.

Data Set	Mean	Standard Deviation	Min.	Max.	Number	Coefficient of Variation
De-clustered <i>Grchan</i>	1.118	1.791	0.05	17.76	321	1.602

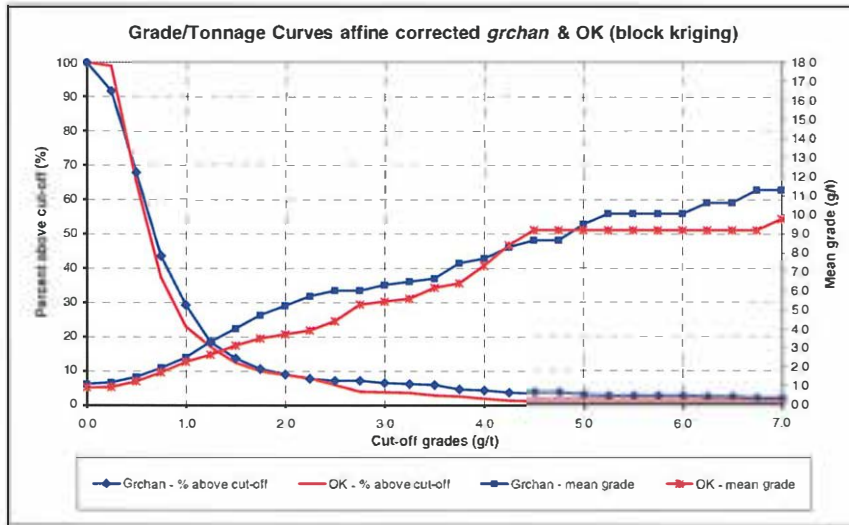
Hence the correction factor is equal to

$$\sqrt{f_v} = \sqrt{\frac{3.08}{3.21}} = 0.98 \quad (7 - 4)$$

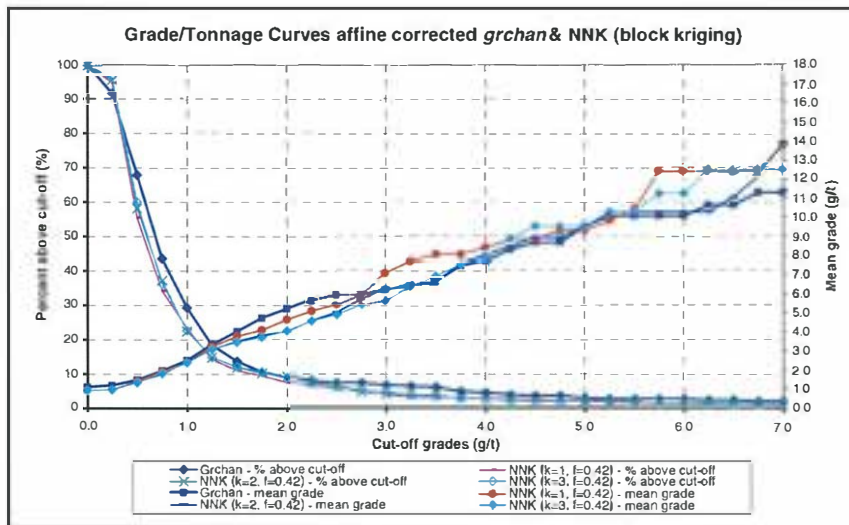
The value of the variance correction factor (7-4) is greater than 0.85.

That means that in this instance the affine correction technique should be adequate.

The outcomes of the affine corrected *grchan* and the kriging estimates using panel size 1 are presented graphically in Figure 7.11. As in previously described cases, charts in Figure 7.11 (b) show the grade-tonnage curves from three NNK estimates for  $k=1, 2$  and 3 (panel size 1) and the grade-tonnage curves of *grchan* data set after the affine correction was applied. As already stated, the correction applied to *grchan* enabled us to account for the support differences between *grchan* and the panel volume, which was used during the kriging runs. For ease of analysis the grade-tonnage curves from OK estimation, along with the corrected *grchan*, are presented separately in Figure 7.11 (a).



(a)



(b)

Figure 7.11 Grade-tonnage curves comparison. **Block kriging.** (a) OK (red curves); (b) NNK  $f=0.42$  ( $k=1$ -brown,  $k=2$ -blue,  $k=3$ -light blue); (a) and (b) affine corrected *grchan* (dark blue curves). Panel size 1 -  $X=12.5m, Y=12.5m, Z=3m$ .

The results shown in this section are discussed in detail in the next section.

Table 7.3 summarises the main statistical properties of the affine corrected *grchan* and, for comparison, descriptive statistics of the kriging estimates are presented.

To accomplish this, a series of kriging estimates of the *finexcomp* grade were generated on the panel size with the support equal to the support of *grchan*. This enables a direct comparison of the distributions of both populations, i.e. *grchan* and the estimated panels. It is the equality of support (volume) represented by one sample from *grchan* and a panel from the grade estimation that makes the comparison possible. This support is our panel size 2, i.e. X=2m, Y=10m, Z=3m.

Table 7.3 Affine corrected *grchan* and grade estimates statistics summary table. Panel size 1 for kriging (12.5m x 12.5x3m).

Data Set	Mean	Standard Deviation	Min.	Max.	Number	Coefficient of Variation
<i>Grchan affine corrected</i>	1.118	1.754	0.070	17.420	321	1.569
OK <sup>[2]</sup>	0.947	1.165	0.200	11.560	420	1.230
NNK <sup>[2]</sup> , f=0.36, k=1	0.943	1.679	0.152	26.369	420	1.780
NNK <sup>[2]</sup> , f=0.36, k=2	0.946	1.514	0.174	22.836	420	1.600
NNK <sup>[2]</sup> , f=0.36, k=3	0.947	1.411	0.170	16.800	420	1.490

Note: [2] – block kriging (block discretisation X=5, Y=5, Z=1)

The correction factor  $f$  for the NNK method was recalculated since the block variance  $\sigma_{bb}^2$  changed due to the smaller panel size. In this case the value of standard deviation is

$$\sigma_{bb} = \sqrt{4.32} = 2.08 \quad (7 - 5)$$

Hence the proportion of our new  $\sigma_{bb}$  to the standard deviation of *finexcomp*  $\sigma_p = 4.91$  (Table 5.3) is equal to

$$f = \frac{2.08}{4.91} = 0.42 \quad (7 - 6)$$

The value shown in (7-6) is the NNK correction factor for the grade estimation using panel size 2.

A visual comparison of the results of kriging estimates (OK and NNK) overlaid with the trench assay data from *grchan* is presented in Figure 7. 12 in the form of bench plans. Panel size 2 (X=2m, Y=10m and Z=3m), i.e. *grchan* support, was used during kriging calculations. Figure 7. 12 (a) shows OK grade estimate contours whereas Figure 7. 12 (b), (c) and (d) are the contoured results of NNK with  $k=1, 2$  and  $3$  nearest samples emphasised, respectively.

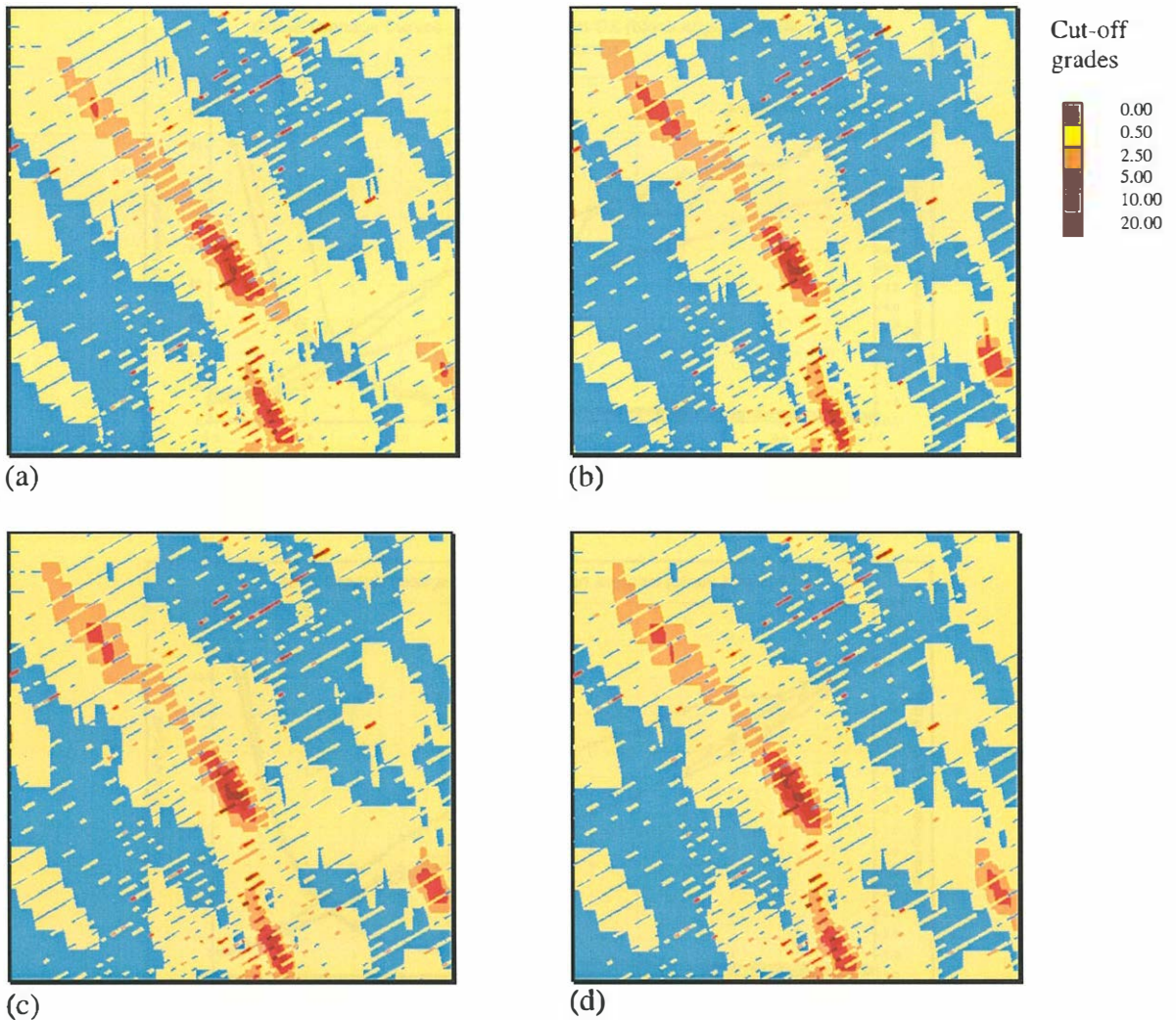
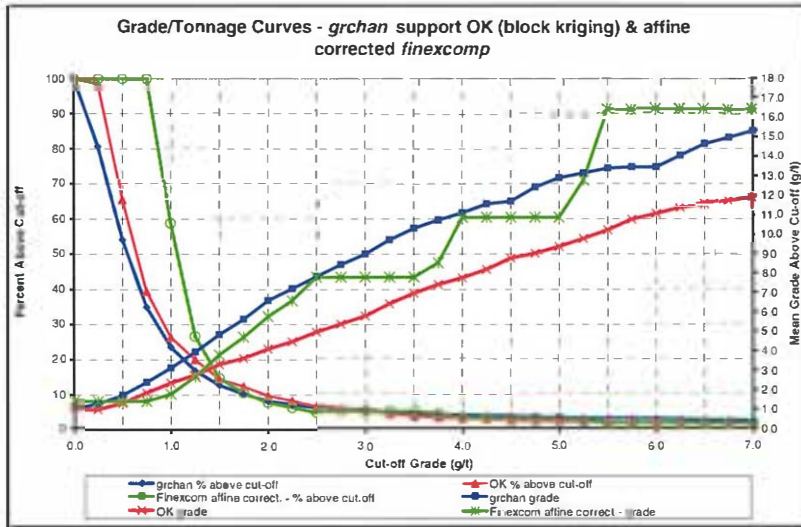
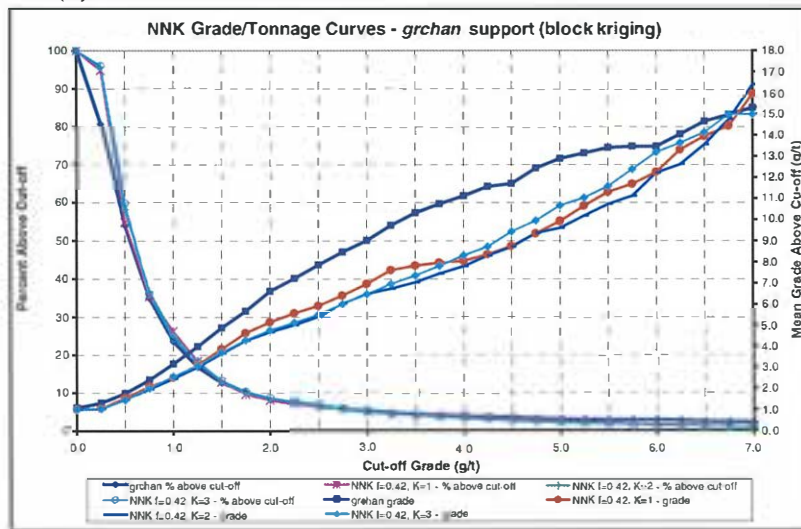


Figure 7.12 Kriging grade estimates and channel assay data. **Block kriging.** OK estimate is shown in (a), NNK estimates are shown in figures (b) –  $f=0.42$ ,  $k=1$ , (c) –  $f=0.42$ ,  $k=2$  and (d) –  $f=0.42$ ,  $k=3$ . Panel size 2 -  $X=2.m$ ,  $Y=10m$ ,  $Z=3m$ .

Grade-tonnage curve comparison between kriging estimates, using panel size 2 and *grchan* data set, is presented in Figure 7.13. In addition, Figure 7.13 (a) shows the *finexcomp* grade-tonnage curves after the affine correction for panel size 2 was applied. The affine correction factor expressed as  $\sqrt{f_v} = 0.42$  and is equal to the NNK factor (7-6).



(a)



(b)

Figure 7.13 Kriging estimates with support equal to *grchan* sample. **Block kriging.** Grade-tonnage curves comparison, block kriging. (a) OK (red curves); (b) NNK  $f=0.42$  ( $k=1$ -brown,  $k=2$ -blue,  $k=3$ -light blue); *grchan* (dark blue curves), (a) *finexcomp* affine corrected (green curves). Panel size 2 - X=2m, Y=10m, Z=3m.

Summary statistics of *grchan* and the kriging estimates, that is OK and NNK for  $k=1, 2$  and  $3$  and  $f=0.42$ , are listed in Table 7.4. The NNK estimate ( $k=1$ ) yields the closest estimate of all in comparison to *grchan* summary statistics.

Table 7.4 *Grchan*, *finexcomp* affine corrected and grade estimates statistics summary table. Panel size 2 for kriging and affine correction (2m x 10m x 3m).

Data Set	Mean	Standard Deviation	Min.	Max.	Number	Coefficient of Variation
<i>Grchan</i>	1.089	2.514	0.010	42.340	2188	2.308
<i>Finexcomp</i> affine correct.	1.464	1.755	0.944	19.852	143	1.199
OK <sup>[2]</sup>	1.029	1.513	0.160	25.100	2530	1.470
NNK <sup>[2]</sup> , f=0.42, k=1	1.015	2.040	0.110	36.870	2530	2.010
NNK <sup>[2]</sup> , f=0.42, k=2	1.000	1.790	0.120	36.200	2530	1.790
NNK <sup>[2]</sup> , f=0.42, k=3	1.016	1.808	0.120	36.120	2530	1.780

Note: [2] – block kriging (block discretisation X=5, Y=5, Z=1)

In the following section the kriging results presented will be analysed in more detail.

### 7.2.3 Analysis of the kriging estimation results

The previous section described the estimation process and presented the results of the kriging (OK and NNK) grade estimations based on the *finexcomp* data set.

Even though the average tonnages are reflected reasonably well by the exploration data set in comparison to the grade control set, the grade at different cut-offs is not. This shows that the support of data plays a very important role and cannot be neglected. The affine correction of

*finexcomp* certainly helped, to some extent, mainly with respect to the grade estimate. The grade curve fluctuates, however there are some points where the two, the *grchan* grade curve and the *finexcomp* grade curve meet. Tonnages are not reflected very well at the cut-offs below the mean value of the data set (the green curves from Figure 7.10), where they are overestimated. The correction method generated unrealistic values in this section of the corrected distribution – hence the overestimated tonnages. This test shows that the affine correction may generate less reliable results when used for distributions with significant differences in variability (*finexcomp* and distribution of panel size 2 i.e. X=2, Y=10 and Z=3m).

For point kriging from NNK (Figure 7.8) the outcome is relatively good. The grade, and especially the tonnages, of our grade control set are quite well estimated. The grade is best estimated by the NNK run with  $k = 1$  (brown curve from the graph) up to the cut-off of about 3.5 (g/t). Then the curve (light blue) representing the run with  $k = 3$  seems to give the best fit. This may suggest (at least in the case of this deposit) that for the higher cut-off estimates it would be more appropriate to increase the number of nearest samples  $k$  during NNK runs. The tonnages are slightly overestimated with low cut-offs (below 0.5 g/t). For the range of cut-offs



from approximately 1.0 to 2.0 (g/t) there is a slight tendency to underestimate the tonnages. Overall the estimates are deemed to produce a good fit. That NNK has improved the kriging technique is apparent when compared with the OK results in Figure 7.8 (a). Indeed, looking at Table 7.1, it is clear that NNK with  $k=1$  gives the best results of all when comparing with *grchan* summary statistics.

Also in the block kriging case (see Figure 7.9 and Table 7.1) NNK proved to be more robust than the traditional OK method. Again when  $k=1$  the closest results to *grchan* were obtained. However the differences between these are not as pronounced as for the point kriging. This can be attributed to the much lower NNK correction factor  $f$  used during the block kriging. This may suggest that more consideration should be given to the value of the correction factor used. Figure 7.9 (a) shows the grade-tonnage curves of *finexcomp* after a change of support correction using the affine method. This time the correction was done to account for the volume of panel size 1. The results of the correction show that although tonnages are overestimated above the mean grade of *finexcomp*, below the mean grade they fit the tonnage curve from kriging quite well. Also the grade fluctuates and again is relatively well estimated close to the mean grade of *finexcomp*. The affine correction test done here used a

correction factor of 0.36, which is lower than suggested in the literature 0.7–0.8 (Section 4.2). Notwithstanding this, as already stated in Section 7.2.2, our purpose is to test the correction techniques, not to reject or accept them, hence the correction performed and analysed above.

Because we wished to compare our estimates against *grchan* we also considered a panel size (panel size 2) with support equal to the support of *grchan*. Actually NNK has the built-in flexibility of enabling one to estimate panels of arbitrary size, taking into account the size of SMU. In our case this means that we could have used panel size 1 during the estimation and only had to re-calculate the correction factor  $f$  using the variance of panel size 2. But OK does not have such flexibility written in, so for the sake of being able to run it along with NNK, panel size 2 was used.

In each of NNK and OK, the change from panel size 1 to panel size 2 brings about a clear improvement in our estimates (compare Figure 7.13 with Figure 7.9). This is an example of how the estimates are affected by different support. If panel size 2 was our SMU and panel size 1 our mining block model panel, we could not and should not simply estimate

the mineral resources without giving consideration to the support differences.

From Figure 7.13, it can be seen that NNK performs better than OK, even though a significant improvement in the case of OK is visible when comparing with Figure 7.9 (a). The better results from NNK are also confirmed by the statistics presented in Table 7.4. In this case also, NNK with  $k=1$  yielded the results closest overall to the *grchan* statistics. The NNK estimates produced very good fit of the tonnages when compared with the grade control data. They were higher only for low cut-offs, below 0.4 (g/t), whereas the tonnages from OK were higher for the range of cut-offs below 2.5 (g/t) and then slightly lower from approximately 3.5 (g/t) onwards. Commonly the grade from the kriging estimates is lower than the grade of *grchan*. This can most likely be attributed to the smoothing introduced by this algorithm. It is even more pronounced here since our data include some considerably high sample values.

Another feature of the support changes is that the larger the support of the panel being estimated the lower the mean grade of the estimates (see Table 7.1 and Table 7.4). For comparison in Figure 7.9 (a) there are also grade-tonnage curves for *finexcomp* after the affine correction technique

was applied for panel size 2. This case has been already discussed at the beginning of this section.

Looking at how our estimates are positioned in space, Figure 7.6, Figure 7.7 and Figure 7.12, it can be seen that they are fairly similar. This was to be expected, since the same data (*finexcomp*) were used in all cases. The NNK estimates are more variable than the OK equivalents. The main feature of these plots is a high grade zone running through the middle and across the study region, with some isolated high grade pods in the middle and left lower (South) sections of the project. Comparing the contoured grade estimates with the trench data, some overestimation occurred in the upper (North) left corner of the region. There is no indication from the trench data of higher grade in that region. In contrast, the grade in the upper middle section of the study area is underestimated. The trench data indicate the grade value between 2.5 and 5.0 (g/t) but it is likely that the exploration drilling (see Figure 5.2) did not intersect any of the higher grade formations in this region and this is reflected in the kriging estimates. Overall the estimation worked well with the results being comparable with the grade control data regarding the spatial position.

The last of the support effect tests carried out was the affine correction in the case of *grchan* distribution. Although theoretical it is deemed to be very useful and gave very interesting results. It is called theoretical here because usually the distribution of the grade control data set is not adjusted to reflect, say, the distribution of the SMU panel, providing that the two have different supports. This kind of exercise may have a practical application for grade control and it makes a lot of sense. If we assume that the grade control data is the exhaustive data set but actual mining occurs on different support/volume of the SMU, then to estimate the recoverable reserve accurately on a per mining bench basis, the distribution of grade control data (*grchan* in our example) should be adjusted to the distribution of the SMU (panel size 1 in our example). The results of correcting *grchan* data to the support of kriging estimates by the use of the affine correction method are shown in Figure 7.11. The correction procedure worked very well in this case. In particular, the curves from the NNK estimates are close to the *grchan* curves. Some fluctuation does occur but the goodness of fit is high with NNK with  $k=2$  being the closest. With respect to the tonnages, after the correcting of *grchan*, the kriging results are lower with some exceptions for cut-off grades below 0.5 (g/t) for OK and below 0.4 (g/t) for NNK. For the

range of cut-offs between 1.5 (g/t) and 2.5 (g/t) the tonnages are nearly equal.

Looking at the statistical characteristics of all the sets compared (see Table 7.3) it was difficult to choose the set which could be considered the closest to *grchan*. However the NNK estimate with  $k=3$  was considered as having the statistical properties most similar to the affine corrected *grchan*.

In summary, the correction for the support changes plays a very important role during the mineral resource estimation. Estimation done using only the exploration data proved to be far less reliable than using alternative methods that account for the difference in the volume on which the data are defined. Nearest Neighbour Kriging produced results closer to the grade control data set used than the ordinary kriging method itself in all of the instances tested. NNK, in the case of the data used in this study, demonstrated more robustness than OK. The improvement introduced by NNK in comparison to OK confirms the fact that correction for the data support improves the results and reduces the bias in the mineral resources estimation.

The outcome of the affine correction method tested in the course of the study produced variable results. Although the results are data specific, this is an example that, under certain circumstances and honouring the assumptions behind the method, it may well be used as a support correction tool.

### **7.3 Change of support by conditional simulation**

#### 7.3.1 Background

In the following section sequential Gaussian conditional simulation (see Section 2.5) using the *finexcomp* data set will be presented. The simulation was performed with a special attention given to the problem of the change of support. This was achieved by the use of a program, namely *bsgsim*, developed by I.M. Glacken (1996) and made available to the author. This program is a modification of the *sgsim* program presented in GSLIB (Deutsch and Journel, 1998) and allows for simulation at the discretised block volume and then, after back-transformation, averages the results into the desired block volume. Effectively the change of support problem is resolved because the simulation can be done on a very fine grid and then the results are averaged to a given support (volume of the SMU for example). Since no

economic parameters were applied to any of the previous estimates the simulation results were not constrained economically in order to avoid a bias in the final outcomes.

### 7.3.2 Sequential Gaussian conditional simulation

The sequential Gaussian simulation paradigm calls for the random function model with multiGaussian distribution (see Section 2.5.2). Our sample set *finexcomp* is not normally distributed (Figure 5.3 and Table 5.3) so, prior to the simulation, a normal score transform was applied. The transformation was done on the declustered *finexcomp*. The declustering weights used were those from the cell declustering algorithm (cell size, X=30m, Y=30m and Z=3m). We refer to the transformed set as *nfinexcomp*. The histogram of *nfinexcomp* is presented in Figure 7.14 and summary statistics are given in Table 7.5.



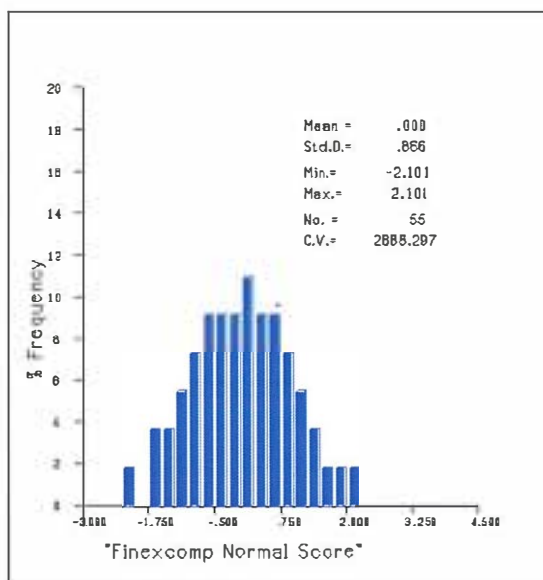


Figure 7.14 Histogram of *nfinexcomp*

Table 7.5 Summary statistics of *nfinexcomp*.

Data Set	Mean	Standard Deviation	Min.	Max.	Number	Coefficient of Variation
<i>Nfinexcomp</i>	0.000	0.866	-2.101	2.101	55	2888.297

Experimental semivariograms for *nfinexcomp* were calculated in directions from N0°E to N180°E with a step of 10° and a tolerance of 25°. Lag distance of 31m (due to the de-clustering cell size) with 15.5m lag tolerance was used. Band widths of 16m and 1.5m were taken in the horizontal and the vertical direction respectively.

In addition, several h-scatter plots were calculated, in the same range of directions and the same angular step as for the semivariograms. This was done in order to check and confirm the major direction of continuity of

the normal scores. This was determined to be N120°E and the minor direction of continuity is then N30°E. Subsequently, based on the results, semivariogram models for the major direction (Figure 7.15 (a)) and the minor direction of continuity (Figure 7.15 (b)) were developed. The models presented in these figures are geometric anisotropy models (see Section 2.3). Table 7.6 summarises the parameters of the semivariogram models shown in Figure 7.15.

Table 7.6 *nfinexcomp* normal scores spatial continuity parameters based on covariance function experimental semivariograms

Nugget:  $C_0=0.06$

	Type of Variogram Model	Anisotropy Type	Sill	Range Max.	Range Min.
Structure 1	Spherical	geometric	0.66	59.62	44.04
Structure 2	Spherical	geometric	0.28	107.03	89.17

The program *bsgsim* was then applied. In our case the simulation was done on a fine grid with the cell size X=2m by Y=2m by Z=3m and then the results were averaged to block size X=2m by Y=10m by Z=3m. This block size is equal to the support of *grchan* which is the exhaustive data set used for comparison. By using equal supports for our simulated values and *grchan* a direct comparison of the statistics and, more importantly, of the grade and tonnage curves is possible.

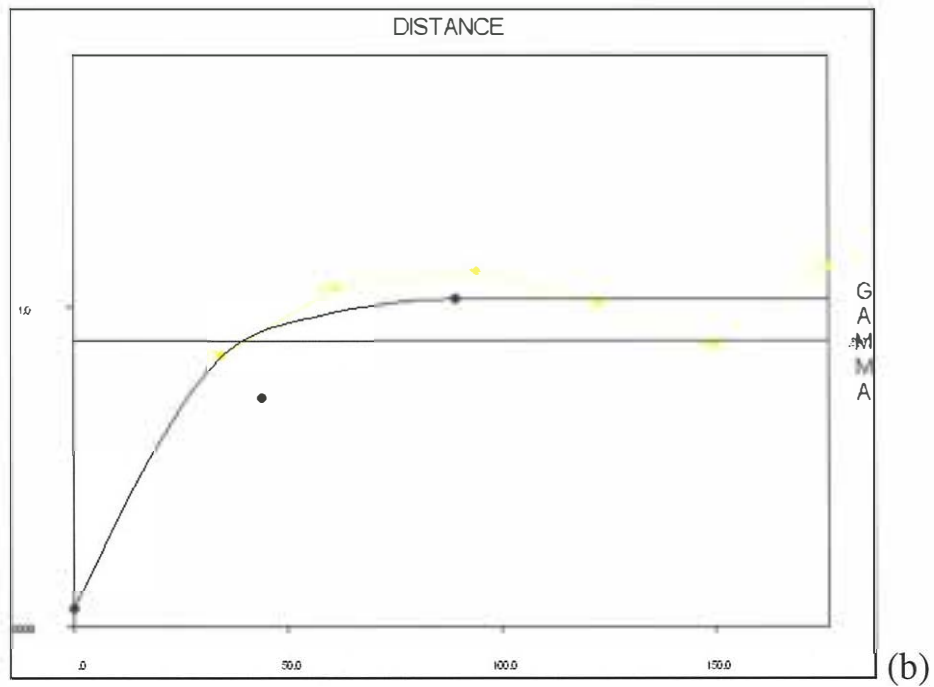
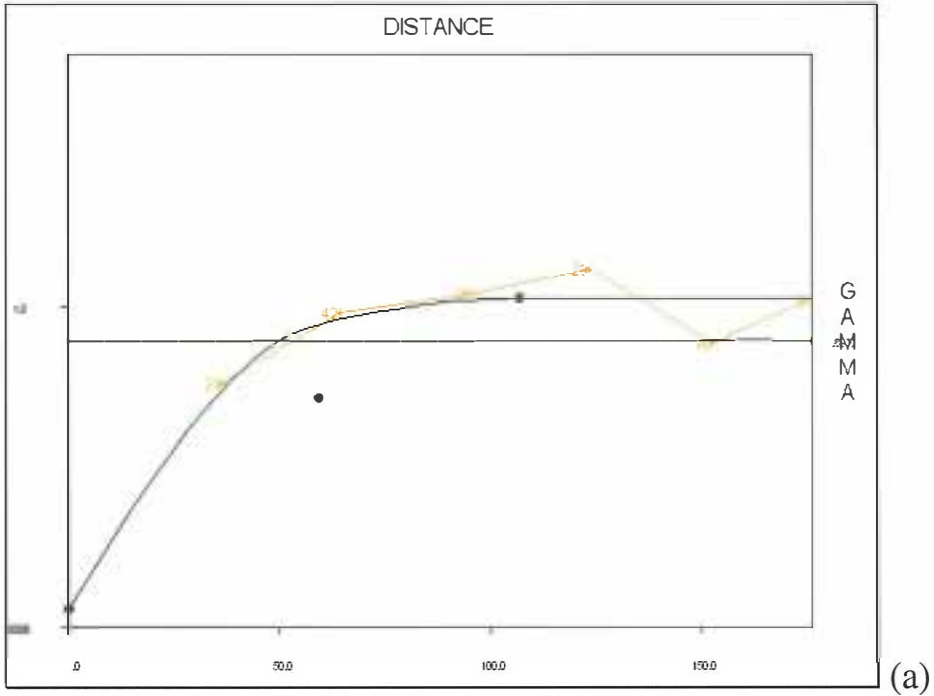


Figure 7.15 *nfinexcomp* normal scores semivariogram models. (a) major direction - N120°E, (b) minor direction - N30°E

The program, *bsgsim*, calls for the non-transformed data set as an input file. Therefore the data from *finexcomp* from the Medsystem® project

were dumped into an ASCII format file and then used with the program. The *bsgsim* parameter file used is given in Appendix 2.

For the upper tail extrapolation (Section 2.5.2) of the back-transform distribution the hyperbolic option (2-46) with  $\omega = 2$  has been used. For this project 50 realisations were generated. Each of these realisations is equally probable and these were analysed by means of their grade/tonnage curves and summary statistics were calculated. Three of these realisations were selected representing the highest, lowest and median values with respect to the tonnages and the grade. This was done in order to present one of the main features of simulation namely the spread of the results.

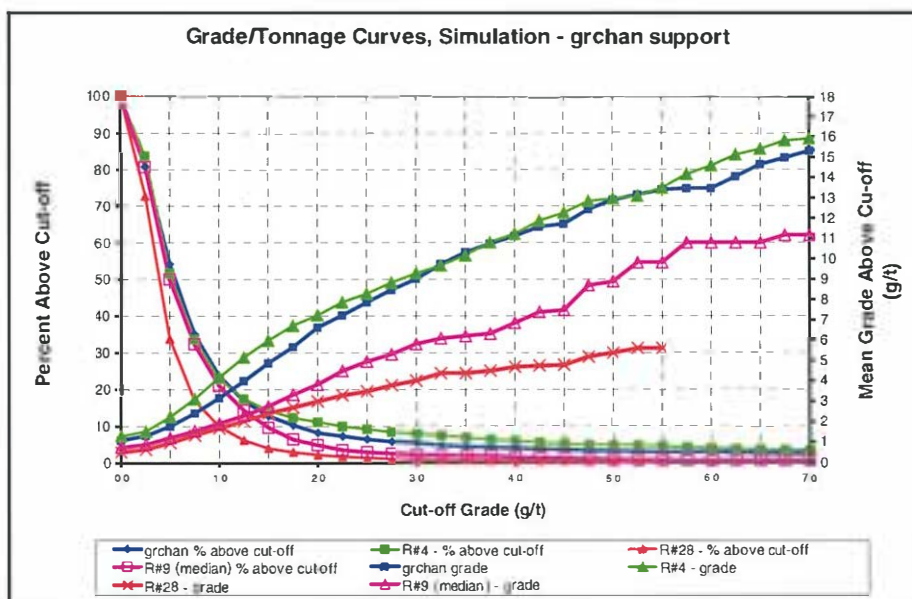


Figure 7.16 Grade/tonnage curves SGCS realisations #4(highest), #9 (median), #28 (lowest) and de-clustered *grchan*.

Figure 7.16 presents the grade/tonnage curves for these three realisations, that is respectively realisation R#4 (green curves), realisation R#9 (purple curves) and realisation R#28 (red curves), together with *grchan* (blue curves).

Summary statistics of each of the data sets from Figure 7.16 are presented in Table 7.7 below.

Table 7.7 Summary statistics of de-clustered *grchan* and realisations #4(highest) #9 (median) and #28(lowest).

<b>Data Set</b>	<b>Mean</b>	<b>Standard Deviation</b>	<b>Min.</b>	<b>Max.</b>	<b>Number</b>	<b>Coefficient of Variation</b>
<i>Grchan</i>	1.089	2.514	0.010	42.340	2188	2.308
<b>R #4</b>	1.304	3.272	0.045	44.888	2640	2.509
<b>R #9</b>	0.756	1.011	0.017	21.375	2640	1.336
<b>R #28</b>	0.516	0.510	0.022	5.595	2640	0.990

The information presented in Figure 7.16 and Table 7.7 will be discussed in the next section.

### 7.3.3 Sequential Gaussian conditional simulation results analysis

Simulation, as already discussed in Sections 2.5 and 7.3.1 is not intended to estimate, for example the grade of a deposit, it is rather designed to reproduce the variability of the distribution of the data set being

considered. Simulation delivers a distribution of values for each estimated panel, modelling the uncertainty about an unsampled location. Conditional simulation, used in this study, honours the sample values at their locations but does not necessarily give the best estimate at unsampled locations. Following this logic the results, that is the realisations, of simulation should be looked at as a whole.

In our study, the spread of the set of 50 realisations that were generated is illustrated by the grade/tonnage curves presented in Figure 7.16. In the same figure the grade and tonnage curves of *grchan* are also presented. The two most extreme grade/tonnage curves, that of R#4 and R#28, provide us with some upper and lower limits of our results. Even though it is not possible to pick “the best realisation” the median realisation, within the tolerance limits provided by the highest and the lowest realisations, may be considered as representative for the whole set.

In Figure 7.16 the tonnage curve (green) of the highest realisation R#4 seems to be very close to that of *grchan* (blue). Just above the cut-off grade of 1.50 (g/t) the green curve departs from the blue one but gets close to it again for the cut-offs above 6.00 (g/t). Now looking at the red curve that illustrates the tonnage of the lowest realisation R#28, it can be

seen that for any given non-zero cut-off this curve is below the tonnage curve of *grchan*. The largest discrepancies take place in the steepest section of both curves for the range of cut-offs from about 0.30 to 3.00 (g/t). The third tonnage curve (purple) of the 'middle' realisation R#9 is remarkably close to that of *grchan* for the range of cut-off grades from 0.0 to 1.00 (g/t) after which it starts to move away from the blue curve and gradually comes closer to the tonnage curve of R#28, following the latter one precisely from the cut-off grade of approximately 3.00 (g/t). Considering these features with respect to the tonnes of our exhaustive data set *grchan*, we may expect, with reasonable confidence, that the estimate should be fairly accurate in the low grade section of the distribution below the 1.00 (g/t) cut-off grade where the curves of the median realisation R#9 as well the highest realisation R#4 follow that of *grchan*. This situation will deteriorate slightly as we move to the higher grade range (above 1.00 (g/t)) where R#9 is below *grchan* and hence some under-estimation may be expected. Overall, however, our set of realisations captured the tonnes distribution of *grchan* quite well.

Looking at the grade curves in Figure 7.16 a rather different situation to the one described above can be seen. For the lower cut-off grade range from 0.75 (g/t) to approximately 1.50 (g/t) the blue curve of *grchan* lies

within the “fan” of results of the simulation, although always closer to R#4 than to R#28 and R#9 which follows the latter one closely within this range. In all other cases the two grade curves, for *grchan* and R#4 are very close to one other. The median realisation R#9 lies in the proximity of the lower bound rather than in the middle of the spread. The median realisation R#9 is also consistently below the *grchan* grade curve, with some improvement for cut-off grades above 4.50 (g/t) where it becomes steeper.

In general, it can be stated that simulation is a functional tool for the correction of the change of support of data. It delivers a set of features which can have very practical application during the mineral resources estimation. Furthermore, the mechanics of the change of support by conditional simulation, as carried out in the study, does not, in fact, require any correction factors. Hence, for this purpose there is no need to know the theoretical variability of the chosen panel or SMU that is being simulated. This is an evident advantage of the method since every additional estimate, i.e. an estimate of the unknown distribution of the SMU, may introduce an additional error.



Under given circumstances, as in the instance of our data set, and with this particular set of 50 realisations returned by the conditional simulation the distribution of grade and tonnage of chosen panel size or SMU were reproduced with a varying level of accuracy (Figure 7.16). Both of these properties, that is the grade and tonnage distributions, were captured by the realisations set. Yet, using the median realisation R#9 as representative for the whole set the latter property was better reproduced than the former one. The results of the conditional simulation performed throughout this section suggest, perhaps, that with a deposit of high variability and positive skewness the realisation returning higher grade and tonnages should be given special consideration when trying to derive the grade and tonnage distribution of this deposit.

## 8. CONCLUSIONS

This final section of the study is intended to summarise the outcomes of the research performed. Conclusions will be drawn from the results of our dissertation regarding the two main topics, namely the change of support effect on the resource estimation and correction for the change of support by two specific methods.

The research presented in this thesis was based on real data acquired from the Boddington Gold Mine (BGM). Because the data come from a region that was already mined out, two sets of data were available, exploration data referred to as *finexcomp* and grade control data referred to as *grchan*. All the calculations, i.e. estimations and simulations were compared against declustered *grchan* which was considered as reality in this case. This was done in order to reflect real mine planning practice and is called *grade and tonnage reconciliation*.

The results obtained from all the estimations and simulations are certainly very valuable and form a very good base for an indication of the way that different methods were performing. Nevertheless due regard should be given to the fact that we were dealing with a specific, real data set. Every data set is unique and, to a certain extent, it would be difficult

to fully predict the performance of the tested methods in any other case. Therefore one must be careful not to overgeneralise the results obtained. This, however, does not detract from the validity of the comparison exercises performed in this study.

The support or volume on which data used for reserve estimation is defined does have a significant effect on the results of estimation. An attempt to estimate the recoverable reserves, which are usually defined on the support of SMU, using the exploration data with no regard to the differences of the volume represented by an exploration sample and the SMU may introduce a serious bias that could have disastrous effects on the economic viability of a mining project.

There is a strong need for correction for change of support during any type of estimation. If the size of a panel or a block from a mining block model, where the estimates of the grade and tonnages are stored, is different from the size of the SMU (the volume on which mining occurs) then the distribution of the blocks from the model has to be corrected to the distribution of the SMU blocks. Only this can ensure that the error of the recoverable reserve estimate will be minimised. The larger the panel size used the lower the mean grade of the estimated reserves.

There are several traditional methods available for the change of support correction (see Section 3 and 4). One of those was tested in this study, namely the affine correction method. For this method to deliver unbiased results it is important that the value of the correction factor used is not too low (not less than 0.7-0.8). This was the case in this study when the affine correction method was applied to *grchan* in one instance, when fully acceptable results were obtained. However, in other cases, where the correction factor was below the limit suggested by geostatistical literature, biased outcomes were observed.

The NNK method accomplishes the correction of the support differences by applying a correction factor that is derived from the proportion of the variance of the data used for estimation and the blocks being estimated. This method, when applied to the study data set, showed a clear improvement of the estimation results in comparison to the ordinary kriging algorithm applied to the same data set. This is evidence that an estimation technique that honours the support of data and adjusts for it is very likely to deliver far more reliable results than one that does not. NNK can be globally unbiased and more robust than OK, especially when applied to a variable deposit with some high grade values, as in case of our study data. It is however suggested that the global

unbiasedness of the NNK method should be checked. It generates estimates which are less smooth than those from OK, giving the user the ability to control the number of samples from the nearest neighbourhood which get the most weight. This is particularly useful with highly variable grade distributions. Since the results of NNK estimation depend on the number  $k$  of nearest samples chosen as well as the smoothing correction factor  $f$ , particular attention should be given to those variables. Our estimation tests demonstrated a clear advantage in this case in using NNK over OK. However NNK may introduce conditional bias when producing more variable results, e.g. estimating regions preferentially drilled. Also the number  $k$  of nearest samples to be emphasised is not categorically defined. This puts a special importance on the user's experience and knowledge of the data set in order to be able to choose a value of  $k$  in such a way so that the "best" possible estimate is obtained.

The change of support by conditional simulation (in this study the sequential Gaussian simulation algorithm was used) is realised by generating point values simulated at a smaller scale (fine grid) and then averaging them to derive the block (or SMU) value. There is basically no limitation when it comes to the block size/volume. What is more important is that there is no need to know the theoretical distribution of

the block being simulated because the method does not call for a correction factor. Simulation has the advantage of generating a set of values for each block estimated, i.e. a distribution of values, which models the uncertainty. This information can be used for determining the optimal grade under different criteria. The analysis of the 50 realisations revealed that the tonnage distribution of *grchan* was well reproduced unlike the grade distribution which was located close to the upper bound of our realisations ensemble. Perhaps larger number of realisations is required in this case to further refine the outcomes. The results obtained also seem to suggest that the realisations with higher grade and tonnages should be given a particular attention, when dealing with data sets like *finexcomp* (high variability, positive skewness with some very high grade values). Interestingly a similar tendency, although not so pronounced, to under-estimate the grade of *grchan* was observed in the case of NNK. These may actually indicate that our exploration data set does not have sufficient amount of information to enable accurate estimation or reproduction of certain properties of *grchan*. Some errors are unavoidable, but as shown, the support correction helped to minimised them. The change of support by conditional simulation using sequential Gaussian simulation can be seen as a global method because it accounts for the covariances between block values. Summarising, the

method is easy to implement and, in the cases tested, gives acceptable results. It should become a “standard step” during the recoverable reserve/resource estimation process.

The two new correction methods, NNK and change of support by conditional simulation proved to be useful and practical. They can both be easily applied to any data set. A direct comparison of the two methods is difficult since one is a simulation method and the other one is an estimation method and these two methods are based upon different underlying assumptions. Nevertheless each of these methods has its apparent advantages and certainly can provide the user with a very helpful analytical tool. They might even be viewed as two complementary methods.

## **APPENDICES**



## **Appendix 1**

**Medsystem®/Minesight® - 3-D search parameters definition for kriging interpolation technique.**

**I. Primary 3-D search parameters defining a box around a block:**

- PAR1 = X-SEARCH DISTANCE
- PAR2 = Y-SEARCH DISTANCE
- PAR3 = Z-SEARCH DISTANCE

NOTE: PAR3 not used for SCAN1-D or SCAN2-D. However, still enter a small non-zero value (e.g. 0.1).

- PAR4 = MAXIMUM 3-D DISTANCE FROM BLOCK CENTROID TO ACCEPT DATA  
(default =  $\text{SQRT}((\text{PAR1})^2 + (\text{PAR2})^2 + (\text{PAR3})^2)$ )

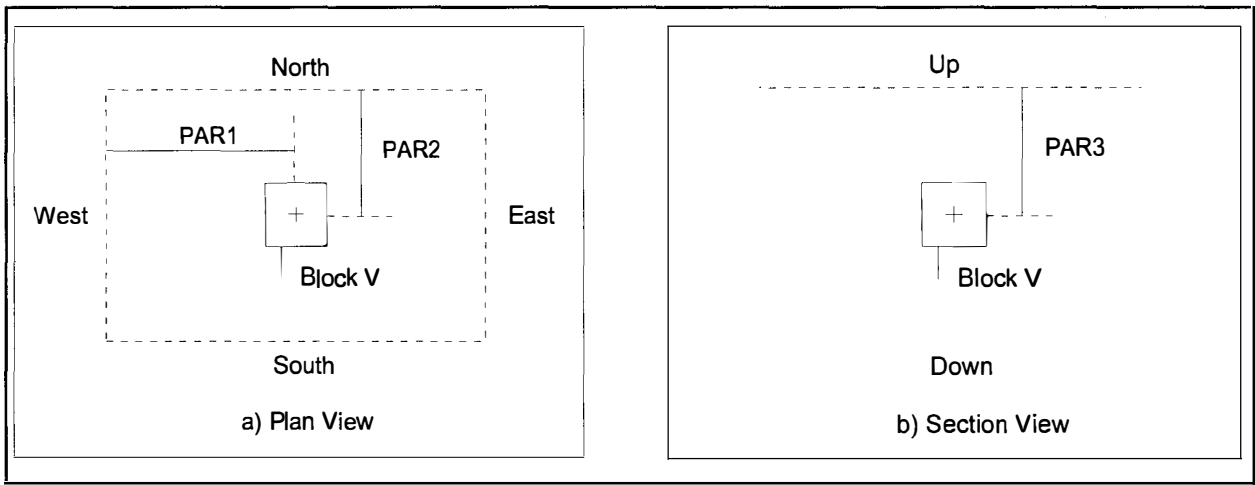


Figure 1. Definition of Primary Coordinate Search Parameters (PAR1, PAR2, and PAR3).

All of the composites within this rectangular “box” are checked against the maximum 3-D search distance (PAR4). The composites that are less than or equal to this distance from the center of the box are retained for further screening, such as geologic matching.

If there are more than “n” number of composites for a given block after all the tests, then the composites are sorted by increasing distance. Only the closest “n” are retained for calculating the weights. Based on these weights, the grade of the block is computed and stored.

**IMPORTANT NOTE:** To interpolate GSM or 2-D surface data, the coordinate selection must be based on X and Y coordinates only. If this is the case, then depending on which source is appropriate, use one of the following command lines in your run file:

- ITMn = CARD DATA INPUT SCAN2-D (ASCII Input Data) OR
- ITMn = FILE DATA INPUT SCAN2-D (Composite File 8)

## II. Optional full 3-D (ellipsoidal) coordinate search definition

To add a full 3-D search within the primary search explained above include the following command in your run file:

```
CMD = SEARCH RY RX RZ ROTN DIPN DIPE
or
CMD = SEARCH GSLIB RY RX RZ ROT1 ROT2 ROT3
or
CMD = SEARCH COORD filename RY RX RZ
where
```

SEARCH = Keyword for the program indicating a 3-D search  
 RY = Search distance (range) in the new north (major-axis) direction  
 RX = Search distance (range) in the new east direction  
 RZ = Search distance (range) in the new up direction  
 ROTN = Rotation from the old north axis to the new north axis( clockwise is a positive rotation)  
 DIPN = Dip of the new north axis measured horizontally (negative dip is plunging down)  
 DIPE = Dip easterly from the new north axis  
 (the horizontal component of this vector is 90 degrees clockwise from the horizontal component of the new north axis. The dip is measured as in DIPN.)  
 GSLIB = Keyword to specify GSLIB rotation entry  
 ROT1 = Horizontal rotation of north axis  
 ROT2 = Rotation of the north axis from horizontal  
 ROT3 = Final rotation around the new north axis  
 COORD = Keyword to specify rotation with three points  
 filename = Name of the ASCII file with coordinates of these points

For a detailed description of rotation parameters, see the 600-series Technical section.

Figures 2, 3, and 4 below and Sample Run File #2 show the relationships of the various parameters for ellipsoidal search.

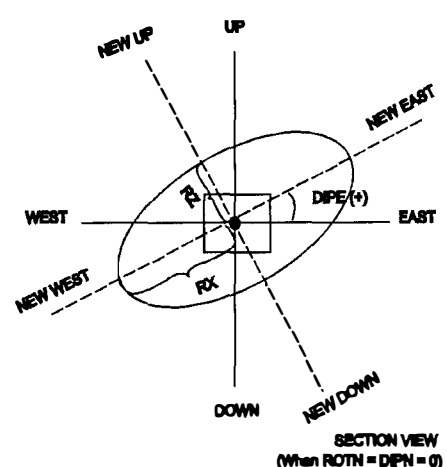
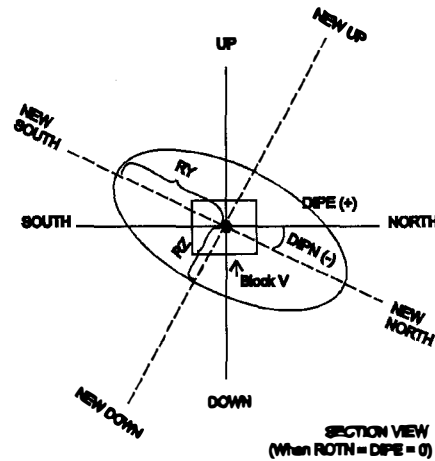
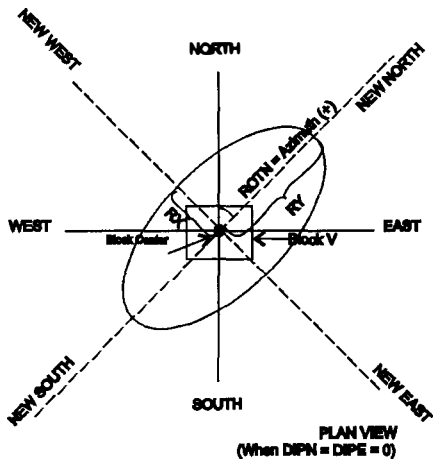


Figure 2. Definition of ROTN, RY and RX used in 3-D Ellipsoidal Coordinate Search

Figure 3. Definition of DIPN, RY and RZ used in 3-D Ellipsoidal Coordinate Search

Figure 4. Definition of DIPE, RX and RZ in 3-D Ellipsoidal Coordinate Search

This search forms an ellipsoid around the center of the block based on the search ranges and angles used. The composites within this ellipsoid are retained for calculations. The 3-D distances (RX, RY, RZ) between the block center and the composites are “adjusted” distances based on anisotropy ratios between the ranges. Therefore, if the full 3-D search is used, the value of the maximum 3-D search distance (PAR4) must reflect the distance in the new coordinates. This option supercedes the IOP3 setting. This option should not be used for the GSM mine model or File 13 interpolation.

### III. Optional interpolation parameters

PAR7 = MAXIMUM DISTANCE TO CLOSEST POINT FOR INTERPOLATION (default = PAR4)  
PAR8 = MAXIMUM DISTANCE TO THE CLOSEST COMPOSITE WHEN THE NUMBER OF COMPOSITES  
WITHIN THE SEARCH = IOP7 (default = PAR7)

NOTE: The difference between PAR7 and PAR8 is that PAR7 is tested at all cases whereas PAR8 is tested only when the number of composites within the search volume is equal to IOP7.

PAR9 = MINIMUM GRADE VALUE (if IOP5=1)  
PAR18 = MAXIMUM ESTIMATION ERROR ALLOWED

NOTE: If the kriging variance for a block exceeds PAR18, the block estimate is not stored.

### IV. Optional 3-D search distance at a specified cutoff

Maximum 3-D search distance can be changed for the assays that are greater than a specified cutoff. For this, add the following lines in your run file:

PAR31 = CUTOFF GRADE FOR CHANGING THE 3-D SEARCH DISTANCE  
PAR32 = THE 3-D SEARCH DISTANCE AT THE SPECIFIED CUTOFF  
(i.e., for composites greater than or equal to PAR31 in value, the maximum 3-D search distance will be PAR32, instead of regular PAR4).  
PAR33 = LOW GRADE CUTOFF TO CHANGE THE SEARCH  
PAR34 = MAX. 3D SEARCH DISTANCE AT PAR33

NOTE: PAR31 - PAR34 apply to the items in the first calculation only.

### V. Specification of variogram model parameters

The M624V1 run file must contain the specifications of one variogram model to be used for kriging. To specify the nugget and sill values for the variogram, enter the following command lines:

CMD = NUGGET nug-value  
CMD = SPH sill-value R1 R2 R3 [ROTN DIPN DIPE]  
or  
CMD = SPH GSLIB sill-value R1 R2 R3 ROT1 ROT2 ROT3  
or  
CMD = SPH COORD filename sill-value R1 R2 R3  
where

NUGGET = Keyword for the program (could be abbreviated NUG)  
nug-value = Nugget value for the program. Enter even when it is zero.  
SPH = Keyword for the program for spherical model.  
Use LIN for a linear variogram or EXP for an exponential.  
sill-value = Individual sill value for the specified variogram (C1 or C2, etc.).  
For a single model, this value equals to "total sill minus the nugget".  
R1 = Range in the new north (major-axis) direction  
R2 = Range in the new east direction  
R3 = Range in the new up direction  
ROTN = Rotation from the old north axis to the new north axis (clockwise is a positive rotation)  
DIPN = Dip of the new north axis measured horizontally (negative dip is plunging down)  
DIPE = Dip easterly from the new north axis (the horizontal component of this vector is 90° clockwise from the new north axis projected in the old horizontal plane. The dip is measured as in DIPN.)  
ROTN, DIPN, DIPE = MEDS rotation angles  
ROT1, ROT2, ROT3 = GSLIB rotation angles  
filename = Name of the ASCII file with coordinates of points defining rotation

See the Technical section for a detailed description of rotation parameters.

## Appendix 2

### Parameter file for **bsgsim**

#### START OF PARAMETERS:

```
declusl.dat          \ file with data
2 3 0 5 6 0         \ columns for X,Y,Z,vr,wt,sec.var.
0.0001 1.0e21       \ trimming limits
2                   \ transform the data (0=no, 1=yes, 2=block av.)
1 5 1               \ discretization factor for block averaging
bsg50.trm           \ file for output trans table
0                   \ consider ref. dist (0=no, 1=yes)
nofile.out          \ file with ref. dist distribution
1 2                 \ columns for vr and wt
0.0 70.0            \ zmin,zmax(tail extrapolation)
1 0.0               \ lower tail option, parameter
4 2                 \ upper tail option, parameter
1                   \ debugging level: 0,1,2,3
bsg50.dbg           \ file for debugging output
bsg50.out           \ file for simulation output
50                  \ number of realizations to generate
110 1.0 2.0         \ nx,xmn,xsiz
120 1.0 2.0         \ ny,ymn,ysiz
1 0.0 1.0           \ nz,zmn,zsiz
112063              \ random number seed
0 20                \ min and max original data for sim
12                  \ number of simulated nodes to use
0                   \ assign data to nodes (0=no, 1=yes)
1 3                 \ multiple grid search (0=no, 1=yes),num
0                   \ maximum data per octant (0=not used)
120.0 10.0 1.50     \ maximum search radii (hmax,hmin,vert)
120.0 0.0 0.0       \ angles for search ellipsoid
0 0.60 1.0          \ ktype: 0=SK,1=OK,2=LVM,3=EXDR,4=COLC
./data/ydata.dat    \ file with LVM, EXDR, or COLC variable
0                   \ column for secondary variable
2 0.06              \ nst, nugget effect
1 0.66 120.0 0.0 0.0 \ it,cc,ang1,ang2,ang3
    59.62 44.04 1.5  \ a_hmax, a_hmin, a_vert
1 0.28 120.0 0.0 0.0 \ it,cc,ang1,ang2,ang3
    107.03 89.17 1.5 \ a_hmax, a_hmin, a_vert
```

By entering 2 at the fourth line of the parameter file the block averaging option is specified

The fifth line contains the block discretisation parameters.

## Appendix 3

### Parameter file for **postsim**

#### Parameters for POSTSIM

\*\*\*\*\*

#### START OF PARAMETERS:

```
bsg50.dat          \ file with simulated realizations
50                 \ number of realizations
-0.001 1.0e21      \ trimming limits
110 24 1           \ nx, ny, nz
CIbsg50.dat        \ file for output array(s)
1                  \ output option [1], output parameter
```

#### Note:

[1] for probability intervals calculation in the last line of the parameter file a digit four followed by 0.95 should appear. Four is the output option and 0.95 is the output parameter for the 95% confidence intervals calculation.

## REFERENCES

- Abramovitz, M. and I.A. Stegun, editors, 1972. Handbook of Mathematical Functions: with Formulas, Graphs and Mathematical Tables, 9<sup>th</sup> (revised) printing. Dover, New York. 1046p.
- Arik, A. (1997). "Practical Mining Geostatistics", Short Course Notes Prepared for Medsystem ® / MineSight® Users, Mintech Inc. Tuscon, AZ USA
- Arik, A. (1990). Effect of Search Parameters on Kriged Reserve Estimates. International Journal of Mining and Geological Engineering, Vol 8, No. 12, pp305 – 318. Mathematical Geology 19 (2), 91-98.
- Arik, A. (1998). "Nearest Neighbor Kriging: A Solution to Control Smoothing Of Kriged Estimates", SME Annual Meeting, Preprint.
- Dagdelen, K., Verly, G., Coskun, B. (1997). Conditional Simulation for Better Reserves Estimation and Grade Control. SME Annual Meeting, Denver, CO. Preprint Number 97 201.
- David, M. (1972). Grade – tonnage curve: use and misuse in ore – reserve estimation. Transactions Institution of Mining and Metallurgy, volume 81, pp 129-132
- David, M. (1977). Geostatistical Ore Reserve Estimation. Elsevier, Amsterdam.
- Deutsch, C.V. and Journel, A.G. (1998). GSLIB: Geostatistical Software Library and User's Guide. Oxford University Press.
- Dimitrakopoulos, R.(ed), (1994). Geostatistics for the Next Century. Kluwer Academic Publishers. Printed in Netherlands.
- Glacken, I.M. (1996). Change of Support by direct conditional block simulation. Master's thesis, Stanford University, Stanford, C.A.

- Glacken, I.M. (1997). Change of Support and Use of Economic Parameters for Block Selection. In Geostatistics Wollongong'92, Vol 2. Kluwer Academic Publishers, Dordrecht, pp. 811-821.
- Goovaerts, Pierre. (1997). Geostatistics for Natural Resources Evaluation. Oxford University Press.
- Huijbregts, Ch. (1976). Selection and Grade – Tonnage Relationship. In M. Guarscio et al (eds), Advanced geostatistics in the mining industry, D.Reidel Publishing Company, Dordrecht-Holland, pp. 113-135.
- Isaaks, E.H. and Srivastava, R.M. (1989). An Introduction to Applied Geostatistics. Oxford University Press.
- Journel, A.G. (1985). Recoverable reserves estimation – the geostatistical approach. Mining Engineering, 563-568, June.
- Journel, A.G. and Huijbregts Ch. J. (1978). Mining Geostatistics. London, Academic Press.
- Khosrowshahi, S. et al (1992). Geological Modelling and Resource Estimation of the Pit F0 Deposit, Boddington WA; for Boddington Gold Mine. Mining and Resource Technology Pty Ltd. Applecross WA.
- Matheron, G. (1971). The theory of Regionalised Variable and its Applications. Les Cahiers du Centre de Morphologie Mathematique, Fasc. 5, CG Fontainebleau.
- Matheron, G. (1975a). Forecasting block grade distributions: the transfer functions. In M. Guarscio et al (eds), Advanced geostatistics in the mining industry, NATO-ASI, series C, v.24, Reidel Dordrecht, pp. 237-251.
- Matheron, G. (1975b). A simple substitute for conditional expectation: the disjunctive kriging. In M. Guarscio et al (eds), Advanced geostatistics in the mining industry, NATO-ASI, series C, v.24, Reidel Dordrecht, pp. 221-236



- Parker, H. (1980). The volume-variance relationship: a useful tool for mine planning in Geostatistics (Mousset-Jones, P., ed.). New York, McGraw Hill.
- Recny, C.J. (1978) Assessment of Economic Scale of Operations Mine Planning Unpublished Masters thesis, Stanford University
- Recny, C.J. (1982). The Influence of Geologic Characteristics on Production Capacity and Their Relation to Cost and Profitability of Mining Project. Mineral Industry Costs, Chapter 4, Northwest Mining Association, Spokane, WA.
- Rossi, M.E., Parker, H.M. (1993). Estimating recoverable reserves: is it hopeless? in Proceeding of Geostatistics for the Next Century Meeting (in press), June 3-5, 1993, Montreal Quebec, Canada.
- Sullivan, J.A., Verly, G. (1983) The estimation of Recoverable Reserves Using Conditional Recovery Functions. Stanford University, Department of Applied Earth Sciences.
- Verly, G.W., Sullivan, J.A. (1985). MultiGaussian and Probability Kriging, Application to Jerritt Canyon Deposit. Mining Engineering, Vol. 37, pp. 568 – 574.
- “Boddington Gold Mine (1998), Ore Deposit Modelling Methodology Report 1998”, Internal report, January 1998 Boddington Gold Mine WA.
- “Boddington Gold Mine (1996), Wandoo Oxide Orebody Methodology Report”. Internal report, Mining Library, Boddington Gold Mine WA.